



LAB-MADE COLORIMETRIC DEVICES FOR EDUCATIONAL AND
FORENSIC APPLICATION

BY

NATTAWAT BAWORNNITHICHAIYAKUL

A THESIS SUBMITTED IN PARTIAL FULFILLMENT OF THE REQUIREMENTS
FOR THE DEGREE OF MASTER OF SCIENCE (CHEMISTRY)
DEPARTMENT OF CHEMISTRY
FACULTY OF SCIENCE AND TECHNOLOGY
THAMMASAT UNIVERSITY
ACADEMIC YEAR 2023

LAB-MADE COLORIMETRIC DEVICES FOR EDUCATIONAL AND
FORENSIC APPLICATION

BY

NATTAWAT BAWORNNITHICHAIYAKUL



A THESIS SUBMITTED IN PARTIAL FULFILLMENT OF THE REQUIREMENTS
FOR THE DEGREE OF MASTER OF SCIENCE (CHEMISTRY)
DEPARTMENT OF CHEMISTRY
FACULTY OF SCIENCE AND TECHNOLOGY
THAMMASAT UNIVERSITY
ACADEMIC YEAR 2023

THAMMASAT UNIVERSITY
FACULTY OF SCIENCE AND TECHNOLOGY

THESIS

BY

NATTAWAT BAWORNNITHICHAIYAKUL

ENTITLED

LAB-MADE COLORIMETRIC DEVICES FOR EDUCATIONAL AND FORENSIC APPLICATION

was approved as partial fulfillment of the requirements for
the degree of Master of Science (Chemistry)

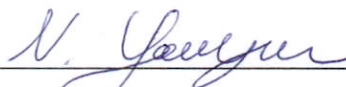
on **June 5**, 2024

Chairman



(Assistance Professor Kamonthip Sereenonchai, Ph.D.)

Advisor



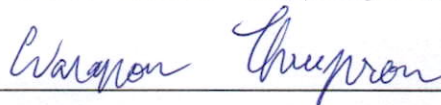
(Associate Professor Napaporn Youngvises, Ph.D.)

Member



(Assistance Professor Saisuree Prateptongkum, Dr. rer. Nat.)

Member



(Assistance Professor Waraporn Threeprom, Ph.D.)

Dean



(Associate Professor Supet Jirakajohnkool, Ph.D.)

Thesis Title	LAB-MADE COLORIMETRIC DEVICES FOR EDUCATIONAL AND FORENSIC APPLICATION
Author	Nattawat Bawornnithichaiyakul
Degree	Master of Science (Chemistry)
Department/Faculty/University	Chemistry Faculty of Science and Technology Thammasat University
Thesis Advisor	Associate Professor Napaporn Youngvises, Ph.D.
Academic Year	2023

ABSTRACT

This work is focused on the invention of a spectrometer for colorimetric analysis of tetracycline hydrochloride (TCH), monosodium glutamate (MSG), delta-9-tetrahydrocannabinol (THC), and ethanol (EtOH) with two systems; laser pointer – light dependence resistor (LDR); and paper-based device with smartphone systems.

Firstly, a simple spectrometer was designed and invented in our laboratory with simple components such as a laser pointer, light-dependent resistor (LDR), plastic holder, and multi-meter. Three wavelengths of light sources, laser pointers (red, green, and blue), were tested for the relationship of signal (R) in ohm unit and absorbance, using sun-protective car films calibrated to a commercial spectrophotometer. It was found that the relationship of absorbance and $\log R$ was linear with the coefficient of determination (R^2) > 0.990.

The systems were applied to determine tetracycline hydrochloride (TCH) and monosodium glutamate (MSG) using blue and red laser pointers, respectively. The determination of TCH and MSG is based on complex formation with Fe(III) and Cu(II), subsequently producing red and blue color solutions. The optimizations of reagent concentrations were studied. The proposed method presented the linearity in the concentration range of TCH and MSG were $1.15 \times 10^{-4} - 5.74 \times 10^{-6} \text{ mol L}^{-1}$ (R^2 0.9987) with LOD $1.44 \times 10^{-6} \text{ mol L}^{-1}$; and $2.96 \times 10^{-3} - 4.73 \times 10^{-2} \text{ mol L}^{-1}$ (R^2 0.9987) with LOD

$6.50 \times 10^{-4} \text{ mol L}^{-1}$; respectively. The relative standard deviations (%RSDs) of repeatability were 1.30 for TCH and 1.24 for MSG. The proposed spectrometers were applied to determine TCH in pharmaceuticals and MSG in flavor enhancers compared to a commercial spectrophotometer, with no significant difference at a 95% confidence level.

Secondly, the capillary-driven microfluidic paper-based device (μ CD-PAD) with smartphone-enabled colorimetric detection for on-site analysis was proposed for the simultaneous detection of delta-9-tetrahydrocannabinol (THC) and ethanol (EtOH) in synthetic saliva; based on coupling reaction with fast blue B salt and oxidation reaction with dichromate, respectively. Synthetic salivas with various viscosity can flow to the detection zone without a sample preparation step. Also, the colorimetric signal can be produced on the detection zone without the effect of viscosity (RSD < 5%). Under optimal conditions, the developed device presented the linearity in the concentration range $0.100 - 10.0 \text{ mg L}^{-1}$, with R^2 0.9967 and $0.100 - 5.00 \text{ \%v/v}$, with R^2 0.9943 for THC and EtOH, respectively. The limits of detection (LOD) were $6.00 \times 10^{-2} \text{ mg L}^{-1}$ of THC and $8.00 \times 10^{-2} \text{ \%v/v}$ of EtOH. The %RSDs for reproducibility were 6.69 (THC) and 4.81 (EtOH). The proposed device was applied to simultaneously detect THC and EtOH in synthetic salivas with acceptable precision and accuracy.

Keywords: Lab-made spectrometer, Tetracycline hydrochloride, Monosodium glutamate, the capillary-driven paper-based microfluidic device, A roadside test kit, Delta-9-tetrahydrocannabinol, Ethanol, Artificial saliva

ACKNOWLEDGEMENTS

Firstly, I would like to thank Associate Professor Napaporn Youngvises for supporting and encouraging me to complete my work.

Secondly, I would like to acknowledge Dr Chawin Srisomwat for supporting and suggesting my work during this hardship.

Acknowledge to Assistance Professor Kamonthip Sereenonchai, Assistance Professor Saisuree Prateeptongkum, and Assistance Professor Waraporn Threeprom to be the thesis examination committee of my thesis to guide important points and making my work better.

I would like to thank the scholarship for talent student to study graduate program in the Faculty of Science and Technology, Thammasat University, Contract No.TB 4/2563. I am grateful to the Department of Chemistry, Thammasat University for providing all equipment and chemicals.

Finally, I would like to give many thanks to my family and friends for supporting me, encouraging me, and helping me with everything.

Nattawat Bawornnithichaiyakul

TABLE OF CONTENTS

	Page
ABSTRACT	(1)
ACKNOWLEDGEMENTS	(3)
LIST OF TABLES	(11)
LIST OF FIGURES	(12)
LIST OF ABBREVIATIONS	(15)
CHAPTER 1 INTRODUCTION	1
1.1 Rationale of the research study	1
1.2 Objectives	3
1.3 Scope of research	4
1.3.1 Lab-made spectrometer	4
1.3.2 Roadside test kit	4
CHAPTER 2 REVIEW OF LITERATURE	5
2.1 Spectrophotometer	5
2.2 Lab-made spectrometer	6
2.3 Colorimetric detection of TCH	11
2.4 Colorimetric detection of MSG	16
2.5 Microfluidic paper-based device for colorimetric detection of THC and EtOH	19
2.6 Simultaneous determination of EtOH and THC	23

2.7 Capillary-driven microfluidic paper-based device	23
2.8 Commercial test kit for detection of THC and ethanol	28
CHAPTER 3 RESEARCH METHODOLOGY	38
3.1 Chemicals	38
3.2 Lab-made spectrometer for detection of TCH and MSG	40
3.2.1 Reagent preparation	40
3.2.1.1 Preparation of acetate buffer pH 2.5	40
3.2.1.2 Preparation of Fe(III) (1.00×10^{-2} mol L ⁻¹)	40
3.2.1.3 Preparation of Cu(II) (6.26×10^{-2} mol L ⁻¹)	40
3.2.2 Standard solution	40
3.2.2.1 Stock standard solution of TCH (1.00×10^{-3} mol L ⁻¹)	41
3.2.2.2 Stock standard solution of MSG (5.91×10^{-2} mol L ⁻¹)	41
3.2.3 Sample preparation	41
3.2.3.1 Sample preparation for TCH determination	41
3.2.3.2 Sample preparation for MSG determination	41
3.2.4 Equipment	41
3.2.5 Design and assembly	41
3.2.6 Calibrate a lab-made spectrometer with a commercial spectrophotometer	43
3.2.7 Apply lab-made spectrometer to determine TCH in pharmaceuticals and MSG in flavor enhancers	44
3.2.7.1 Study spectrum of the complexes	45
3.2.7.2 Reaction time and stability	45
3.2.7.3 Stoichiometric study of the complex	45
3.2.7.4 Optimization	46
3.2.7.5 Some analytical features	47

3.3 Roadside test kit using the capillary-driven microfluidic paper-based device for the simultaneous colorimetric detection of THC and ethanol in artificial saliva samples	49
3.3.1 Reagents	49
3.3.1.1 Preparation of potassium dichromate (0.400 mol L^{-1})	49
3.3.1.2 Preparation of fast blue B salt (2.0 %w/v)	49
3.3.2 Standard solutions	49
3.3.2.1 Standard solution of THC (1, 10, 100, 1000 mg L^{-1})	49
3.3.2.2 Standard solution of EtOH (1.00 %v/v)	50
3.3.3 Synthetic saliva	50
3.3.3.1 Preparation of synthetic saliva (1.17 %SCMC)	50
3.3.3.2 Preparation of synthetic saliva (0.10, 0.25, 0.50, 1.00 %SCMC)	50
3.3.4 Ion and compounds for interference test	50
3.3.4.1 Preparation of HCO_3^- , Na^+ (80.0 mmol L^{-1}) in the synthetic saliva	50
3.3.4.2 Preparation of SCN^- (2.00 mmol L^{-1}) in 1.17% of the synthetic saliva	51
3.3.4.3 Preparation of Ca^{2+} (4.00 mmol L^{-1}) in the synthetic saliva	51
3.3.4.4 Preparation of K^+ , Cl^- (4.00 mmol L^{-1}) in the synthetic saliva	51
3.3.4.5 Preparation of Mg^{2+} ($0.200 \text{ mmol L}^{-1}$) in the synthetic saliva	51
3.3.4.6 Preparation of PO_4^{3-} (4.00 mmol L^{-1}) in the synthetic saliva	51
3.3.4.7 Preparation of glucose ($0.250 \text{ mmol L}^{-1}$) in the synthetic saliva	51
3.3.4.8 Preparation of sucrose ($5.00 \times 10^{-2} \text{ mmol L}^{-1}$) in the synthetic saliva	51

3.3.4.9 Preparation of ascorbic acid (1.00×10^{-2} mmol L ⁻¹) in the synthetic saliva	52
3.3.5 Design of a capillary-driven microfluidic paper-based device	52
3.3.6 Preparation of a capillary-driven microfluidic paper-based device for the detection of ethanol and THC	54
3.3.7 The operation of the capillary-driven microfluidic paper-based device for colorimetric detection of THC and ethanol in artificial saliva samples	55
3.3.8 Flow behavior of synthetic salivas with varying viscosity	56
3.3.9 The effect of viscosity of synthetic salivas for colorimetric detection	56
3.3.10 Optimization parts	56
3.3.10.1 Channel thickness	56
3.3.10.2 Channel width	57
3.3.10.3 Sample volume	57
3.3.10.4 Concentration of dichromate	58
3.3.10.5 The reaction time for the colorimetric detection of ethanol	58
3.3.10.6 The volume of fast blue B salt reagent	58
3.3.10.7 The reaction time for colorimetric detection of THC	59
3.3.11 Analytical performance	59
3.3.11.1 Linearity	59
3.3.11.2 Limit of detection (LOD)	60
3.3.11.3 Precision	60
3.3.11.4 Stability	61
3.3.11.5 Interference	62
3.3.12 Feasibility of the developed device for simultaneous detection of ethanol and THC	63
3.3.12.1 Cross-talk between ethanol and THC	63

3.3.12.2 Recovery	64
CHAPTER 4 RESULTS AND DISCUSSION	65
4.1 Lab-made spectrometer	65
4.1.1 Design and assembly of laser-LDR spectrometer	65
4.1.2 The relationship between signal (resistance, ohm) and transmittance	67
4.2 Application of blue laser-LDR spectrometer	70
4.2.1 Spectrum of the complex solution	70
4.2.2 Reaction time and stability	70
4.2.3 Stoichiometric ratio	71
4.2.4 Optimization	73
4.2.4.1 Stability of signal	73
4.2.4.2 Effect of pH	73
4.2.4.3 Concentration of Fe(III)	74
4.2.5 Some analytical features	74
4.2.5.1 Linearity	74
4.2.5.2 Limit of detection (LOD) and limit of quantification (LOQ)	75
4.2.5.3 Precision and Accuracy	76
4.2.6 Application	77
4.3 Red laser-LDR spectrometer for determination of MSG	78
4.3.1 Absorption spectrum of complex	78
4.3.2 Reaction time and stability	78
4.3.3 Stoichiometric ratio	79
4.3.4 Optimization	81
4.2.4.1 Effect of Cu(II)	81
4.3.5 Some analytical features	82
4.3.5.1 Linearity	82

4.3.5.2 Limit of detection (LOD) and limit of quantification (LOQ)	83
4.3.5.3 Precision and Accuracy	83
4.3.6 Application	84
4.4 Roadside test kit using the capillary-driven microfluidic paper-based device for the simultaneous colorimetric detection of THC and ethanol in synthetic saliva samples	85
4.4.1 Flow behavior of synthetic salivas with varying viscosity	85
4.4.2 The effect of viscosity of synthetic salivas for colorimetric detection	86
4.4.3 Optimization of the device design	87
4.4.3.1 Channel thickness	87
4.4.3.2 Channel width	88
4.4.4 Optimization of the assay condition	89
4.4.4.1 Sample volume	89
4.4.4.2 Concentration of dichromate	90
4.4.4.3 Reaction time of colorimetric detection of ethanol	91
4.4.4.4 Reagent volume of fast blue B salt	92
4.4.4.5 Reaction time of colorimetric detection of THC	93
4.4.5 Some Analytical Features	94
4.4.5.1 Linearity	94
4.4.5.2 Limit of detection (LOD)	95
4.4.5.3 Reproducibility	98
4.4.6 Stability	98
4.4.7 Interference study	99
4.4.7.1 Interference study for ethanol detection	100
4.4.7.2 Interference study for THC detection	101
4.4.8 Feasibility of developed device for simultaneous detection of ethanol and THC	102
4.4.9 Recovery	103

	(10)
CHAPTER 5 CONCLUSIONS AND RECOMMENDATIONS	107
5.1 Lab-made spectrometer	107
5.2 The capillary-driven microfluidic paper-based device	108
REFERENCES	109
BIOGRAPHY	125



LIST OF TABLES

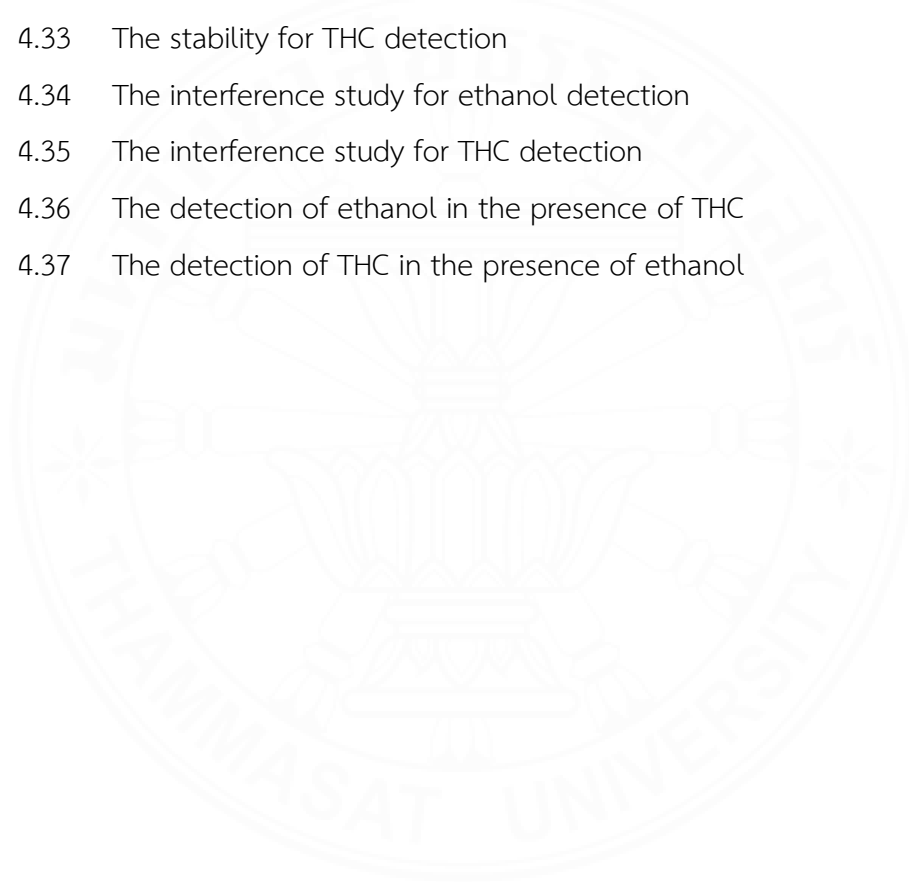
Tables	Page
2.1 The review of the lab-made spectrometer for educational application	7
2.2 The review of the determination of tetracycline hydrochloride	12
2.3 The review of the research that uses colorimetric reaction for the detection of TCH	14
2.4 The review of MSG determination	16
2.5 The review of colorimetric reaction for detection of MSG in food	18
2.6 The review of paper-based platforms with colorimetric detection of THC	21
2.7 The review of paper-based platforms with colorimetric detection of EtOH	22
2.8 The review of a capillary-driven microfluidic device with μ PAD	25
2.9 The review of commercial test kit for the detection of THC	30
2.10 The review of the commercial test kit for the detection of EtOH	32
2.11 The review of commercial test kit for the detection of THC and EtOH	36
3.1 List of all chemicals used in this research	38
4.1 The recovery studies of TCH	76
4.2 Assay of TCH in samples	77
4.3 The recovery studies of MSG	83
4.4 The amount of MSG in samples	84
4.5 The determination of EtOH and THC in saliva	97
4.6 The concentration of common ions and compounds in human saliva	99
4.7 The feasibility of simultaneous detection of EtOH and THC	105

LIST OF FIGURES

Figures		Page
3.1	The complex reaction between Fe(III) and TCH	42
3.2	The complex reaction between Cu(II) and MSG	42
3.3	The design of a lab-made spectrometer and its arrangement: A: a lab-made spectrometer using a blue laser pointer, B: a black box.	43
3.4	The preparation of a cuvette that is fitted with car film	44
3.5	Cuvettes fixed with sun protection film	44
3.6	(a) a schematic and (b) components of the capillary-driven microfluidic paper-based device.	53
3.7	The fabrication of the capillary-driven microfluidic paper- based device	53
3.8	The preparation of paper-based devices before laminating	54
3.9	The paper-based device is assembled with a capillary-driven microfluidic channel	54
3.10	The operation of a proposed microfluidic device for colorimetric detection of THC and ethanol in a synthetic saliva sample	55
4.1	The design and the invention of the blue laser-LDR spectrometer	65
4.2	The design and the invention of the red laser-LDR spectrometer	66
4.3	The design and the invention of the green laser-LDR spectrometer	66
4.4	The setup of a multimeter outside the black box	68
4.5	The linear graph of log R vs. absorbance at 405 nm (blue laser-LDR spectrometer)	68

4.6	The linear graph of log R vs. absorbance at 650 nm (red laser-LDR spectrometer)	69
4.7	The linear graph of log R vs. absorbance at 532 nm (green laser-LDR spectrometer)	69
4.8	The absorption spectrum of Fe-TCH complex	70
4.9	Reaction time and stability of complex between Fe(III) and TCH	71
4.10	Job's method, a graph represents log R as a function of mole fraction of TCH	72
4.11	Mole ratio method, a graph represents log R as a function of mole ratio (TCH: Fe)	72
4.12	Effect of pH of acetate buffer	73
4.13	Effect of concentrations of Fe(III)	74
4.14	The linear graph of the laser-based spectrometer and spectrophotometer for determination of TCH	75
4.15	The absorption spectrum of Cu-MSG	78
4.16	The reaction time and stability of complex between Cu(II) and MSG	79
4.17	Job's method, a graph represents log R as a function of the mole fraction of Cu(II)	80
4.18	Mole ratio method, a graph represents log R as a function of mole ratio (MSG: Cu)	80
4.19	Effect of concentrations of Cu(II)	81
4.20	The linear graph of the laser-based spectrometer and spectrophotometer for determination of MSG	82
4.21	The effect of viscosity on time to reach the detection zone	86
4.22	The effect of viscosity on the delta blue intensity of ethanol	87
4.23	The optimization of channel thickness	88
4.24	The optimization of channel width	89
4.25	The optimization of sample volume	90

4.26	The optimization concentration of dichromate	91
4.27	The optimization of the reaction time of ethanol	92
4.28	The optimization of reagent volume of fast blue B salt	93
4.29	The optimization of the reaction time of THC	94
4.30	The calibration curve of ethanol	95
4.31	The calibration curve of THC	95
4.32	The stability study for ethanol detection	98
4.33	The stability for THC detection	99
4.34	The interference study for ethanol detection	101
4.35	The interference study for THC detection	102
4.36	The detection of ethanol in the presence of THC	103
4.37	The detection of THC in the presence of ethanol	103



LIST OF ABBREVIATIONS

Symbols/Abbreviations	Terms
%BAC	Percentage of blood alcohol concentration
%RSD	The percentage relative standard deviation
%v/v	Volume/volume percentage
%VLT	Percentage of visible light transmission
%w/v	Weight/volume percentage
(FeNO ₃) ₃ .9H ₂ O	Iron (III) nitrate nonahydrate
°C	Degree Celsius
μ	The viscosity of the solution
μL	Micro liter
A	Absorbance
ABTS	3-ethylbenzothiazoline-6-sulfonic acid
B	Path length
BLMB	N-benzoyl leucomethylene blue
C	Concentration
Cap	Capsule
CDs	Carbon dots
Cm	Centimeters
COVID	Coronavirus disease
c-P4VB	Carboxy-bis(4-pyridyl)dineopentoxyl-p-phenylenedivinylene
CTAB	Cetyltrimethylammonium bromide
CuNCs	Copper nanoclusters
DG	Diffraction grating
D _H	Hydraulic diameter

Symbols/Abbreviations

Terms

DNPH	Dinitrophenylhydrazine
ePAD	Electrochemical paper-based analytical device
EtOH	Ethanol
FBBBS	Fast blue BB salt
FBBS	Fast blue B salt
FBRRS	Fast blue RR salt
HRP	Anti-THC-horseradish peroxidase
I	Intensity of light transmitted the sample
I_0	Intensity of light transmitted the reference
iOS	iPhone operating system
L	Liter
LDR	Light dependence resistor
LED	Light emitting diode
LOD	Limit of detection
LOQ	Limit of quantification
M	Milli
Mg	Milligrams
Min	Minute
MSG	Monosodium glutamate
N	Nano
θ	The contact angle
PAD	Paper-based analytical device
PMMA	Poly(methyl methacrylate)
R	Resistance (ohm)
S	The slope of the calibration curve

Symbols/Abbreviations**Terms**

SCMC	Sodium carboxymethyl cellulose
T	Transmittance
T	Time
TCH	Tetracycline hydrochloride
THC	Delta-9-tetrahydrocannabinol
TLC	Thin-layer chromatography
USP	United States Pharmacopeia
UV	Ultraviolet
W	Watt
Z	The distance of the interface from the inlet
Γ	Surface tension between liquid and air
E	Molar absorptivity
Λ	The wavelength
λ_{\max}	The wavelength at which a substance has its strongest photon absorption
μ PADs	Microfluidic paper-based devices
Σ	The standard deviation of the blank solution

CHAPTER 1

INTRODUCTION

1.1 Rationale of the research study

Colorimetric detection is a widely employed analytical technique that relies on measuring color changes to determine the concentration of a target analyte in a sample. One of the most commonly utilized instruments based on the principles of absorption and transmission is the UV-visible spectrophotometer. Spectrometer offers several advantages: simplicity, sensitivity, and good performance. It enables rapid and accurate analysis, making it suitable for a wide range of applications in various fields. However, a general spectrometer or spectrophotometer is enormous and cannot be held in one hand as portable equipment; it is unsuitable for field analysis. It is not only limited in terms of on-site analysis but is also too expensive to make it available for every student, especially for lab-in-house study during the COVID crisis.

Several lab-made or homemade or lab-made spectrometers were constructed using various materials and simple components. Some spectrometers utilize smartphones for light intensity detection. The trend to invent lab-made spectrometers is going to increase with the development of microelectronics, digital cameras, and smartphones. Especially in the COVID crisis in 2020-2022, an online learning chemistry laboratory is necessary, and simple tools and experiments are preferred in this situation. Furthermore, they can be integrated into small projects to determine some analytes in food, pharmaceuticals, and environmental samples.

Tetracycline hydrochloride (TCH) is an antibiotic with anti-inflammatory, immune-modulating, and neuroprotective effects. Nevertheless, TCH has side effects such as nausea, vomiting, photosensitizing, diarrhea, allergic reactions, and reduced appetite. There are several techniques to determine the amount of TCH in pharmaceuticals, such as high-performance liquid chromatography, electrophoresis, and spectrophotometry. All these instruments provided a low detection limit with good

sensitivity, precision, and accuracy. However, these instruments are expensive and huge, which makes them unsuitable for field analysis. Some colorimetric reagents for TCH analysis are toxic and not suitable to apply in the lab at home.

Monosodium glutamate (MSG) is a flavor-enhancing food additive. However, some foods contain large amounts of MSG. Some people are irritated by MSG and get the effect of “Chinese restaurant syndrome.” Therefore, several techniques, such as chromatography and spectrophotometer, were used to determine MSG in food and food enhancers, which required expensive instruments and some toxic chemicals. Therefore, they are unsuitable for field analysis and as an experiment at home.

Besides on-site colorimetric sensing platforms, microfluidic paper-based devices (μ PADs) with colorimetric detection have emerged as innovative platforms combining the advantages of microfluidics and paper technology for various analytical applications. These devices represent a microfluidic system that utilizes porous paper as the substrate for fluid manipulation and analysis. The fluid flow is controlled by the capillary action of the cellulose fiber, eliminating the need for external pumps or power sources. The key advantages of μ PADs include their low cost, simplicity, minimal sample volume requirement, and rapidity. These devices can rapidly and visually detect target analytes by integrating colorimetric detection approaches, such as using color-changing reagents. The colorimetric μ PADs offer numerous benefits, including affordability, portability, qualitative and semi-quantitative results, and rapid analysis time. Moreover, these devices provide a user-friendly and accessible platform for conducting rapid on-site analysis without complex instrumentation. Consequently, the paper-based colorimetric device can serve as an effective on-site detection platform for various applications.

Colorimetric paper-based devices for saliva detection have emerged as a promising tool for non-invasive and rapid analysis of various biomarkers, thanks to the advantages offered by paper-based platforms. However, due to the high viscosity of saliva samples, a sample pretreatment step is still necessary before colorimetric

detection on these devices. Capillary-driven microfluidic technology has been integrated with paper-based platforms to address this issue.

A capillary-driven microfluidic paper-based device utilizes capillary forces to manipulate fluids within microchannels. The passive flow of fluids is achieved through the interaction between the fluid and the surface tension of the microchannel walls, resulting in the generation of capillary forces. This integration overcomes the challenges posed by high-viscosity samples, eliminating the need for a pretreatment step. The benefits of a capillary-driven microfluidic paper-based device are rapid analysis, portability, cost-effectiveness, and the capability to detect high-viscosity samples without requiring additional pretreatment steps. These exploits make them ideal for point-of-care applications, home testing, roadside testing, and resource-limited settings.

Alcohol and cannabis, being the most commonly used psychoactive drugs, are frequently used together. The growing concern lies in the rise of driving under the influence of both substances, as their combined effect can be synergistic or additive. To mitigate the risk of fatal road accidents caused by drivers who have consumed a combination of alcohol and cannabis, there is an urgent need to develop non-invasive, rapid, accurate, and simple roadside tests capable of detecting tetrahydrocannabinol (THC) and alcohol. Thus, integrating a capillary-driven microfluidic channel with a paper-based device for saliva analysis can serve as an ideal sensing platform for roadside testing, enabling the detection of THC and alcohol.

1.2 Objectives

- To design and invent a lab-made spectrometer using a laser pointer, LDR and multimeter, then calibrate with a commercial spectrometer.

- To apply the designed lab-made spectrometer for the determination of tetracycline (TCH) in pharmaceuticals and monosodium glutamate (MSG) in flavor enhancers, compared to a commercial spectrometer for the experiment examples for students.

- To design and invent a roadside test kit using a capillary-driven microfluidic channel integrated with a paper-based device for simultaneous colorimetric detection of THC and EtoH in artificial saliva samples

1.3 Scope of research

1.3.1 Lab-made spectrometer (laser pointer)

- Design and fabricate a lab-made spectrometer based on a laser pointer, LDR and multi-meter
- Calibrate the design equipment with a commercial spectrometer using sun-protective car films.
- Apply to determine TCH in pharmaceuticals and MSG in flavor enhancers based on colorimetric reaction after optimization and method validation process.

1.3.2 Roadside test kit

- Design and fabricate a capillary-driven microfluidic paper-based device.
- Study about optimization of the device design and colorimetric reaction and some analytical features
- Detecting both THC and EtOH in artificial saliva samples

CHAPTER 2

REVIEW OF LITERATURE

2.1 Spectrophotometer

A spectrophotometer is a scientific instrument used to measure light intensity at various wavelengths, allowing for the analysis of the absorption, transmission, and reflection of light by a sample. It is commonly used in various fields, including chemistry, biochemistry, physics, and environmental science. The instrument consists of a light source, a monochromator to separate the light into its different wavelengths, a sample holder, and a detector to measure light intensity. The sample is placed in the sample holder, and the light source emits a broad range of wavelengths covering the visible or ultraviolet (UV) range. The monochromator allows only a specific wavelength or a narrow range of wavelengths to pass through the sample. The light that passes through the sample is then detected by a photodetector, which converts the light into an electrical signal. The light that passes through the sample is then detected by a photodetector, which converts the light into an electrical signal. The intensity of the detected light is proportional to the amount of light absorbed, and “I and I₀” refer to the intensity of light transmitted the sample and reference, respectively, whereas “T” is transmittance, and “A” is absorbance, following the Beer’s Law;

$$A = -\log T = -\log I/I_0$$

$$A = \epsilon bC$$

“ ϵ ”, “b”, and “C” refer to molar absorptivity, pathlength, and concentration (Molar unit). However, if the unit of concentration is not a molar, the equation will use “E” (Extinction coefficient) instead of “ ϵ ” (Driscoll, 1969). There are a large number of researches utilizing spectrophotometers with colorimetric detection to determine the amount of analyte in various areas such as agriculture (Haché, Shibusawa, Sasao, Suhama, & Sah, 2007; McCaig, 2002; H. Yang, 2011), foods (Altunay, Elik, Tuzen, Lanjwani, & Mogaddam, 2023; Chapman, Gangadoo, Truong, & Cozzolino, 2019),

environments (Al Momani & Örmeci, 2014; Kawamura, Nagayoshi, & Yao, 2010; Wang & Hsieh, 2001), pharmaceuticals, and forensics (Bourquin & Brenneisen, 1987; Lo, Donahue, & Brown, 1993; Paiva, Ribessi, Pereira, & Rohwedder, 2020).

2.2 Lab-made spectrometer

Although commercial spectrometers will provide good sensitivity and reliability, the drawbacks are the high cost and the large size, especially since they are not suitable for application to a large number of students in laboratory classes both in school and university. A lab-made spectrometer is an alternative built or assembled by students using common materials or readily available components.

Several lab-made or home-made spectrometers were constructed using various materials and simple components such as a monochromatic light source (such as LED and laser, no need for wavelength selector) and a detector to detect and measure the intensity of light, such as a photodiode, light dependence resistor (LDR). Moreover, several spectrometers utilized smartphones to detect light intensity (Kovarik, Clapis, & Romano-Pringle, 2020). The benefits of a lab-made spectrometer are reduced cost, the size of instruments, and the complications of the invention. So, it is suitable for small projects of students in invention and utilized for onsite analysis.

A significant amount of research utilizes a lab-made spectrometer for many applications, including educational support, as shown in **Table 2.1**. Project-based learning and context-based learning approaches were implemented with students. The primary advantage of lab-made spectrometers for academic support is their affordability, enabling students to construct them independently and better understand a spectrophotometer's fundamental components. By conducting experiments and following instructions, students could understand the principles of the Beer-Lambert law. The learning outcomes were assessed through questioning and evaluating the students' experimental results.

Table 2.1

The review of the lab-made spectrometer for educational application.

Subject	Lab-made spectrometer	Learning outcome	Educational level	Reference
General chemistry	LED, Transmission diffraction-grating (DG) foils (1,000 lines/inch), Cuvette, Camera	Basic spectrometry (Absorption/fluorescence) Beer's law (Viking Spectrophotometer)	High school	(Kolesnichenko, Eriksson, Lindh, Zigmantas, & Uhlig, 2023)
General chemistry	LED, collimator lens, a slit, transmissive diffraction grating, cuvette, photodiode and Raspberry Pi (RPi)	Enhance the confidence of students to troubleshoot unexpected results, and students gain the actual ability to reconstruct the working principles of a light spectrophotometer	Undergraduate	(Chng & Patuwo, 2021)

Table 2.1

The review of the lab-made spectrometer for educational application. (Cont.)

Subject	Lab-made spectrometer	Learning outcome	Educational level	Reference
General chemistry Physical chemistry	LED, slit, lens, grating, webcam Lego for housing and fixing	Beer's law, Quantitative Absorption/fluorescence, Spectral	Undergraduate	(Lietard et al., 2021)
General chemistry	Camera of smartphone or computer RGB	To understand the concept of acid-base, titration, pH measurement, buffer, van't hoff analysis	Undergraduate	(Andrews et al., 2020)
General chemistry	LED, plastic cuvette, LDR, multimeter	To understand the concepts of the Beer-Lambert law through experimental work, comprehend the	High school	(O'Donoghue, 2019)

Table 2.1

The review of the lab-made spectrometer for educational application. (Cont.)

Subject	Lab-made spectrometer	Learning outcome	Educational level	Reference
		components of a spectrophotometer, and recognize the correlation between colorimetry and its practical applications in the real world.		
General chemistry	LED, UV cuvette, millivolt meter	To understand the concept of UV-photometer, Beer-Lambert law. To construct the simple UV-photometer	Undergraduate, teacher training students	(Kvittingen, Kvittingen, Sjursnes, & Verley, 2016)
General chemistry	Computer with a color screen, a transparent	To understand the concepts and equations	High school	(Kuntzleman & Jacobson, 2016)

Table 2.1

The review of the lab-made spectrometer for educational application. (Cont.)

Subject	Lab-made spectrometer	Learning outcome	Educational level	Reference
	cup, smartphone, RGB analyzer program	involved in absorption spectrometry.		
General chemistry	LED, diffraction grating, cuvette, smartphone, ImageJ program.	To understand the relationship of light and wavelength, converting image to spectrum, pixel calibration, resolution and the Beer-Lambert law.	High school	(Grasse, Torcasio, & Smith, 2016)

2.3 Colorimetric detection of TCH

Tetracycline hydrochloride (TCH) is an antibiotic medication that belongs to the tetracycline class of drugs. TCH inhibits the growth and reproduction of bacteria by binding to the bacterial ribosomes (Papich, 2021). The advantage of TCH is used to treat various bacterial infections, including respiratory tract infections, urinary tract infections, skin and soft tissue infections, sexually transmitted infections, and certain types of acne. However, the disadvantage of TCH is side effects such as nausea, vomiting, diarrhea, abdominal pain, and the risk of inflammatory bowel disease (Aronson, 2012).

Several techniques were applied to determine the concentration of tetracycline hydrochloride in various samples, as summarized in **Table 2.2**. These techniques offer a low detection limit and wide linearity range; however, the disadvantages are high cost and unsuitable for schools or universities with limited budgets. In an educational setting, specific learning outcomes, such as understanding the Beer-Lambert law, require the observation of colorimetric reactions and the resulting color changes because the visual observation of color changes is often easier for students to understand.

A wide range of research utilizes colorimetric reactions for THC detection, as shown in **Table 2.3**. These colorimetric reactions involve various reagents, such as complexing reagents, nanoparticles, and coupling reagents. Among these options, complexing agents are preferred for educational purposes due to their lower cost and more straightforward reaction.

Table 2.2

The review of the determination of tetracycline hydrochloride

Sample	Detection method	Range (mg L ⁻¹)	LOD (mg L ⁻¹)	Reference
River water	Colorimetric paper-based analytical device with a smartphone	0.38 - 192.36	0.057	(Huy, Nghia, & Lee, 2020)
Milk, liver, and breast meat of chicken	High-performance liquid chromatography	0.065 – 0.8	0.021	(Saridal & Ulusoy, 2019)
Aqueous solution	Fluorescent quenching	0 – 480.9	2.00	(G.-N. Liu et al., 2019)
Milk and serum	Electrochemical aptasensor	7.21×10^{-4} - 1.68	2.16×10^{-4}	(Taghdisi, Danesh, Ramezani, & Abnous, 2016)
Honey and Milk	Time-of-flight mass spectrometer	0.016 – 0.81	0.01	(Xu et al., 2016)
Milk	Capillary electrophoresis	0.027 – 0.25	0.009	(Ibarra, Rodriguez, Miranda, Vega, & Barrado, 2011)

Table 2.2

The review of the determination of tetracycline hydrochloride. **(Cont.)**

Sample	Detection method	Range (mg L ⁻¹)	LOD (mg L ⁻¹)	Reference
Milk and water	High-performance liquid chromatography	0.002 – 0.050	0.0009	(Tsai, Huang, Huang, Hsue, & Chuang, 2009)
Bovine milk and powder milk samples	High-performance liquid chromatography	0.26 - 248	0.267	(Casella & Picerno, 2009)
Milk	Lab on valve	6×10 ⁻³ - 10	2×10 ⁻³	[(M. Yang, Xu, & Wang, 2006)]
Drugs	Flow injection analysis	2.40 - 288.54	10 ng	[(Palaharn, Charoenraks, Wangfuengkanagul, Grudpan, & Chailapakul, 2003)]

Table 2.3

The review of the research that uses colorimetric reaction for the detection of TCH.

Samples	Colorimetric reagent	Detection method	λ_{\max} (nm)	Reference
Milk	Silver nanoparticle	Spectrophotometer	550	(D. Liu, Huang, & Wu, 2022)
Drugs	2,4-dinitrophenylhydrazine (2,4-DNPH) and potassium periodate	Spectrophotometer	488	(Hameedi, 2021)
Drugs	Fe (III)	Spectrophotometer	430	(Senee Kruanetr, 2021)
Drugs	Sodium nitroprusside and hydroxylamine hydrochloride	Spectrophotometer	529	(Hind & Ghadah, 2018)
Drugs	Sulphanilic Acid	Spectrophotometer	403	(Jumaev, Sadiq Hawezy, & Abdullah, 2018)
Drugs	Ferric ammonium sulphate	Spectrophotometer	420	(Bagheri, 2015)
Urine	Gold nanoparticle	Spectrophotometer	526	(Shen, Chen, Li, He, & Li, 2014)
-	Ferric chloride	Spectrophotometer	430	(Burckhardt-Herold et al., 2007)]

2.4 Colorimetric detection of MSG

Monosodium glutamate (MSG) is a flavor-enhancing food additive commonly used in cooking and the food industry. It is the sodium salt of glutamic acid, a naturally occurring amino acid found in various foods. MSG is known for enhancing the savory or umami taste in foods (Henry-Unaeze, 2022). MSG can also be found in various packaged and processed food products, including snacks, canned soups, salad dressings, and ready-made meals. Some individuals may be sensitive or have adverse reactions to MSG. These reactions are referred to as "MSG symptom complex" or "Chinese Restaurant Syndrome." Symptoms can include headache, flushing, sweating, chest tightness, and a sensation of general discomfort. However, scientific research has not consistently found a causal relationship between MSG and these symptoms, and many people can consume MSG without experiencing any adverse effects. The acceptable daily intake of MSG established by European regulations, set at 30 mg/kg body weight, exceeds the level at which no adverse effects are observed. Product labels include specific requirements for proper MSG labeling. Additionally, there is a need for further research to explore the impact of MSG consumption on the human diet (Walker & Lupien, 2000).

There are many techniques for the determination of MSG in various samples, as shown in **Table 2.4**. These techniques provide a low detection limit and a wide linearity range; however, their instruments are high-cost and sophisticated, which is unsuitable in onsite analysis. These instruments are appropriate for high levels of education, such as in the third or fourth year of undergraduate students studying chemistry or related fields.

A wide range of research utilizes colorimetric reactions for MSG detection, as shown in **Table 2.5**. These colorimetric reactions encompass enzymatic, electrophilic aromatic substitutions and complex reactions. However, most of them are complicated, excluding the complexing agent, Cu^{2+} , which is the most straightforward reaction.

Table 2.4

The review of MSG determination.

Sample	Analytical method	Range (mg L ⁻¹)	LOD (mg L ⁻¹)	Reference
Noodles	Spectrofluorometric method	4.230 – 42.28	0.29	(Kamal, El-Malla, Elattar, & Mansour, 2023)
Instant noodles and Chinese salt	Spectrophotometric methods by using ligand exchange complexation	42.23 – 422.78	12.09	(Elattar, Kamal, Mansour, & El-Malla, 2023)
Food	Spectrophotometric method	5 – 35	0.897	(Ali, Hammad, & El-Malla, 2021)
Food	Electrochemical	8.50×10^{-3} – 33.82	5.07×10^{-3}	(Devi et al., 2019)
Chips, taste cubes, sauces, and soups	Liquid chromatography-tandem mass spectrometry	0.005 - 0.2	1.0	(Cebi, Dogan, Olgun, & Sagdic, 2018)
Food	Potentiometric method	1.69×10^{-4} – 1.69	1.69	(Anirudhan & Alexander, 2015)

Table 2.4

The review of MSG determination. **(Cont.)**

Sample	Analytical method	Range (mg L ⁻¹)	LOD (mg L ⁻¹)	Reference
Food	High-performance liquid chromatography	1300 - 10000	5	(Shrestha et al., 2016)
Food	Capillary electrophoresis	2 - 40	0.46	(Aung & Pyell, 2016)
Broths	Flow-batch system with nephelometric measurements	2.8 - 11	0.097	(Acebal, Insausti, Pistonesi, Lista, & Band, 2010)
Flavor enhancers	Spectrophotometric method	447.6 - 1398.6	16.1	(Acebal, Lista, & Fernández Band, 2008)

Table 2.5

The review of colorimetric reaction for detection of MSG in food.

Samples	Colorimetric reagent	Detection method	λ_{\max} (nm)	Reference
Soup powder	N-benzoyl leucomethylene blue (BLMB), horseradish peroxidase and glutamate oxidase	Paper-based microfluidic devices with smartphone detection	-	(Danchana, Iwasaki, Ochiai, Namba, & Kaneta, 2022)
Food	1,2-naphthoquinone-4-sulfonate sodium salt	Spectrophotometer	475	(Ali et al., 2021)
Soup	Copper (II) Nitrate	Spectrophotometer	621	(Marlina, Amran, & Ulianas, 2018)
Food	Glutamate oxidase, peroxidase, 4-aminoantipyrine and phenol	Spectrophotometer	502	(Alnokkari, Mounir, & Zaid, 2013)

2.5 Microfluidic paper-based device for colorimetric detection of THC and EtOH

A microfluidic paper-based analytical device (μ PAD) is a tool that integrates microfluidics with paper-based materials. It is designed to perform chemical and biological analyses using small volumes of liquid samples. μ PADs have gained significant attention due to their simplicity, affordability, and ease of use (Benhabib & Li, 2021). The device comprises a hydrophilic paper substrate as a fluidic channel network. The paper is typically impregnated with hydrophobic barriers or treated with chemical agents to create flow paths. These hydrophobic barriers or channels direct the flow of liquids and samples through the paper matrix. μ PADs can be used for various applications, including medical diagnostics, environmental monitoring, food safety testing, and water quality analysis (Hasanzadeh & Hashemzadeh, 2021). Usually, microfluidic paper-based analytical devices (μ PAD) use with colorimetric detection (Cai, Wu, Xu, & Chen, 2013; Badra Manori Jayawardane, McKelvie, & Kolev, 2015; B. Manori Jayawardane, Wei, McKelvie, & Kolev, 2014; Jiang et al., 2019; Kudo, Maejima, Hiruta, & Citterio, 2020; C. Liu, Gomez, Miao, Cui, & Lee, 2019; M.-M. Liu et al., 2020; Placer, Lavilla, Pena-Pereira, & Bendicho, 2023; Tang et al., 2022; Thongkam & Hemavibool, 2020). A microfluidic paper-based analytical device (μ PAD) with colorimetric detection is a μ PAD that utilizes color-based signals to detect and quantify analytes. This μ PAD is designed to produce a visual color change in response to the presence or concentration of the target analyte (Silva-Neto, Sousa, & Coltro, 2022).

A few research studies utilize microfluidic paper-based devices for the colorimetric detection of THC, as shown in **Table 2.6**. The first study introduces a paper-based immunoassay. In this study, the paper was conjugated with antibodies on the test zone and control zone, specifically Anti-IC Fab and Anti-mouse IgG. When THC is present, it binds to the active site of the Anti-IC Fab antibody. Subsequently, anti-THC-horseradish peroxidase (HRP) binds to THC on the test zone, while on the control zone, anti-THC-HRP binds to the active site of the Anti-mouse IgG antibody. The anti-THC-HRP then reacts with 2,2'-azino-bis(3-ethylbenzothiazoline-6-sulfonic acid) (ABTS) in the presence of hydrogen peroxide, resulting in a green color. The presence of THC

results in a green color in the test zone, while the control zone exhibits a green color regardless of the presence of THC, allowing for visual observation. The second study utilizes a colorimetric reagent called Fast blue B salt (FBB) under basic conditions. When THC is present, it reacts with the FBB reagent and exhibits a red color. The paper with the red color is then extracted in a methanol solution, and the intensity is analyzed using a UV-Vis spectrophotometer. Among these three studies, the colorimetric reaction using the FBB reagent in basic conditions is suitable due to its simplicity and not complicated compared to the first work. Thin-layer chromatography (TLC) is widely used for the separation and identification of cannabinoids, including THC and other cannabinoids (Huang et al., 2022; Y. Liu, Brettell, Victoria, Wood, & Staretz, 2020; Mano-Sousa et al., 2021; Tsujikawa et al., 2022). In this technique, a colorimetric reagent known as a diazonium salt, such as FBB, Fast blue BB salt (FBBB), and Fast blue RR salt (FBRR), is used in basic conditions as a coupling reagent. These diazonium salts react with the phenol ring in THC and other cannabinoids to form color products.

Several research studies utilize microfluidic paper-based devices for the colorimetric detection of EtOH, as shown in **Table 2.7**. These studies employ different types of reagents. The first type is based on the oxidation of metals to observe a color change, using reagents such as potassium dichromate ($K_2Cr_2O_7$) and potassium permanganate ($KMnO_4$). The second type involves the use of the enzyme alcohol oxidase to convert EtOH to hydrogen peroxide (H_2O_2), followed by the protonation of carboxy-bis(4-pyridyl)dineopentoxyl-p-phenylenedivinylene (c-P4VB), resulting in a fluorescent color change from blue to orange (Thungon et al., 2022). The third type is based on ratiometric fluorescence using copper nanoclusters (CuNCs) and carbon dots (CDs). In this approach, EtOH causes the aggregation of CuNCs ($\lambda = 612$ nm) while having little effect on CDs ($\lambda = 445$ nm), allowing for measuring the ratio between the fluorescent intensities at 612 and 445 nm to detect EtOH. Among these reviewed approaches, potassium dichromate is considered suitable as a colorimetric reagent due to its simplicity compared to the second and third approaches.

Table 2.6

The review of paper-based platforms with colorimetric detection of THC.

Samples	Colorimetric reagent	Device detection unit	LOD (mg L ⁻¹)	Reference
Spiked THC in blood and milk	Anti-THC-HRP, ABTS	Naked eye	-	(Solin, Vuoriluoto, Khakalo, & Tammelin, 2023)
Extracted marihuana	FBB, NaOH	UV-Vis spectrophotometer	0.1	(Krishna, Patil, Dixit, Joseph, & Pandey, 2022)
Synthesized THC	FBB, NH ₃	Naked eye	100	(Tsujikawa et al., 2022)
Extracted cannabis	FBBB, NaOH	Smartphone with ImageJ program	5.5	(Huang et al., 2022)
Extracted cannabis	FBB, FBRR, HCl, NH ₄ OH	Photoshop CC 2019 version 20.0.0 and Sci-Chromus® program	-	(Mano-Sousa et al., 2021)
Extracted marihuana and hemp	FBB	TLC visualizer with VisionCATS CAMAG HPTLC SOFTWARE	-	(Y. Liu et al., 2020)

Table 2.7

The review of paper-based platforms with colorimetric detection of EtOH.

Samples	Colorimetric reagent	Device detection unit	LOD (%v/v)	Reference
Alcoholic beverages	$K_2Cr_2O_7$, H_2SO_4	Smartphone with Colorímetro application	1.5	(Caroline Nava Pinheiro, Souza Ferreira, & Gabriel Lucca, 2022)
Vodkas	c-P4VB, alcohol oxidase	Smartphone with RGB program	0.5	(Thungon et al., 2022)
Mice blood	Alcohol oxidase, HRP, ABTS	Digital camera with Image J program	-	(Thepchuay et al., 2020)
Whiskeys	$KMnO_4$, H_2SO_4 , $C_2H_2O_4$ (Oxalic acid)	Naked eye	2.1	(Nogueira et al., 2019)
Alcoholic beverages and pharmaceutical products	$K_2Cr_2O_7$, H_2SO_4	Digital camera with Image J program	-	(Sitanurak et al., 2019)
-	CuNCs, CDs	Spectrofluorometer	-	(Wen et al., 2019)

2.6 Simultaneous determination of EtOH and THC

Although Thailand is the first country in Asia to have decriminalized cannabis, which has led to significant interest in cannabis-based products among people and tourists, the rules and regulations concerning cannabis and its products are unclear. In other countries such as the USA, cannabis and alcohol are popularly used as a combination of psychoactive drugs, and the number of drivers who consume cannabis and alcohol has dramatically increased in recent years (Mishra et al., 2020). On-site analysis of both substances (THC and EtOH) is essential to monitoring drivers for reducing fatal accidents and side effects from both (Mishra et al., 2020) designed and invented a wearable electrochemical ring sensor for rapid road-site testing of salivary THC and alcohol. However, this work needs a sample preparation step due to the viscosity of saliva.

2.7 Capillary-driven microfluidic paper-based device

A capillary-driven microfluidic device is a type of microfluidic system that utilizes capillary action to control the flow of fluids within a network of microchannels or porous materials. It relies on the natural wicking of the materials to drive the fluid movement, eliminating the need for external pumps (Bao & Nagayama, 2023). The advantages of capillary-driven microfluidic devices include their simplicity, low cost, and ease of use, and they can be used with samples without the need for a preparation step. These devices have applications in various fields, including diagnostics, environmental monitoring, chemical analysis, and biological assays. A capillary-driven microfluidic device can be integrated with a paper-based analytical device to incorporate the benefits of both devices, such as fast and low cost. It can be used with viscous samples without needing preparation steps such as saliva.

Table 2.8 presents studies that utilize a capillary-driven microfluidic device with μ PAD. When compared with conventional μ PADs, a capillary-driven microfluidic device with μ PAD can increase flow rates, reduce liquid retention,

minimize sample evaporation, and require a smaller sample volume compared to a paper-based device (Songok & Toivakka, 2016).



Table 2.8

The review of a capillary-driven microfluidic device with μ PAD.

Analyte	Detail	Analysis time	LOD (mg L ⁻¹)	Reference
Ni(II), Cu(II), and Fe(III) in water	The μ PAD was combined with capillary flow-driven microfluidics. The μ PAD consists of five layers of filter paper. The top three layers of the μ PAD were printed using the wax printing technique, while the other two layers serve as waste pads. Capillary flow-driven microfluidics utilizes a transparency film and double-sided adhesive. The device employs dimethylglyoxime, bathocuproine, and bathophenanthroline as colorimetric reagents for the detection of Ni(II), Cu(II), and Fe(III) in water. A smartphone with the ImageJ program serves as the detection unit.	20 min	2 for Ni(II), 0.3 for Cu(II), and 1.1 for Fe(III)	(Aryal, Brack, Alexander, & Henry, 2023)

Table 2.8

The review of a capillary-driven microfluidic device with μ PAD. (Cont.)

Analyte	Detail	Analysis time	LOD (mg L ⁻¹)	Reference
Thiocyanate in saliva	The microcapillary pump paper-based analytical device consists of a colorimetric PAD (cPAD) and an electrochemical PAD (ePAD). Both PADs are printed using the wax printing technique. The cPAD features a hollow capillary, which is created through etching. The colorimetric reagent in the cPAD contains Fe(III), CTAB, and HNO ₃ . The ePAD includes three printed electrodes. The cPAD is placed onto the ePAD to enable analysis. A smartphone with the ImageJ program is utilized as the detection unit.	5 min	11.62	(Pungjunun et al., 2021)
Organophosphate pesticide in foods	The device consists of transparency film, filter paper, and double-sided adhesive. It is a mixing device composed of five layers. The device includes two inlets, two channels, and one outlet connected to a fan-	15 min	1.34×10 ⁻³	(Jang, Carrão, Menger, Moraes de

Table 2.8

The review of a capillary-driven microfluidic device with μ PAD. (Cont.)

Analyte	Detail	Analysis time	LOD (mg L-1)	Reference
	shaped paper layer. The colorimetric reagent used in the device is acetylcholinesterase. A smartphone is used as the detection unit.			Oliveira, & Henry, 2020)
-	The device consists of a paper board coated with TiO ₂ , spacers, and a hydrophobic layer. The hydrophilic channel of this device was created by exposing the paper board to UV radiation using a photo mask. Compare this device with a paper-based device using different liquids that cover a range of surface tensions and viscosities. It has been found that using capillary-driven flow in a closed channel can increase flow rates, reduce liquid retention, minimize sample evaporation, and require a smaller sample volume compared to a paper-based device.	-	-	(Songok & Toivakka, 2016)

2.8 Commercial test kit for detection of THC and EtOH

A test kit is a tool used for qualitative analysis of analytes in a sample, typically observed visually using the naked eye. The test kit provides a binary “yes” or “no” result. A “yes” indicates the presence of the analyte in the sample, typically above the cut-off threshold of the test kit. On the other hand, a “no” means either the analyte's absence or the analyte's presence below the test kit's cut-off threshold. A test kit comprises various components and reagents necessary for a specific test. These components may include sample collection tools, chemical reagents, reaction vessels, test strips, and colorimetric indicators. Test kits are designed to be user-friendly and accessible, intended for individuals without extensive laboratory training. They are developed to provide rapid results within a short timeframe, enabling real-time analysis, such as the detection of COVID-19.

Table 2.9 presents several commercial test kits for the detection of THC. These test kits use the naked eye to observe the test line visually. The detection limits of these kits range from 0.015 to 0.3 mg L⁻¹. Results can be obtained within 5 minutes. All these test kits utilize urine as the sample for testing.

Table 2.10 presents various commercial test kits for the detection of EtOH. These kits can be used for qualitative and semi-quantitative analysis by observing the color change in the test line and comparing it to a color chart to determine the concentration of EtOH. These test kits can detect EtOH in various samples, including urine, breath, saliva, and breast milk. The cutoff thresholds of these kits range from 0.00005% to 0.02% blood alcohol concentration (BAC). Results can be obtained within 5 minutes.

Table 2.11 presents commercial test kits to detect EtOH and THC in saliva samples. These kits offer qualitative and semi-quantitative analysis by observing color changes in the test line and referring to a color chart to determine the concentration of THC and EtOH. The EtOH cutoff provided by these kits is below the legal limit in the USA (0.08 %BAC), while the THC cutoff exceeds the legal limit (0.005 mg L⁻¹). However, it's worth noting that these test kits are relatively expensive, ranging from

318 to 546 baht per test. To address the critical issue of preventing fatal road accidents caused by drivers under the influence of a combination of alcohol and cannabis, there is an urgent need for the development of non-invasive, rapid, accurate, low-cost, and user-friendly roadside tests capable of detecting THC and EtOH.



Table 2.9

The review of commercial test kit for the detection of THC



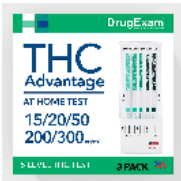
Samples and pictures of the test kit	Detail	Device detection unit	Cutoff (mg L ⁻¹)	Reference
Urine 	Dip the test in urine and read the results in 5 minutes.	Naked eye	0.05	(Amazon, 2023c)
Urine 	Dip the strip in urine, wait 5 minutes, and observe the result.	Naked eye	0.05	(Amazon, 2023d)
Urine 	Remove the cap from the end of the test kit, then dip the test kit in urine and wait until the c line appears. Afterwards, place the cap back on to the test, lay it on a flat surface, and read the results in 5 minutes.	Naked eye	0.015-0.300	(Amazon, 2023b)

Table 2.9

The review of commercial test kit for the detection of THC. (Cont.)




Samples and pictures of the test kit	Detail	Device detection unit	Cutoff (mg L ⁻¹)	Reference
Urine 	Dip the test in urine for 30 seconds and read the results in 5 minutes.	Naked eye	0.015	(Amazon, 2023f)
Urine 	Remove the cap from the end of the test kit and then dip the test kit 30 seconds in urine, place the cap back onto the test, and lay it on a flat surface.	Naked eye	0.015-0.300	(Amazon, 2023e)
Urine 	Remove the cap from the end of the test kit, then dip the test kit in urine and wait until the c line appears. Afterwards, place	Naked eye	0.015	(Amazon, 2023a)

Table 2.9

The review of commercial test kit for the detection of THC. (Cont.)

Samples and pictures of the test kit	Detail	Device detection unit	Cutoff (mg L ⁻¹)	Reference
	the cap back onto the test, lay it on a flat surface, and read the results in 5 minutes.			

Table 2.10

The review of the commercial test kit for the detection of EtOH


Samples and pictures of the test kit	Detail	Device detection unit	Cutoff (%BAC)	Reference
Urine 	Remove the test dipstick from the sealed pouch and ensure it is used within one hour. Dip the test into the urine sample for at least 10-15 seconds. Wait for the colored line(s) to appear. Read the results for 5 minutes.	Naked eye	0.0001	(UK, 2023a)

Table 2.10

The review of the commercial test kit for the detection of EtOH. (Cont.)



Samples and pictures of the test kit	Detail	Device detection unit	Cutoff (%BAC)	Reference
 <p>Breath</p>	<p>Ensure that the test is performed at least 15 minutes after the last alcohol consumption. Take a deep breath and blow into the mouthpiece of the breathalyzer, following the direction indicated by the arrows, for 10 seconds. Compare the test result with the color scale chart located on the side of the breathalyzer within 2 to 4 minutes.</p>	<p>Naked eye</p>	<p>0.02</p>	<p>(UK, 2023c)</p>
 <p>Saliva</p>	<p>Dip the pad in saliva for 8 seconds. After 2 minutes, read the result. Compare the color of the reaction pad with the color chart on the foil pouch to determine the relative blood alcohol level.</p>	<p>Naked eye</p>	<p>0.02</p>	<p>(UK, 2023b)</p>

Table 2.10

The review of the commercial test kit for the detection of EtOH. (Cont.)



Samples and pictures of the test kit	Detail	Device detection unit	Cutoff (%BAC)	Reference
 <p>Breastmilk</p>	<p>Open the foil package and take out the test dipstick. Saturate the reactive pad on the dipstick with breast milk from the collection cup. Wait for 3-5 minutes for the results to appear. Compare the color of the reaction pad on the dipstick with the provided standard color chart to determine the relative alcohol concentration in the breast milk.</p>	<p>Naked eye</p>	<p>0.01</p>	<p>(UK, 2023d)</p>
 <p>Saliva</p>	<p>Dip the pad in saliva. After 2 minutes, read the result. Compare the color of the reaction pad with the color chart provided.</p>	<p>Naked eye</p>	<p>0.02</p>	<p>(UKDrugTesting, 2023c)</p>

Table 2.10

The review of the commercial test kit for the detection of EtOH. (Cont.)


Samples and pictures of the test kit	Detail	Device detection unit	Cutoff (%BAC)	Reference
 <p>Urine</p>	<p>Remove the ETG test strips from the sealed tube. Dip the test strip into the urine for 15-30 seconds. Start a timer for 5 minutes and wait for the colored band to appear. After 5 minutes, check the result.</p>	<p>Naked eye</p>	<p>0.00005</p>	<p>(PharmaDrugTest, 2023)</p>

Table 2.11

The review of commercial test kit for the detection of THC and EtOH.




Samples and pictures of the test kit	Detail	Device detection unit	Cutoff 1.(THC mg L ⁻¹) 2.(%BAC)	Reference
<p>Saliva</p> 	<p>Remove the collector from the sealed pouch. Place the sponge top in your mouth and chew until it becomes soft, usually taking 3-5 minutes. After chewing, place the saturated oral fluid collector into the test cup. Remove the peel-off label from the test cup. Wait for the colored line to appear. Read the results for 10 minutes.</p>	<p>Naked eye</p>	<p>0.012, 0.02</p>	<p>(UKDrugTesting, 2023a)</p>
<p>Saliva</p> 	<p>Wipe the swab tongue collector around the mouth to collect saliva. Ask the donor to release saliva onto the collector, holding it in their mouth. Watch as the drug test membranes start running in the results windows.</p>	<p>Naked eye</p>	<p>0.012, -</p>	<p>(UKDrugTesting, 2023d)</p>

Table 2.11

The review of commercial test kit for the detection of THC and EtOH

Samples and pictures of the test kit	Detail	Device detection unit	Cutoff 1.(THC mg L ⁻¹) 2.(%BAC)	Reference
	Once the control lines have formed, remove the test. Read the result for 5 minutes.			
 <p>Saliva</p>	Remove the collector from the sealed pouch. Ask the donor to release saliva onto the collector, holding it in their mouth. Watch as the drug test membranes start running in the results windows. Once the control lines have formed, remove the test. Read the result for 10 minutes.	Naked eye	0.05, 0.02	(UKDrugTesting, 2023b)

CHAPTER 3

RESEARCH METHODOLOGY

3.1 Chemicals

All chemicals used in this research were of analytical reagents grade. Chemicals and their manufacturer are listed in **Table 3.1**. Type II water was used for all solutions throughout the experiments.

Table 3.1

List of all chemicals used in this research.

Chemicals	Formula	Manufacturer
Iron (III) nitrate nonahydrate	$(\text{FeNO}_3)_3 \cdot 9\text{H}_2\text{O}$	QReC, New Zealand
Acetic acid glacial	CH_3COOH	QReC, New Zealand
Hydrochloric acid, 37 % (w/w)	HCl	RCI Labscan, Thailand
Sodium hydroxide pellets	NaOH	QReC, New Zealand
Nitric acid, 70 % (w/w)	HNO_3	QReC, New Zealand
Sodium acetate anhydrous	$\text{C}_2\text{H}_3\text{NaO}_2$	QReC, New Zealand
Tetracycline hydrochloride	$\text{C}_{22}\text{H}_{24}\text{N}_2\text{O}_8$	Glentham, United Kingdom
Copper(II) sulfate anhydrous	CuSO_4	Merck, Germany
Monosodium glutamate	$\text{C}_5\text{H}_8\text{NO}_4\text{Na}$	Sigma-Aldrich, France

Table 3.1

List of all chemicals used in this research. (Cont.)

Chemicals	Formula	Manufacturer
Potassium dichromate	$K_2Cr_2O_7$	Univar, United State
Sulfuric acid, 98 % (w/w)	H_2SO_4	RCI Labscan, Thailand
Ethanol	C_2H_5OH	Merck, Germany
Methanol	CH_3OH	RCI Labscan, Thailand
FBBS	$C_{14}H_{12}N_4O_2Cl_2 \cdot ZnCl_2$	Univar, United State
Potassium chloride	KCl	Univar, United State
Potassium dihydrogen phosphate	KH_2PO_4	Univar, United State
Dipotassium mono hydrogen phosphate	K_2HPO_4	Rankem, India
Calcium chloride	$CaCl_2$	Kemaus, Australia
Magnesium chloride hexahydrate	$MgCl_2 \cdot 6H_2O$	Ajax Finechem, Australia
Sodium Carboxy Methyl Cellulose	$C_8H_{15}NaO_8$	Univar, United State
Sodium bicarbonate	$NaHCO_3$	Univar, United State

Table 3.1

List of all chemicals used in this research. (Cont.)

Chemicals	Formula	Manufacturer
Potassium thiocyanate	KSCN	Univar, United State
Glucose	C ₆ H ₁₂ O ₆	Carlo Erba German
Sucrose	C ₁₂ H ₂₂ O ₁₁	Univar, United State
Ascorbic	C ₆ H ₈ O ₆	Sigma-Aldrich, France
Sodium dihydrogen phosphate	NaH ₂ PO ₄	M Chemical, United State
Tetrahydrocannabinol	C ₂₁ H ₃₀ O ₂	Pharm GmbH, Thailand

3.2 Lab-made spectrometer for detection of TCH and MSG

3.2.1 Reagent preparation

3.2.1.1 Preparation of acetate buffer pH 2.5

A 0.100 mol L⁻¹ acetate buffer solution was prepared by dissolving 0.062 grams of sodium acetate in 250 mL of water, then adding 1.39 mL of acetic acid and adjusting the pH to 2.5 with 2 mol L⁻¹ hydrochloric acid.

3.2.1.2 Preparation of Fe(III) (0.01 mol L⁻¹)

A 0.010 mol L⁻¹ of Fe(III) solution was prepared by dissolving 0.2020 grams of Iron (III) nitrate nonahydrate in 50.0 mL of 0.1 mol L⁻¹ nitric acid.

3.2.1.3 Preparation of Cu(II) (6.26 × 10⁻² mol L⁻¹)

A solution of 6.26 × 10⁻² mol L⁻¹ of Cu(II) was prepared by dissolving 0.6270 grams of copper (II) sulphate in 25.0 mL of water.

3.2.2 Standard solution

3.2.2.1 Stock standard solution of TCH ($1.0 \times 10^{-3} \text{ mol L}^{-1}$)

Stock standard solution of TCH ($1.0 \times 10^{-3} \text{ mol L}^{-1}$) was prepared by dissolving 0.0240 grams of TCH in 50.0 mL of water.

3.2.2.2 Stock standard solution of MSG ($5.91 \times 10^{-2} \text{ mol L}^{-1}$)

Stock standard solution of MSG ($5.91 \times 10^{-2} \text{ mol L}^{-1}$) was prepared by dissolving 1.0000 grams of MSG in 100.0 mL of water.

3.2.3 Sample preparation

3.2.3.1 Sample preparation for TCH determination

Six brands of TCH capsules were purchased from drugstores in Pathum Thani, Thailand. The powder in 10 capsules of each sample was weighed and mixed, then the mixed powder was accurately weighed equivalent to 250 mg of TCH (0.260 mmol), transferred to a beaker then dissolved in 50.0 mL of water, sonicated for 5 minutes and filtered with Whatman filter paper No.1, and then diluted to 100.0 mL with water. Finally, the sample solutions were diluted 10 times.

3.2.3.2 Sample preparation for MSG determination

Three brands of flavor enhancers were purchased from stores in Pathum Thani, Thailand. Weighed 0.250 grams, dissolved in 10 mL water, and then transferred to a volumetric flask 25.00 mL, making it to volume with DI water.

3.2.4 Equipment

Spectrophotometer (MAPADA, Shanghai), LDR (photoresistor, GL5516, 5 mm, China), laser blue, green, red (405, 532, 650 nm, 5 mW, Newegg, China), multimeter (model UT30D, China and using Banana plug to Alligator clip test cable pair), wood board (size 14.5 × 20 cm), car film (FilmEx, PT-2, 3, 5, 7, 8, 9, 14, 17 with 69, 81, 82, 37, 13, 20, 60, 47 %VLT), plastic cuvette (1 × 1 cm), black box (40 × 40 × 40 cm), Acrylic piece with rectangular shape (1.4 × 1.4 cm).

3.2.5 Design and assembly

The lab-made spectrometer was designed and fabricated to determine TCH and MSG based on complex formation with Fe(III) and Cu(II), subsequently producing red and blue color solutions. The maximum absorption

wavelength of Fe(III)-TCH complex was 420 nm ((Senee Kruanetr, 2021),(Bagheri, 2015),(Burckhardt-Herold et al., 2007)), whereas those of Cu(II)-MSG complex was 621 nm (Marlina et al., 2018), the reactions were shown in **Figure 3.1** and **3.2**.

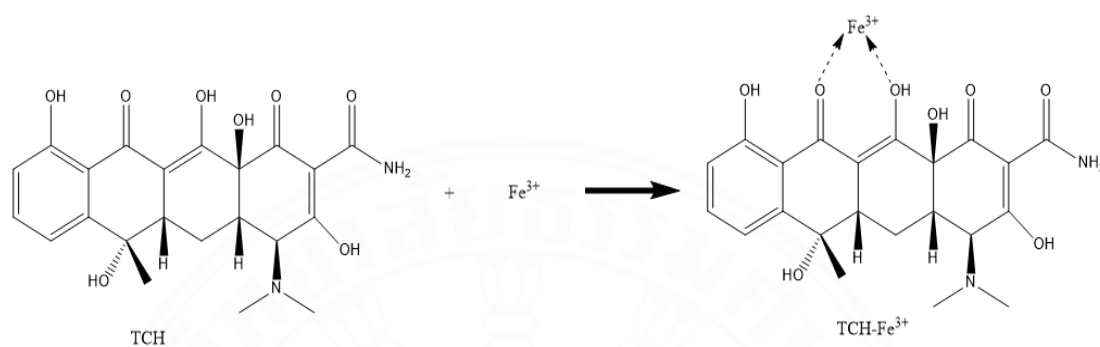


Figure 3.1. The complex reaction between Fe(III) and TCH.

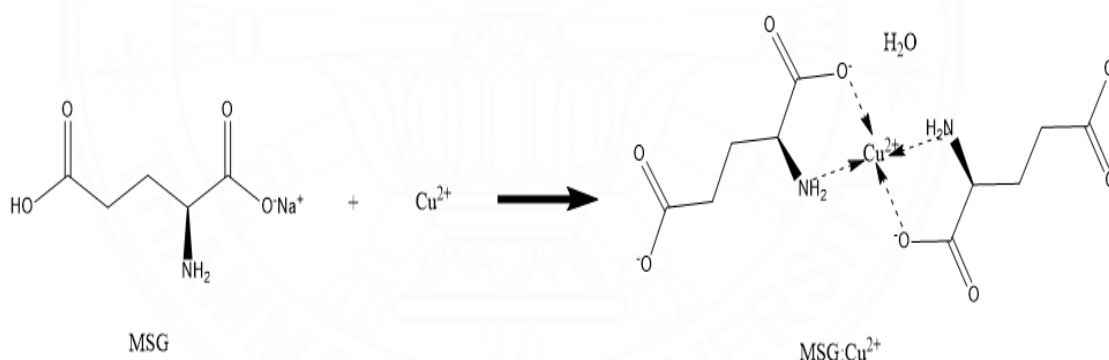


Figure 3.2. The complex reaction between Cu(II) and MSG.

This designed spectrometer is arranged on the wooden cutting board in the following order: 1) laser pointer with clamp holder (as a light source); 2) an acrylic piece with rectangular shape, size 1.4 x 1.4 cm (as a cuvette holder); 3) light dependence resistor, LDR (as a photodetector) and its holder; 4) two electric cables for connecting LDR to the readout; and 5) multimeter (as a readout device). The design of the lab-made spectrometer and its arrangement are shown in **Figure 3.3**. Three different light laser pointers (blue 405 nm, red 650 nm, and green 532 nm) were tested.

The multi-meter displays the resistance readings, providing a means of quantifying the intensity of the light detected by the LDR. The laser pointer clamp, cuvette holder, and LDR holder were fixed on the board using glue.

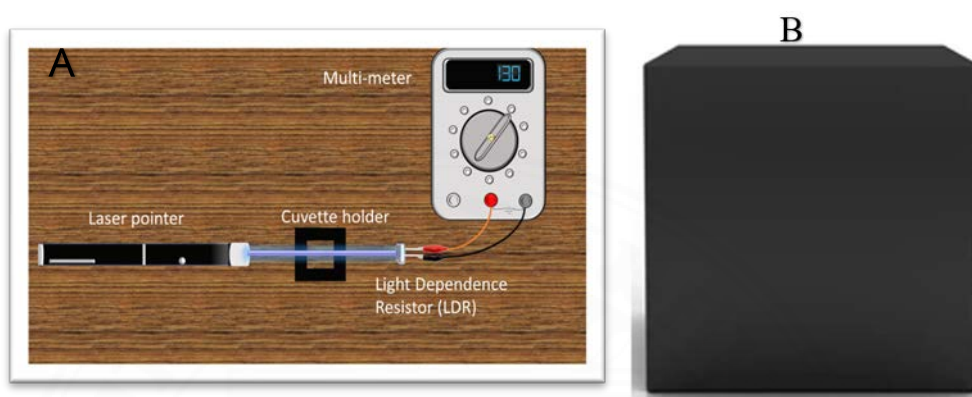


Figure 3.3. The design of a lab-made spectrometer and its arrangement: A: a lab-made spectrometer using a blue laser pointer, B: a black box.

3.2.6 Calibrate a lab-made spectrometer with a commercial spectrophotometer.

Eight pieces of cuvette that were fixed with various car films (10-80 % VLT) were utilized for calibrating the lab-made spectrometer, as shown in **Figure 3.4** and **3.5**. Three lab-made spectrometers (using red, green and blue laser pointers) were tested by measuring the light transmission of the car films (that were fixed on the cuvettes), and the signal was read by multimeter in a unit of resistance (ohm) calibrating to commercial spectrophotometer in the mode of transmittance. The relationship between resistance (lab-made spectrometer) and transmittance (commercial spectrophotometer) was plotted and solved in the linear equation.

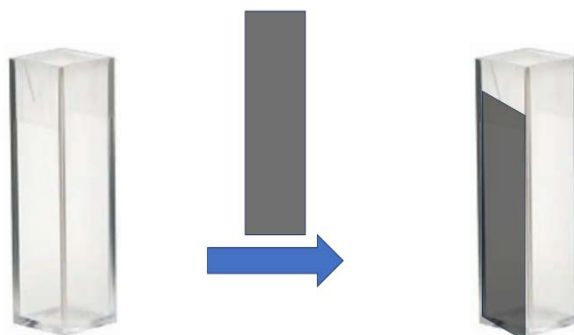


Figure 3.4. The preparation of a cuvette that fitted with car film.

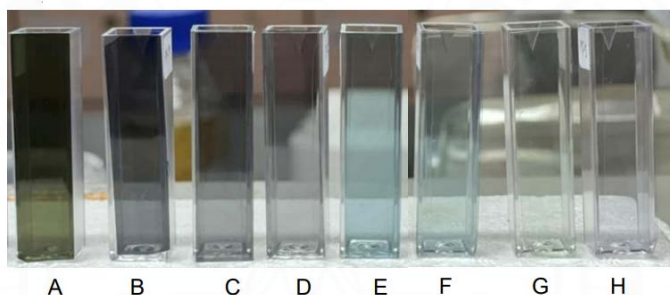


Figure 3.5. Cuvettes fixed with sun protection film (A PT-08:13%VLT, B PT-09: 20%VLT, C PT-07:37%VLT, D PT-17:47%VLT, E PT-14:60%VLT, F PT-12:69%VLT, G PT-03:81%VLT, H PT-05:82%VLT).

3.2.7 Apply lab-made spectrometer to determine TCH in pharmaceuticals and MSG in flavor enhancers.

3.2.7.1 Study spectrum of the complexes

A 1.0-mL of TCH $1.00 \times 10^{-3} \text{ mol L}^{-1}$ was added to a mixture of acetate buffer pH 2.5 8.0 mL, and 1.0 mL of Fe(III) $1.00 \times 10^{-2} \text{ mol L}^{-1}$ solution in a disposable centrifuge tube (15 mL). In the case of MSG-Cu(II) complex, a 3.0-mL of MSG $5.91 \times 10^{-2} \text{ mol L}^{-1}$ was mixed with a 7.0-mL of $6.26 \times 10^{-2} \text{ mol L}^{-1}$ Cu (II) in a disposable centrifuge tube (15 mL). The absorbance of these two complex solutions was measured by UV/Vis Spectrophotometer SHIMADZU UV-1700 from 380 - 600 nm. The maximum wavelengths obtained were used to select a suitable laser.

3.2.7.2 Reaction time and stability

A 1.0-mL of TCH $1.00 \times 10^{-3} \text{ mol L}^{-1}$ was added to a mixture of acetate buffer pH 2.5 8.0 mL, and 1.0 mL of Fe(III) $1.00 \times 10^{-2} \text{ mol L}^{-1}$ solution in a disposable centrifuge tube (15 mL). The solution was shaken and left for 10 min. In the case of MSG-Cu(II) complex, 5.0 mL of MSG $5.91 \times 10^{-2} \text{ mol L}^{-1}$ was mixed with 1.0 mL of $6.26 \times 10^{-2} \text{ mol L}^{-1}$ Cu (II) and 4 mL of water in a disposable centrifuge tube (15 mL). The absorbance of the complex solutions, TCH-Fe (III) and MSG-Cu(II), were measured by spectrophotometer (MAPADA). The absorbance was observed from 0 - 120 minutes.

3.2.7.3 Stoichiometric study of the complex

3.2.7.3.1 Job's method

Into a series of 15.0 mL disposable centrifuge tubes containing 1.80×10^{-6} – 20.0×10^{-6} mol of TCH, aliquots equivalent to 1.80×10^{-6} – 20.0×10^{-6} mol of Fe(III) were accurately transferred from their stock solution ($1.00 \times 10^{-3} \text{ mol L}^{-1}$) to make the total number of moles in each tube 20.0. The tubes were completed to 10.0 mL volume with sodium acetate buffer pH 2.50. Resistance (ohm) was measured by a blue laser-LDR spectrometer. The log R value was plotted against the TCH mole fraction.

Into a series of 15.0 mL disposable centrifuge tubes containing 1.00×10^{-4} – 9.00×10^{-2} mol of MSG, aliquots equivalent to 1.00×10^{-4} – 9.00×10^{-2} mol of Cu(II) were accurately transferred from their stock solution ($1.00 \times 10^{-1} \text{ mol L}^{-1}$) to make the total number of moles in each tube 9.01×10^{-2} mol. Absorbance was measured at 650 nm and plotted against MSG mole fraction. Resistance(ohm) was measured by a red laser-LDR spectrometer. The log R value was plotted against the MSG mole fraction.

3.2.7.3.2 Mole ratio method

Into a series of 15.0 mL centrifuge tubes containing 1.80×10^{-6} of Fe(III), aliquots equivalent to 0.300×10^{-6} – 3.30×10^{-6} mol of TCH were accurately transferred from their stock solution ($1.00 \times 10^{-3} \text{ mol L}^{-1}$). The tubes were completed to 10.0 mL volume with sodium acetate buffer pH 2.50. The absorbance

was measured at 405 nm and plotted against the mole ratio of TCH to Fe(III). Resistance(ohm) was measured by a blue laser-LDR spectrometer. The log R value was plotted against the TCH mole fraction.

Into a series of 15.0 mL centrifuge tubes containing 2.00×10^{-4} mol of Cu(II), aliquots equivalent to 1.00×10^{-4} – 8.00×10^{-4} mol of MSG were accurately transferred from their stock solution (0.1 mol L^{-1}). The tubes were completed to 10.0 mL volume with water. The absorbance was measured at 650 nm and plotted against the mole ratio of MSG to Cu(II). Resistance(ohm) was measured by a red laser-LDR spectrometer. The log R value was plotted against the MSG mole fraction.

3.2.7.4 Optimization

Some parameters were optimized, including the light stability from a laser and the concentration of the reagents. The starting condition for the determination of TCH in pharmaceuticals was $1.00 \times 10^{-3} \text{ mol L}^{-1}$ of TCH standard solution and a reagent of $1.00 \times 10^{-2} \text{ mol L}^{-1}$ Iron (III) nitrate nonahydrate in 0.1 mol L^{-1} nitric acid. The starting condition for the determination of monosodium glutamate in flavor enhancer was $5.91 \times 10^{-2} \text{ mol L}^{-1}$ of MSG standard solution and a reagent of $6.26 \times 10^{-2} \text{ mol L}^{-1}$ Copper (II) sulphate. Log R unit, where R is the ratio of the resistance of complex solution (R1) to the resistance of blank (R0), whereas blank is the solution without analyte and absorbance unit.

3.2.7.4.1 Stability of light from laser

The blue laser-LDR spectrometer and the red laser-LDR spectrometer were used to test the stability of light by turning on the laser. The lights from both lasers are directly illuminated to the LDR. The resistance of both LDRs was measured by a multimeter for 0 - 60 minutes.

3.2.7.4.2 Effect of pH formation complex of Fe(III)-TCH

Each 1.0 mL of TCH $1.00 \times 10^{-3} \text{ mol L}^{-1}$ and Fe(III) $1.0 \times 10^{-2} \text{ mol L}^{-1}$ were mixed in a 10.0 mL volumetric flask and made to volume with acetate buffer pH 0.5 – 3.0 Study the effect of pH by measuring the resistance of each solution. Then, the relationship between log R and pH was plotted.

3.2.7.4.3 Concentration of reagent

1.0 mL of tetracycline hydrochloride 1.00×10^{-3} mol L^{-1} was mixed with $1.25 \times 10^{-3} - 2.50 \times 10^{-2}$ mol L^{-1} of Fe(III) 1.0 mL, then the solutions were adjusted the final volume to 10.0 mL with acetate buffer pH 2.50. The solution was measured to determine the resistance of LDR with the blue laser-LDR spectrometer. The result was plotted between log R and concentrations of Fe(III).

5.0 mL of Monosodium glutamate 5.91×10^{-2} mol L^{-1} was mixed with 6.26×10^{-2} mol L^{-1} of Cu(II) 0.20-3.0 mL, and then the solution was adjusted the final volume to 10.0 mL with water. The solutions were measured to determine the resistance of LDR by the red laser-LDR spectrometer. The result was plotted between log R and concentrations of Cu(III).

3.2.7.5 Some analytical features

3.2.7.5.1 Reaction Procedure

For TCH determination, a standard/sample of 1.0 mL was added to a mixture of acetate buffer 8.0 mL and 1.0 mL of Fe(III) solution (at the optimized condition) in a disposable centrifuge tube (15 mL). The solution was shaken, left for 10.0 min, and then measured by the blue laser-LDR spectrometer and commercial spectrophotometer (MAPADA).

For MSG determination, a standard/sample of 2.0 mL was mixed with 2.0 mL of Cu(II) solution (at optimized condition) and 6.0 mL of water in a disposable centrifuge tube (15 mL). The solution was shaken and measured using a red laser-LDR spectrometer and commercial spectrophotometer (MAPADA).

3.2.7.5.2 Linearity

The linearity of TCH determination was studied in the concentration range 5.74×10^{-6} , 1.15×10^{-5} , 2.30×10^{-5} , 4.59×10^{-5} , 6.89×10^{-5} , 9.18×10^{-5} and 1.15×10^{-4} mol L^{-1} of TCH with three replicate measurements for each concentration. The graph was plotted between TCH concentration and log R.

The linearity of MSG determination was studied in the concentration range 5.91×10^{-3} , 1.18×10^{-2} , 1.77×10^{-2} , 2.37×10^{-2} , 2.96×10^{-2} , 3.55×10^{-2} , 4.14×10^{-2} and 4.73×10^{-2} mol L^{-1} of MSG with three replicate

measurements for each concentration. The graph was plotted between MSG concentration and log R.

3.2.7.5.3 Limit of detection (LOD) and Limit of quantification (LOQ)

The limit of detection and Limit of quantification are calculated by equations $LOD = 3.3\sigma/S$ and $LOQ = 10\sigma/S$, respectively, where σ is the standard deviation of the blank solution, and S is the slope of the calibration curve. Blank of TCH and MSG determinations are reagents of each method.

3.2.7.5.4 Precision

The precision of TCH and MSG determinations were studied in terms of repeatability and reproducibility using ten times measurements and ten bottles of complex solution, respectively, with the concentration 2.30×10^{-5} mol L⁻¹ of TCH and 2.36×10^{-2} mol L⁻¹ of MSG. The obtained log R value was used to calculate the percent relative standard deviation (%RSD).

3.2.7.5.5 Recovery

The recovery of TCH determination in pharmaceutical was evaluated by spiking a standard solution of TCH 0, 1.04×10^{-5} , 2.08×10^{-5} , 3.12×10^{-5} and 4.16×10^{-5} mol L⁻¹ to the sample solution with three replicate measurements for each concentration. Each concentration was calculated by the standard curve to be found amount, and then percentage recovery was evaluated by $\frac{\text{standard found}}{\text{standard added}} \times 100$.

The recovery of MSG determination in flavor enhancer was evaluated by spiking a standard solution of MSG 5.91×10^{-3} , 1.18×10^{-2} , 1.77×10^{-2} and 2.36×10^{-2} mol L⁻¹ into the sample solution with three replicate measurements for each concentration. The % recovery of MSG was calculated as same as the TCH recovery process.

3.2.7.5.6 TCH and MSG determinations in real samples.

For TCH determination, a 1.0 mL sample solution of TCH was pipetted into a 15.0 mL disposable centrifuge tube, the 1.0 mL of Fe(III) solution (0.01 mol L⁻¹) was added, and followed by 8.0 mL of acetate buffer solution

(pH 2.50, 0.10 mol L^{-1}). The solution was measured in the 10 mm cuvette and by the blue laser-based spectrometer, compared to a commercial spectrophotometer (MAPADA, Shanghai) at 405 nm.

For MSG determination, a 2.0 mL sample solution of MSG was pipetted into a 15.0 mL disposable centrifuge tube, the 2.0 mL of Cu(II) solution ($6.26 \times 10^{-2} \text{ mol L}^{-1}$) was added, followed by water until 10.0 mL. The solution was poured in a 10 mm cuvette (PMMA, 10 mm pathlength, 12.5 x 12.5 x 45 mm) and measured by the red laser-based spectrometer, compared to the commercial spectrophotometer (MAPADA, Shanghai) at 405 nm.

The results obtained from the laser-LRD spectrometers were compared to those of commercial spectrometers (MAPADA) using a paired T-test at a 95% confidence level.

3.3 Roadside test kit using the capillary-driven microfluidic paper-based device for the simultaneous colorimetric detection of THC and EtOH in artificial saliva samples.

3.3.1 Reagents

3.3.1.1 Preparation of potassium dichromate (0.4 mol L^{-1})

A solution of 4.0 mol L^{-1} of $\text{K}_2\text{Cr}_2\text{O}_7$ was prepared by dissolving 0.5883 grams of potassium dichromate in 5.0 mL of 4 mol L^{-1} hydrochloric acid.

3.3.1.2 Preparation of fast blue B salt (2.0 %w/v)

A solution of 2.0 %w/v of fast blue B salt was prepared by dissolving 10.0×10^{-2} grams of fast blue B salt in 5.0 mL of absolute methanol. The solution was sonicated 1.5 hr.

3.3.2 Standard solution

3.3.2.1 Standard solution of THC (1, 10, 100, 1000 mg L^{-1})

A standard solution of THC (1000 mg L^{-1}) was prepared by diluting a stock solution of 10000 mg L^{-1} of THC 100 μL in SCMC-based synthetic saliva and adjusting the final volume to 1.00 mL.

A standard solution of THC (100 mg L^{-1}) was prepared by diluting 1000 mg L^{-1} of THC $100 \mu\text{L}$ in SCMC-based synthetic saliva and adjusting the final volume to 1.00 mL .

Stock standard solution of THC (10 mg L^{-1}) was prepared by diluting 100 mg L^{-1} of THC $100 \mu\text{L}$ in SCMC-based synthetic saliva and adjusting the final volume to 1.00 mL .

Stock standard solution of THC (1.00 mg L^{-1}) was prepared by diluting 10.0 mg L^{-1} of THC $100 \mu\text{L}$ in SCMC-based synthetic saliva and adjusting the final volume to 1.00 mL .

3.3.2.2 Standard solution of EtOH (1 %v/v)

A standard solution of EtOH (1.00 %v/v) was prepared by diluting absolute ethanol $10.0 \mu\text{L}$ in SCMC-based synthetic saliva and adjusting the final volume to 1.00 mL .

3.3.3 Synthetic saliva

3.3.3.1 Preparation of synthetic saliva (1.17 %SCMC)

The synthetic saliva (1.17 %w/v SCMC) was prepared by dissolving K_2HPO_4 0.804 gram, KCl 0.625 gram, KH_2PO_4 0.366 gram, CaCl_2 0.166 gram, MgCl_2 5.90×10^{-2} gram and sodium carboxy methyl cellulose 11.7 gram in 1000 mL of water.

3.3.3.2 Preparation of synthetic saliva (0.100, 0.250, 0.500, 1.00 %SCMC)

The synthetic saliva (0.10, 0.25, 0.50, 1.00 %w/v SCMC) was prepared by dissolving K_2HPO_4 0.0804 gram, KCl 0.0625 gram, KH_2PO_4 0.0366 gram, CaCl_2 0.0166 gram, MgCl_2 0.0059 gram and sodium carboxy methyl cellulose 0.10, 0.25, 0.50, 1.00 gram in 100 mL of water, respectively.

3.3.4 Ion for interference test

3.3.4.1 Preparation of HCO_3^- , Na^+ (80.0 mmol L^{-1}) in the synthetic saliva

HCO_3^- , Na^+ (80.0 mmol L^{-1}) in 1.17 %w/v SCMC was prepared by dilute stock solution $79.0 \mu\text{L}$ in 1.00 mL of 1.17 %SCMC-based synthetic saliva.

3.3.4.2 Preparation of SCN^- (2.00 mmol L⁻¹) in 1.17% of the synthetic saliva

SCN^- (2.00 mmol L⁻¹) in 1.17 %w/v SCMC was prepared by dilute stock solution 36.0 μL in 1 mL of 1.17 %SCMC-based synthetic saliva.

3.3.4.3 Preparation of Ca^{2+} (4.00 mmol L⁻¹) in the synthetic saliva

Ca^{2+} (4.00 mmol L⁻¹) in 1.17 %w/v SCMC was prepared by dilute stock solution 74.0 μL in 1.00 mL of 1.17 %SCMC-based synthetic saliva.

3.3.4.4 Preparation of K^+ , Cl^- (100 mmol L⁻¹) in the synthetic saliva

K^+ , Cl^- (100 mmol L⁻¹) in 1.17 %w/v SCMC was prepared by dilute stock solution 97.0 μL in 1.00 mL of 1.17 %SCMC-based synthetic saliva.

3.3.4.5 Preparation of Mg^{2+} (0.200 mmol L⁻¹) in the synthetic saliva

Mg^{2+} (0.200 mmol L⁻¹) in 1.17 %w/v SCMC was prepared by dilute stock solution 26.0 μL in 1.00 mL of 1.17 %SCMC-based synthetic saliva.

3.3.4.6 Preparation of PO_4^{3-} (4.00 mmol L⁻¹) in the synthetic saliva

PO_4^{3-} (4.00 mmol L⁻¹) in 1.17 %w/v SCMC was prepared by dilute stock solution 75.0 μL in 1.00 mL of 1.17 %SCMC-based synthetic saliva.

3.3.4.7 Preparation of glucose (0.250 mmol L⁻¹) in the synthetic saliva

Glucose (0.250 mmol L⁻¹) in 1.17 %w/v SCMC was prepared by dilute stock solution 21.0 μL in 1.00 mL of 1.17 %SCMC-based synthetic saliva.

3.3.4.8 Preparation of sucrose (5.00×10^{-2} mmol L⁻¹) in the synthetic saliva

Sucrose (5.00×10^{-2} mmol L⁻¹) in 1.17 %w/v SCMC was prepared by dilute stock solution 9.00 μL in 1.00 mL of 1.17 %SCMC-based synthetic saliva.

3.3.4.9 Preparation of ascorbic acid (1.00×10^{-2} mmol L⁻¹) in the synthetic saliva

Ascorbic acid (1.00×10^{-2} mmol L⁻¹) in 1.17 %w/v SCMC was prepared by dilute stock solution 12.0 μ L in 1.00 mL of 1.17 %SCMC-based synthetic saliva.

3.3.5 Design of a capillary-driven microfluidic paper-based device

The design of a capillary-driven microfluidic paper-based device is shown in **Figure 3.6**. The overall design consists of two main components: a capillary-driven microfluidic device and a paper-based device. Both components are designed using Adobe Illustrator 2022 software.

The microfluidic channel is a 3.5 \times 2.0 cm device with a top hydrophilic transparency sheet (TPS). Below the transparency film, a flow channel is created by CO₂ laser cutting of three layers of 0.2 mm thick double-sided adhesive (DSA) sheet, 0.1 mm thick TPS, and 0.2 mm thick DSA sheet, respectively. The flow channel within the microfluidic device is 1.6 cm in length, 3.5 mm in width, and 0.5 mm in thickness. The top transparent layer has a 1 cm \times 1 cm sample insertion zone, enabling the solution to the flow channel. Additionally, a reagent insertion zone with a diameter of 1 mm was fabricated for introducing colorimetric reagents into the detection zone. This integration of these designs facilitates the capillary-driven flow of fluids within the microfluidic channel.

The paper-based device is a 3.5 cm \times 2.0 cm device that consists of three folds of Whatman grade 1. The top three layers are the detection pad, reagent pad, and waste pad, respectively. These layers are wax printed using the Xerox ColorQube 8570 printer. When folded, the paper device leaves two 4.5 mm detection zones in each layer, touching each other. To create the hydrophobic barrier of the paper device, the wax-printed paper is then heated by the oven at 120 °C for 45 s, allowing the wax to penetrate entirely into both sides of the paper. With heating, the detection pad size shrunk to 0.4 cm. Then, the three layers of wax paper were folded and attached using laminating with a laminating sheet. The microfluidic channel is then attached to the top of the laminated paper-based device. The sample insertion zone

of the microfluidic channel is connected to the detection zone of the paper device, facilitating the flow of the sample to the detection area, as shown in **Figure 3.7**. This integration ensures proper alignment and interaction between the sample and the detection zones of the paper device.

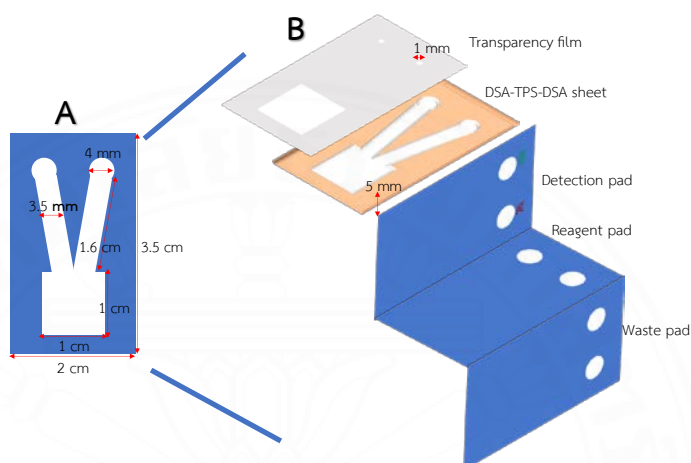


Figure 3.6. (a) a schematic and (b) components of the capillary-driven microfluidic paper-based device.

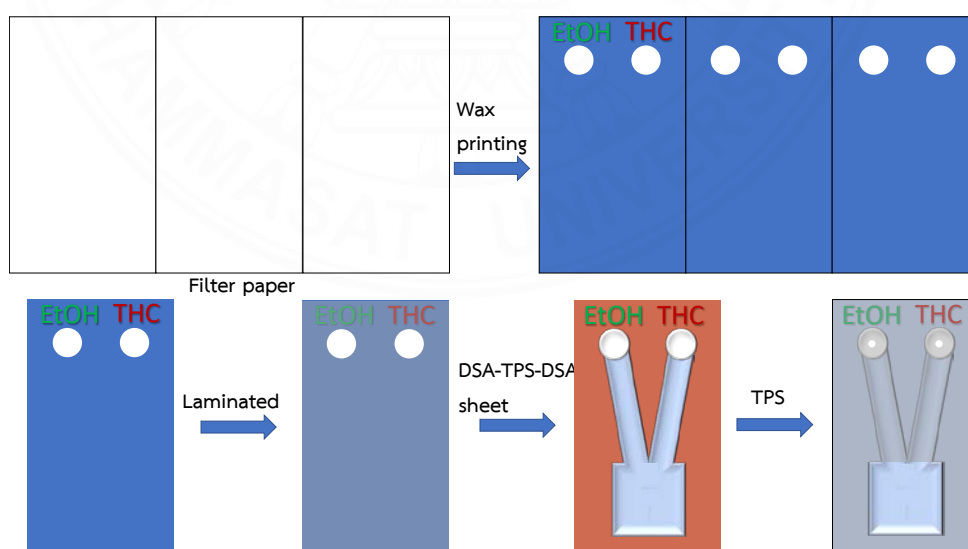


Figure 3.7. The fabrication of the capillary-driven microfluidic paper-based device

3.3.6 Preparation of a capillary-driven microfluidic paper-based device for the detection of ethanol and THC.

The PAD with 2 detection zones was designed for EtOH (left-hand side) and THC (right-hand side). Before the detection of THC, 2.00 μL NaOH 0.100 mol L^{-1} was dropped onto the right-hand side of the reagent pad and allowed to dry for 30.0 seconds, as shown in **Figure 3.8**. After that, the paper-based device assembled with the capillary-driven microfluidic channel is shown in **Figure 3.9**.

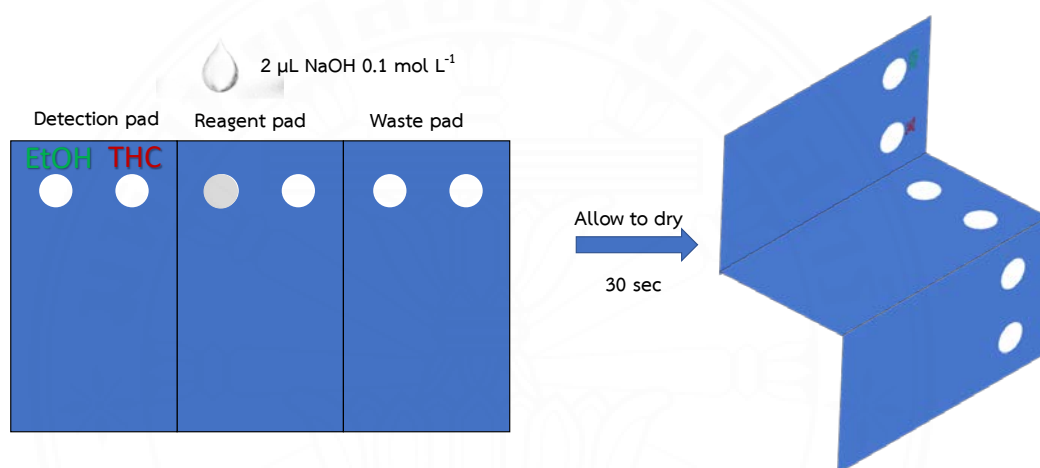


Figure 3.8. The preparation of paper-based devices before laminating.

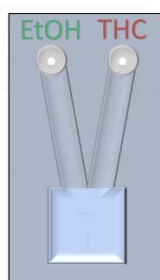


Figure 3.9 The paper-based device is assembled with a capillary-driven microfluidic channel.

3.3.7 The operation of the capillary-driven microfluidic paper-based device for colorimetric detection of ethanol and THC in artificial saliva samples.

The operation of the proposed device is shown in **Figure 3.10**. Colorimetric reagents specific to each target analyte are introduced. For the detection of EtOH, 1 μL of 0.4 mol L^{-1} of dichromate reagent is used, while 3 μL of 2.0 %w/v of fast blue B salt reagent is employed for THC analysis. After introducing the reagents, the 125 μL of artificial saliva solution containing EtOH and THC is loaded onto a sample insertion zone. It is then allowed to flow ultimately toward the detection zone. Once the solution reaches the detection zone, a waiting period of 30 minutes is observed to allow the colorimetric reaction to be thoroughly performed. The color change in each detection zone is visually assessed upon completion of the reactions. In the presence of EtOH in saliva, the color changes from yellow to green. For the THC analysis, the color change from yellow-brown to red is observed with the presence of THC in saliva. A smartphone's camera (iPhone 10) is utilized under controlled lighting conditions provided by a lightbox to capture and analyze the observed colors. The position of the smartphone (12 cm height) and the position of the device was fixed. The intensity of RGB values associated with the observed colors in each detection zone is analyzed using a Color-meter application (available for iOS).



Figure 3.10. The operation of a proposed microfluidic device for colorimetric detection of ethanol and THC in a synthetic saliva sample.

3.3.8 Flow behavior of synthetic salivas with varying viscosity

The SCMC-based synthetic saliva in different concentrations of SCMC (0.10, 0.25, 0.50, 1.00, 1.17 %w/v) was mixed with red dye to get better observations for the flow of the solution. The 50 μL of the synthetic saliva in different concentrations of SCMC was dropped onto the sample insertion zone of the device. Then, the time the solution flowed to the detection zone was observed with three replicates. The result was plotted between %SCMC and the time of the solution flow to the detection zone completely.

3.3.9 The effect of viscosity of synthetic salivas for colorimetric detection

The absolute ethanol 10.0 μL was diluted in 1 mL of the synthetic saliva with the different concentrations of SCMC of 0.10, 0.25, 0.50, 1.00, and 1.17 %, respectively. The 1 μL of 0.4 mol L^{-1} of dichromate reagent was dropped onto the detection zone. The 50 μL of 1.00 %v/v of EtOH in the synthetic saliva with different concentrations of SCMC was dropped onto the sample insertion zone. After the solution flowed to the detection zone entirely, it waited for 30 minutes and observed the color on the detection zone. Then, the color was captured and analyzed using a smartphone camera and Colormeter application with three replicates. The result was plotted between delta blue intensity to provide the best sensitivity and concentration of SCMC. Delta blue intensity is the value calculated from the blue intensity of the analyte – the blue color intensity of blank.

3.3.10 Optimization parts

Some parameters were optimized, consisting of three parts: device design, the colorimetric reaction of THC, and EtOH.

Several parameters were considered to optimize the device design. These include channel thickness and channel width.

3.3.10.1 Channel thickness

The device was fabricated by varying the number of layers of the DSA and TPS from 0.1 to 0.5 mm. 0.1 mm channel thickness was fabricated from a layer of 0.1 mm thick DSA (0.1-DSA), while 0.2 mm channel thickness was fabricated

from a 0.2 mm thick DSA (0.2-DSA) layer. 0.3 mm channel thickness was developed from 3 layers of 0.2 mm DSA-0.1/TPS/DSA-0.1. 0.4 mm and 0.5 mm channel thickness were performed with 3 three layers of DSA-0.2/TPS/DSA-0.1 and DSA-0.2/TPS/DSA-0.2, respectively. The 1.17 %SCMC-based synthetic saliva was mixed with red color dye to get better observations for the solution flow. The 100 μL of the saliva solution was dropped on the sample insertion zone of the device, and then the time of the solution flowed to the detection zone was observed with three replicates. The result was plotted between the time of the solution flow to the detection zone completely and the channel thickness.

3.3.10.2 Channel width

The device was fabricated by varying the channel width from 1.5 - 3.5 mm. The 1.17 %SCMC-based synthetic saliva was mixed with red color dye to get better observations for the solution flow. The 100 μL of the saliva solution was dropped on the sample insertion zone of the device, and then the time of the solution flowed to the detection zone was observed with three replicates. The result was plotted between the time of the solution flow to the detection zone completely and the channel thickness.

Sample volume, dichromate concentration, and reaction time were optimized for colorimetric detection of EtOH on the developed device. Similarly, for the colorimetric reaction of THC, reagent volume and the reaction time were optimized.

3.3.10.3 Sample volume

A 1.00 %v/v EtOH solution was prepared by diluting the absolute ethanol 10 μL in 1.00 mL of 1.17 %SCMC-based synthetic saliva. The 1 μL of 0.4 mol L^{-1} of dichromate reagent was dropped onto a detection zone. Then, 1.00 %v/v of EtOH in the saliva with different sample volumes (125 – 200 μL) was dropped onto the sample insertion zone. After the solution flowed to the detection zone completely, it waited for 30 minutes and observed the color on the detection zone. Then, the color was captured and analyzed using a smartphone camera and Colormeter

application with three replicates. The result was plotted between delta blue intensity ($B_{\text{EtOH}} - B_{\text{blank}}$) to provide the highest sensitivity and sample volume.

3.3.10.4 Concentration of dichromate

The stock solution of 1 mol L^{-1} of potassium dichromate was prepared by dissolving 1.4709 grams of potassium dichromate in 5 mL of 4 mol L^{-1} of hydrochloric acid. The stock solution of 1 mol L^{-1} of potassium dichromate was used to prepare 0.1, 0.2, 0.4, and 0.8 mol L^{-1} of potassium dichromate. The absolute ethanol of $10 \mu\text{L}$ was diluted in 1 mL of 1.17 %SCMC-based synthetic saliva. The $1 \mu\text{L}$ of dichromate reagent with different concentrations ($0.10\text{-}1.00 \text{ mol L}^{-1}$) was dropped onto the detection zone. The $125 \mu\text{L}$ of 1.0 %v/v of EtOH in 1.17 %SCMC-based synthetic saliva solution was dropped onto the sample insertion zone. After the solution flowed to the detection zone completely, it waited for 30 minutes and observed the color on the detection zone. Then, the color was captured and analyzed using a smartphone camera and Colormeter application with three replicates. The result was plotted between delta blue intensity ($B_{\text{EtOH}} - B_{\text{blank}}$) to provide the highest sensitivity and concentration of dichromate.

3.3.10.5 The reaction time for the colorimetric detection of EtOH

The absolute ethanol of $10 \mu\text{L}$ was diluted in 1.00 mL of 1.17 %SCMC-based synthetic saliva. The $1 \mu\text{L}$ of 0.4 mol L^{-1} of dichromate reagent was dropped onto a detection zone. The $125 \mu\text{L}$ of 1.0 %v/v of EtOH in 1.17% SCMC-based synthetic saliva was dropped onto the sample insertion zone. After the solution flowed to the detection zone completely, it waited for 10, 20, 30, 60, 90, and 120 minutes and observed the color on the detection zone. Then, the color was captured and analyzed using a smartphone camera and Colormeter application with three replicates. The result was plotted between delta blue intensity ($B_{\text{EtOH}} - B_{\text{blank}}$) to provide the highest sensitivity and time.

3.3.10.6 The volume of fast blue B salt reagent

According to 2.0 %w/v of fast blue B salt reagent, which is the highest concentration that can be prepared, the volume of fast blue B salt reagent was studied to get the highest signal of analyte (THC).

The 100 mg L⁻¹ of THC stock solution 10 µL was diluted in 1.00 mL of 1.17 %SCMC-based synthetic saliva. The different volume of fast blue B salt reagent (1-5 µL) was dropped onto the detection zone. The 125 µL of 1 mg L⁻¹ THC in 1.17 %SCMC-based synthetic saliva was dropped onto the sample insertion zone. After the solution flowed to the detection zone completely, it waited for 30 minutes and observed the color on the detection zone. Then, the color was captured and analyzed using a smartphone camera and Colormeter application with three replicates. The result was plotted between delta green intensity ($G_{\text{blank}} - G_{\text{THC}}$) due to providing the highest sensitivity and fast blue B salt volume.

3.3.10.7 The reaction time for colorimetric detection of THC

The 100 mg L⁻¹ of THC stock solution 10 µL was diluted in 1.00 mL of 1.17 %SCMC-based synthetic saliva. The 3 µL of 2.0 %w/v of fast blue B salt reagent was dropped onto the detection zone. The 125 µL of 1 mg L⁻¹ THC in 1.17 %SCMC-based synthetic saliva was dropped onto the sample insertion zone. After the solution flowed to the detection zone completely, it waited for 10, 20, 30, 60, 90, and 120 minutes and observed the color on the detection zone. Then, the color was captured and analyzed using a smartphone camera and Colormeter application with three replicates. The result was plotted between delta green intensity ($G_{\text{blank}} - G_{\text{THC}}$) due to providing the highest sensitivity and fast blue B salt volume.

3.3.11 Analytical performance

3.3.11.1 Linearity

The 1 µL of 0.4 mol L⁻¹ of dichromate reagent was dropped onto the detection zone. 125 µL of 0.1, 0.5, 1.0, 3.0, and 5.0 %v/v EtOH in 1.17 %SCMC-based synthetic saliva was dropped onto the sample insertion zone. After the solution flowed to the detection zone completely, it waited for 30 minutes and observed the color on the detection zone. Then, the color was captured and analyzed using a smartphone camera and Colormeter application with three replicates. The result was plotted between delta blue intensity ($B_{\text{EtOH}} - B_{\text{blank}}$) to provide the highest sensitivity and the concentration of EtOH.

The 3.00 μL of 2.0 %w/v of fast blue B salt reagent was dropped onto the detection zone. 125 μL of 0.1, 0.5, 1, 5, 10 mg L^{-1} THC in 1.17 %SCMC-based synthetic saliva was dropped onto the sample insertion zone. After the solution flowed to the detection zone completely, it waited for 30 minutes and observed the color on the detection zone. Then, the color was captured and analyzed using a smartphone camera and Colormeter application with three replicates. The result was plotted between delta green intensity ($G_{\text{blank}} - G_{\text{THC}}$) due to provide the highest sensitivity and the concentration of THC.

3.3.11.2 Limit of detection (LOD)

The 1 μL of 0.4 mol L^{-1} of dichromate reagent was dropped onto the detection zone. The 125 μL of 1.17 %SCMC-based synthetic saliva was dropped to the sample insertion zone. After the solution flowed to the detection zone completely, it waited for 30 minutes and observed the color on the detection zone. Then, the color was captured and analyzed using a smartphone camera and Colormeter application with three replicates. The standard deviation of the obtained blue intensity of blank was used to calculate the limit of detection.

The 3 μL of 2.0 %w/v of fast blue B salt reagent was dropped onto the detection zone. The 125 μL of 1.17 %SCMC-based synthetic saliva was dropped to the sample insertion zone. After the solution flowed to the detection zone completely, it waited for 30 minutes and observed the color on the detection zone. Then, the color was captured and analyzed using a smartphone camera and Colormeter application with three replicates. The standard deviation of the obtained green intensity of the blank was used to calculate the limit of detection.

The limit of detection is calculated by equations $\text{LOD} = 3\sigma/S$, where σ is the standard deviation of the blank solution, and S is the slope of the calibration curve.

3.3.11.3 Reproducibility

The 1 μL of 0.4 mol L^{-1} of dichromate reagent was dropped onto a detection zone. The 125 μL of 1.0 %v/v of EtOH in 1.17 %SCMC-based synthetic saliva was dropped onto the sample insertion zone. After the solution flowed to the

detection zone completely, it waited for 30 minutes and observed the color on the detection zone. Then, the color was captured and analyzed using a smartphone camera and Colormeter application with seven replicates. The standard deviation of the obtained delta blue intensity ($B_{\text{EtOH}} - B_{\text{blank}}$) was used to calculate the reproducibility.

The 3 μL of 2.0 %w/v of fast blue B salt reagent was dropped onto the detection zone. The 125 μL of 1 mg L^{-1} of THC in 1.17 %SCMC-based synthetic saliva was dropped onto the sample insertion zone. After the solution flowed to the detection zone completely, it waited for 30 minutes and observed the color on the detection zone. Then, the color was captured and analyzed using a smartphone camera and Colormeter application with seven replicates. The standard deviation of the obtained delta green intensity ($G_{\text{blank}} - G_{\text{THC}}$) was used to calculate the reproducibility.

The precision was described in terms of reproducibility. Seven times measurements of THC solution (1 mg L^{-1} of THC) and (1.0 %v/v of EtOH) are measured and shown in the percent relative standard deviation (%RSD).

3.3.11.4 Stability

The device was fabricated and stored NaOH solution. Then, it was kept in desiccator (temperature = 34 $^{\circ}\text{C}$, Humidity = 27 %RH) for 7 days. The fabricated device was used to test the stability of the signal for EtOH and THC detection for 7 days (1,3,5 and 7).

The 1 μL of 0.4 mol L^{-1} of dichromate reagent was dropped onto a detection zone. The 125 μL of 1.0 %v/v of EtOH in 1.17 %SCMC-based synthetic saliva was dropped onto the sample insertion zone. After the solution flowed to the detection zone completely, it waited for 30 minutes and observed the color on the detection zone. Then, the color was captured and analyzed using a smartphone camera and Colormeter application with three replicates. The %error of the obtained delta blue intensity ($B_{\text{EtOH}} - B_{\text{blank}}$) was used to calculate the stability.

The 3 μL of 2.0 %w/v of fast blue B salt reagent was dropped onto the detection zone. The 125 μL of 1 mg L^{-1} of THC in 1.17 %SCMC-based synthetic

saliva was dropped onto the sample insertion zone. After the solution flowed to the detection zone completely, it waited for 30 minutes and observed the color on the detection zone. Then, the color was captured and analyzed using a smartphone camera and Colormeter application with three replicates. The %error of the obtained delta green intensity ($G_{\text{blank}} - G_{\text{THC}}$) was used to calculate the stability.

The stability of the signal was express in %error unit. While

$$\%error = \text{absolute} \left(\frac{(\text{intensity of day 3,5,7}) \times 100}{\text{intensity of day 1}} - 100 \right).$$

3.3.11.5 Interference

The 1 μL of 0.4 mol L^{-1} of dichromate reagent was dropped onto the detection zone. The 125 μL of 1.0 %v/v EtOH in HCO_3^- , Na^+ (80 mmol L^{-1}), SCN^- (2 mmol L^{-1}), Ca^{2+} (4 mmol L^{-1}), K^+ (100 mmol L^{-1}), Cl^- (100 mmol L^{-1}), Mg^{2+} (0.2 mmol L^{-1}), PO_4^{3-} (4 mmol L^{-1}), glucose (0.25 mmol L^{-1}), sucrose (0.05 mmol L^{-1}), ascorbic acid (0.01 mmol L^{-1}) in 1.17 %SCMC-based synthetic saliva was dropped on to the sample insertion zone. After the solution flowed to the detection zone completely, it waited for 30 minutes and observed the color on the detection zone. Then, the color was captured and analyzed using a smartphone camera and Colormeter application with three replicates, respectively. The result was plotted between delta blue intensity ($B_{\text{EtOH}} - B_{\text{blank}}$) to provide the highest sensitivity and the concentration of EtOH and the interference ion. The result was compared between the delta blue intensity ($B_{\text{EtOH}} - B_{\text{blank}}$) of 1.00 %v/v of EtOH and the delta blue intensity ($B_{\text{EtOH}} - B_{\text{blank}}$) of 1.0 %v/v of EtOH with interference. The result was described in terms of %error.

The 3 μL of 2.0 %w/v of fast blue B salt reagent was dropped onto the detection zone. The 125 μL of 1 mg L^{-1} THC in HCO_3^- , Na^+ (80 mmol L^{-1}), SCN^- (2 mmol L^{-1}), Ca^{2+} (4 mmol L^{-1}), K^+ (100 mmol L^{-1}), Cl^- (100 mmol L^{-1}), Mg^{2+} (0.2 mmol L^{-1}), PO_4^{3-} (4 mmol L^{-1}), glucose (0.25 mmol L^{-1}), sucrose (0.05 mmol L^{-1}), ascorbic acid (0.01 mmol L^{-1}) in 1.17 %SCMC-based synthetic saliva was dropped on to the sample insertion zone. After the solution flowed to the detection zone completely, it waited for 30 minutes and observed the color on the detection zone. Then, the color was captured and analyzed using a smartphone camera and Colormeter application with three replicates, respectively. The result was plotted between delta green intensity

($G_{\text{blank}} - G_{\text{THC}}$) due to providing the highest sensitivity and the interference ion. The result was compared between the delta green intensity ($G_{\text{blank}} - G_{\text{THC}}$) of 1 mg L^{-1} of THC and the delta green intensity ($G_{\text{blank}} - G_{\text{THC}}$) of 1 mg L^{-1} of THC with interference. The result was described in terms of %error.

3.3.12 Feasibility of the developed device for simultaneous detection of EtOH and THC

3.3.12.1 Cross-talk between EtOH and THC

The simultaneous detection of EtOH and THC was studied to ensure no interference effect between both analytes.

The $1 \mu\text{L}$ of 0.4 mol L^{-1} of dichromate reagent was dropped onto the detection zone. The $125 \mu\text{L}$ of 1.0 \%v/v of EtOH in 1.17 \%SCMC -based synthetic saliva was dropped onto the sample insertion zone. After the solution flowed to the detection zone completely, it waited for 30 minutes and observed the color on the detection zone. Then, the color was captured and analyzed using a smartphone camera and Colormeter application with three replicates. The delta blue intensity was compared to the delta blue intensity ($B_{\text{EtOH}} - B_{\text{blank}}$) of the $125 \mu\text{L}$ of 1.0 \%v/v , 1 mg L^{-1} of EtOH, and THC in 1.17 \%SCMC -based synthetic saliva. The result was described in terms of %error.

The $1 \mu\text{L}$ of 0.4 mol L^{-1} of dichromate reagent was dropped onto the detection zone. The $125 \mu\text{L}$ 1 mg L^{-1} of THC in 1.17 \%SCMC -based synthetic saliva was dropped onto the sample insertion zone. After the solution flowed to the detection zone completely, it waited for 30 minutes and observed the color on the detection zone. Then, the color was captured and analyzed using a smartphone camera and Colormeter application with three replicates. The obtained delta blue intensity ($B_{\text{EtOH}} - B_{\text{blank}}$) was used to describe the interference effect of THC.

The $3 \mu\text{L}$ of 2.0 \%w/v of fast blue B salt reagent was dropped onto the detection zone. The $125 \mu\text{L}$ 1 mg L^{-1} of THC in 1.17 \%SCMC -based synthetic saliva was dropped onto the sample insertion zone. After the solution flowed to the detection zone completely, it waited for 30 minutes and observed the color on the detection zone. Then, the color was captured and analyzed using a smartphone camera and Colormeter application with three replicates. The obtained delta green

intensity was compared to the delta green intensity ($G_{\text{blank}} - G_{\text{THC}}$) of the 125 μL of 1.0 %v/v, 1 mg L^{-1} of EtOH, and THC, respectively, in 1.17 %SCMC-based synthetic saliva. The result was described in terms of %error.

The 3 μL of 2.0 %w/v of fast blue B salt reagent was dropped onto the detection zone. The 125 μL of 1.0 %v/v of EtOH in 1.17 %SCMC-based synthetic saliva was dropped onto the sample insertion zone. After the solution flowed to the detection zone completely, it waited for 30 minutes and observed the color on the detection zone. Then, the color was captured and analyzed using a smartphone camera and Colormeter application with three replicates. The obtained delta green intensity ($G_{\text{blank}} - G_{\text{THC}}$) was used to describe the interference effect of EtOH.

3.3.12.2 Recovery

The 1 μL of 0.4 mol L^{-1} of dichromate reagent was dropped onto the left-hand side of the detection zone, while the 3 μL of 2.0 %w/v of fast blue B salt reagent was dropped onto the right-hand side of the detection zone. The 125 μL of 0.8, 2.0 %v/v of EtOH and 0.8, 3 mg L^{-1} of THC in 0.10, 0.25, 0.50, 1.00 and 1.17 % SCMC-based synthetic saliva was dropped onto the sample insertion zone. After the solution flowed to the detection zone completely, it waited for 30 minutes and observed the color on the detection zone. Then, the color was captured and analyzed using a smartphone camera and Colormeter application with three replicates. The delta blue and green intensity were used to calculate the %recovery to evaluate the trueness.

CHAPTER 4

RESULTS AND DISCUSSION

4.1 Lab-made spectrometer

4.1.1 Design and assembly of laser-LDR spectrometer

The design and assembly of the blue, red, and green laser-LDR spectrometer is shown in **Figure 4.1-4.3**. The three laser-LDR spectrometers consisted of a base that can be made from acrylic plate, wooden board, and paper box, laser holders, cable tie to fix the switch of the laser (for turn on/off laser) and cuvette holder (made from acrylic), and LDR. Three laser pointers (red, green, and blue) were used as a light source for each spectrometer. LDR is a detector connected to a multimeter outside the black box, shown in **Figure 4.4**. A black box was used to protect light from the environment.



Figure 4.1. The design and the invention of the blue laser-LDR spectrometer.

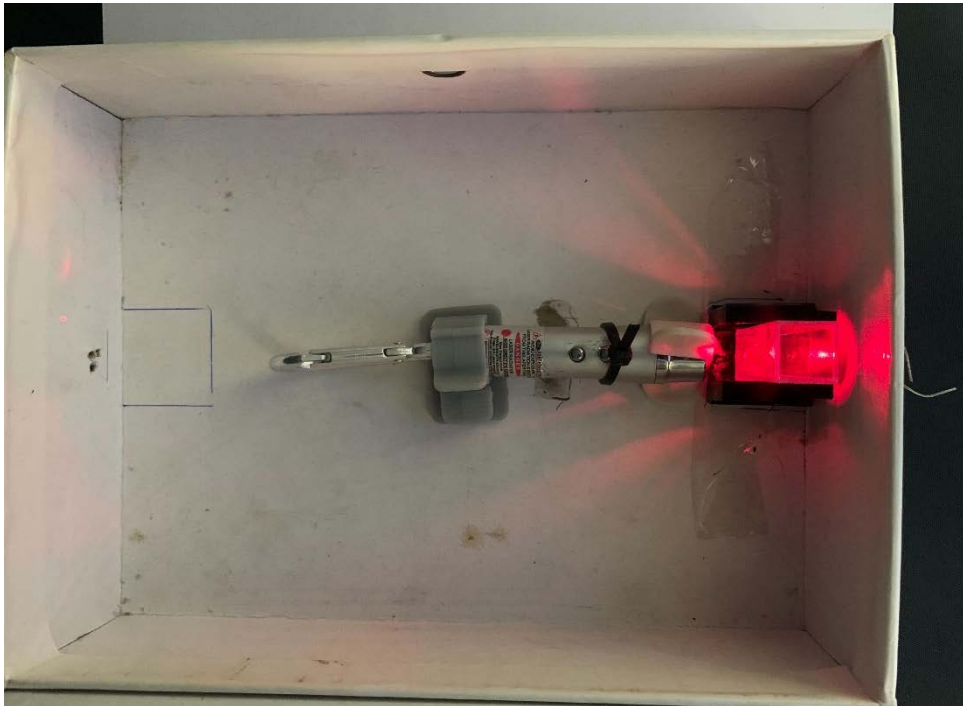


Figure 4.2. The design and invention of the red laser-LDR spectrometer.



Figure 4.3. The design and invention of the green laser-LDR spectrometer.

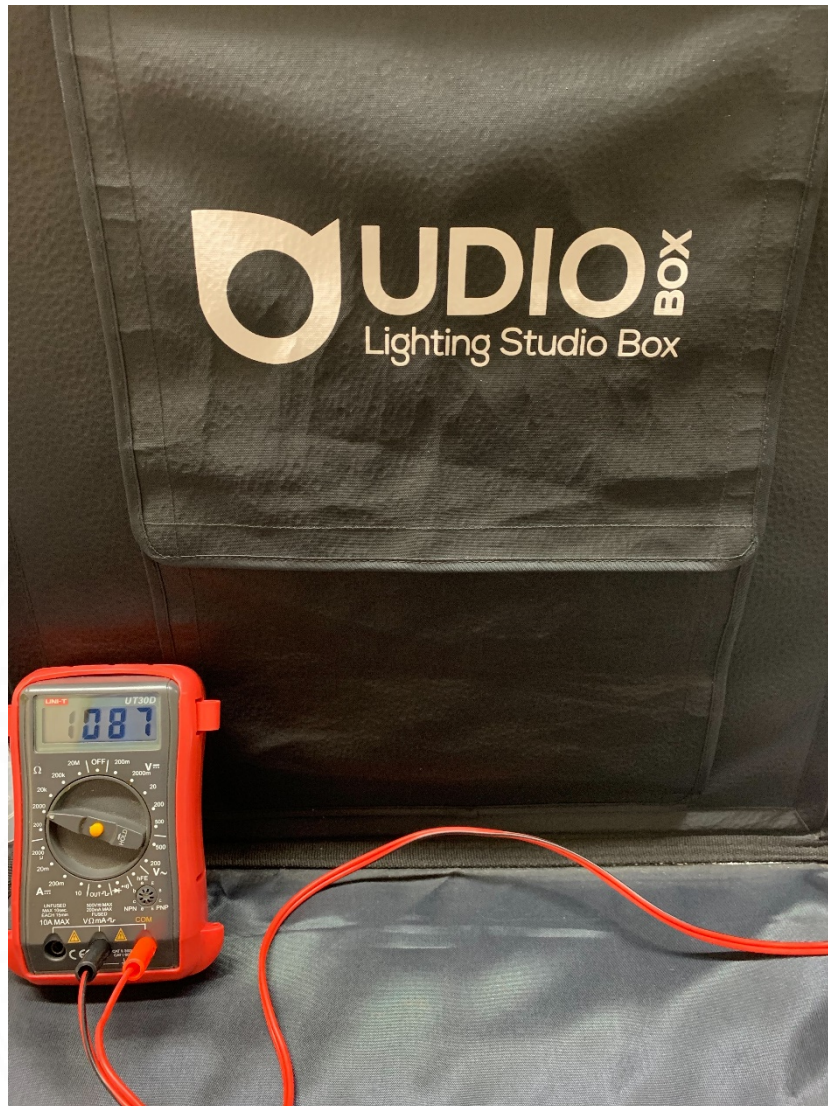


Figure 4.4. The setup of a multimeter outside the black box.

4.1.2 The relationship between signal (resistance, ohm) and transmittance

To calibrate the signal of each laser-LDR spectrometer system, the transmittance of various car films fixed to the cuvettes was measured by a spectrophotometer (MAPADA). After that, they were placed in the cuvette holder of laser-LDR spectrometers, and the signal was read in a resistance unit by a multi-meter. It was found that the resistances (R_f) were related to transmittance in the exponential equation. A logarithm was applied to describe Beer's Lambert Law, and “-log T” was

replaced by absorbance (A). An example of solving the equation is shown in the following equation.

$$R_i = 820.76T^{-0.5559} \quad \text{---(4.1)}$$

$$\log R_i = \log(820.76) - 0.5559(\log(T)) \quad \text{---(4.2)}$$

due to $-\log(T) = A$, so, $\log R_i = 0.5559A + 2.914 \quad \text{---(4.3)}$

Therefore, $\log R_i$ of the blue laser-LDR spectrometer was linear to the absorbance of the spectrophotometer (MAPADA). To minimize the Y intercept, the absorbance of the blank is necessary to be measured by using a cuvette without film.

It was found that the linear graph was obtained by plotting $\log R$ vs. A (where "R" is R_i/R_0), which is shown in equation (4.4).

$$\log R = 0.5559A - 0.0169 \quad \text{---(4.4)}$$

After calibrating the three systems of the laser pointer LDR spectrometers (red, green, blue) with a commercial spectrophotometer (MAPADA), the "log R" signals were plotted with "A" values, the linearities were obtained as shown in **Figure 4.5-4.7**. The results showed that these laser-LDR systems should be used to determine compounds like a commercial spectrometer.

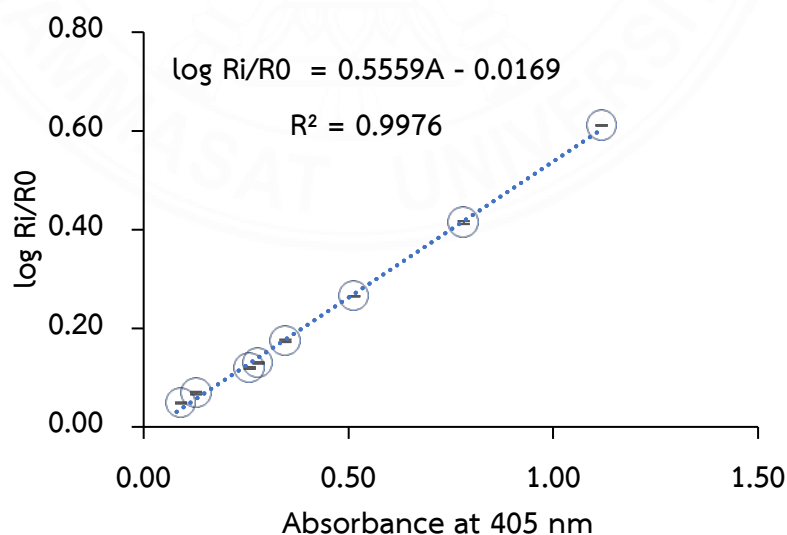


Figure 4.5. The linear graph of $\log R$ vs absorbance at 405 nm (blue laser-LDR spectrometer).

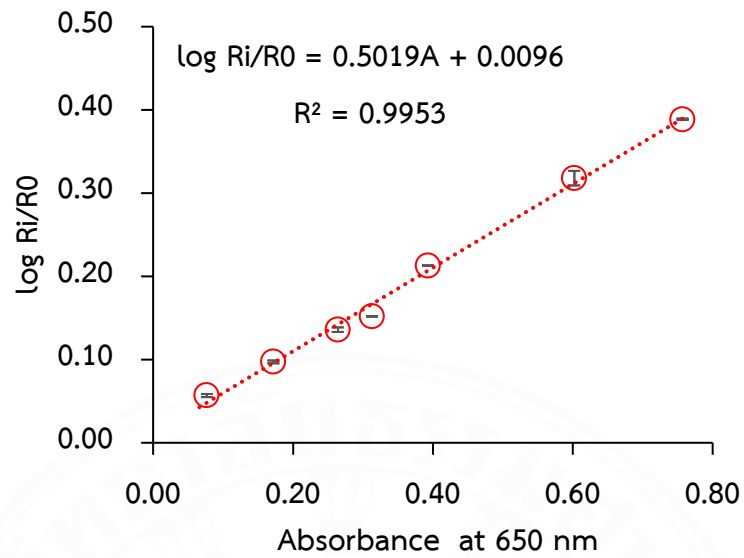


Figure 4.6. The linear graph of log R vs absorbance at 650 nm (red laser-LRD spectrometer).

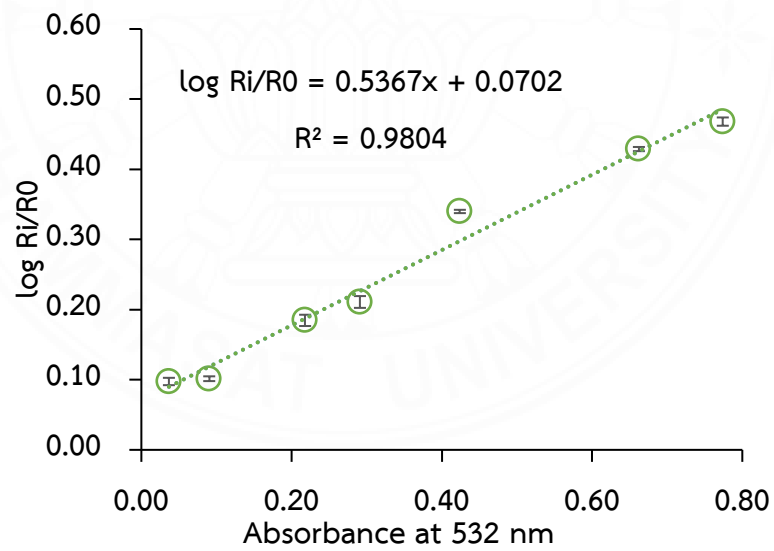


Figure 4.7. The linear graph of log R vs absorbance at 532 nm (green laser-LDR spectrometer).

4.2 Application of blue laser-LDR spectrometer

4.2.1 Absorption spectrum of the complex solution

The absorption spectrum of the Fe-TCH complex is shown in **Figure 4.8**. The maximum wavelength of the complex solution is 430 nm. Thus, the blue laser pointer was chosen as a light source because its wavelength was close to the maximum wavelength.

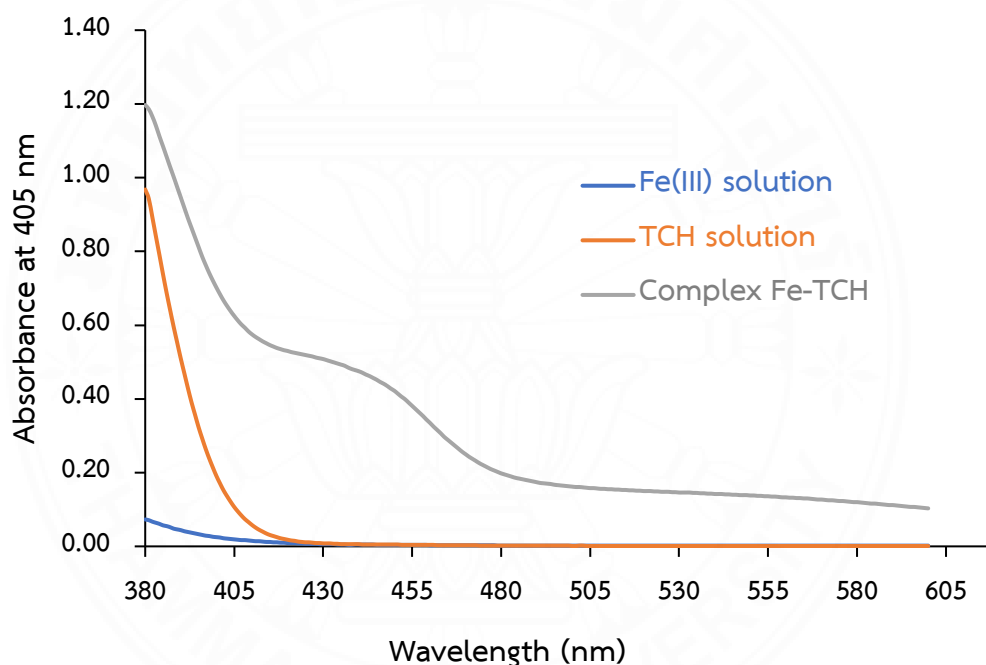


Figure 4.8. The absorption spectrum of Fe-TCH complex.

4.2.2 Reaction time and stability

The complex reaction time between Fe(III) and TCH took 10 minutes. After that, the signal was relatively stable for at least 120 minutes (**Figure 4.9**). Therefore, the reaction process should be kept for at least 10 minutes, and the complex was stable for at least 2 hrs. This reaction is suitable for the determination of TCH in real samples and is also used as an example of a colorimetric experiment in undergraduate chemistry students.

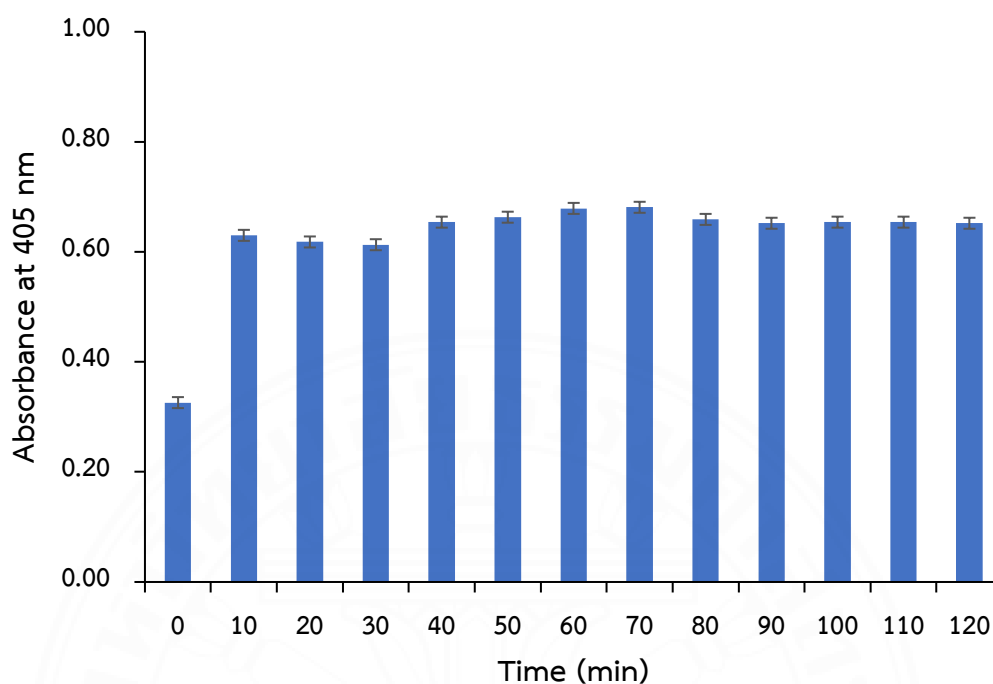


Figure 4.9. Reaction time and stability of complex between Fe(III) and TCH.

4.2.3 Stoichiometric ratio

The stoichiometric ratio between Fe(III) and TCH was studied using Job's method and the mole ratio method. The log R was measured by a laser-based spectrometer. The results are shown in **Figures 4.10 and 4.11** for Job's method and mole ratio method, respectively. Both methods showed that the stoichiometric ratio of Fe: TCH was 1:1. This result was consistent with the work of (Korać Jačić et al., 2022) that Fe(III) and TCH formed a stable complex with 1:1 stoichiometric ratio at pH 3.

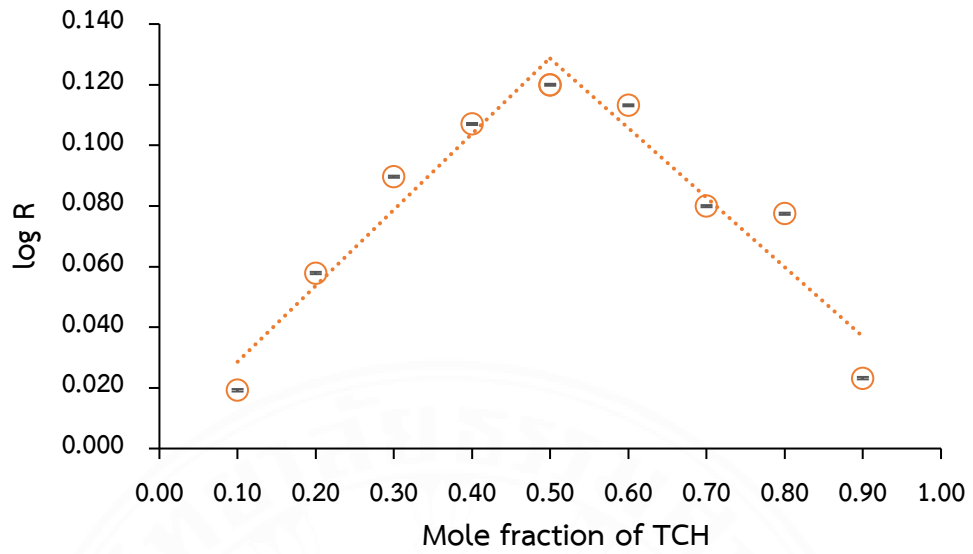


Figure 4.10. Job's method, a graph represents log R as a function of the mole fraction of TCH.

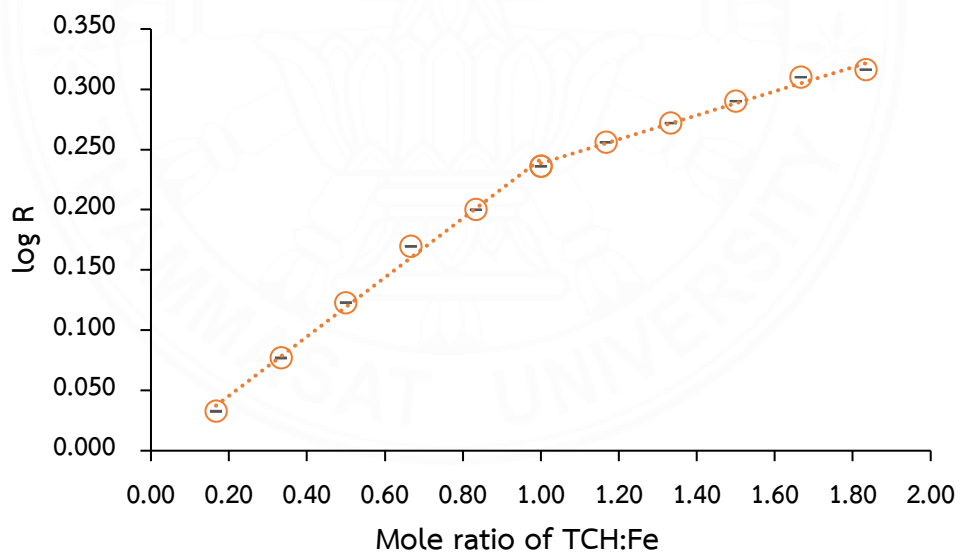


Figure 4.11. In the mole ratio method, a graph represents log R as a function of the mole ratio (TCH: Fe).

4.2.4 Optimization

Prior to the use of this lab-made spectrometer for the determination of TCH, the univariate optimization was studied, and the initial conditions consisted of Fe(III), TCH and acetate buffer at concentration 1.00×10^{-2} , 1.00×10^{-3} and 1.00×10^{-1} mol L⁻¹, respectively.

4.2.4.1 Stability of signal

The intensity of the laser pointer is not stable for long-term analysis, depending on brands and the power of light. The stability of this laser pointer was studied, and the signal was found to be relatively stable in 5 - 60 minutes with a % deviation of less than 10. However, to minimize the deviation, a blank solution needed to be measured before a complex solution throughout the experiment.

4.2.4.2 Effect of pH

The effect of pH was studied by varying the pH of the acetate buffer in the range of pH 0.5-3 (Figure 4.12). A higher signal was obtained at a higher pH, and pH 2.5 after that, the signal was relatively constant. Therefore, pH 2.5 was selected as an optimal condition.

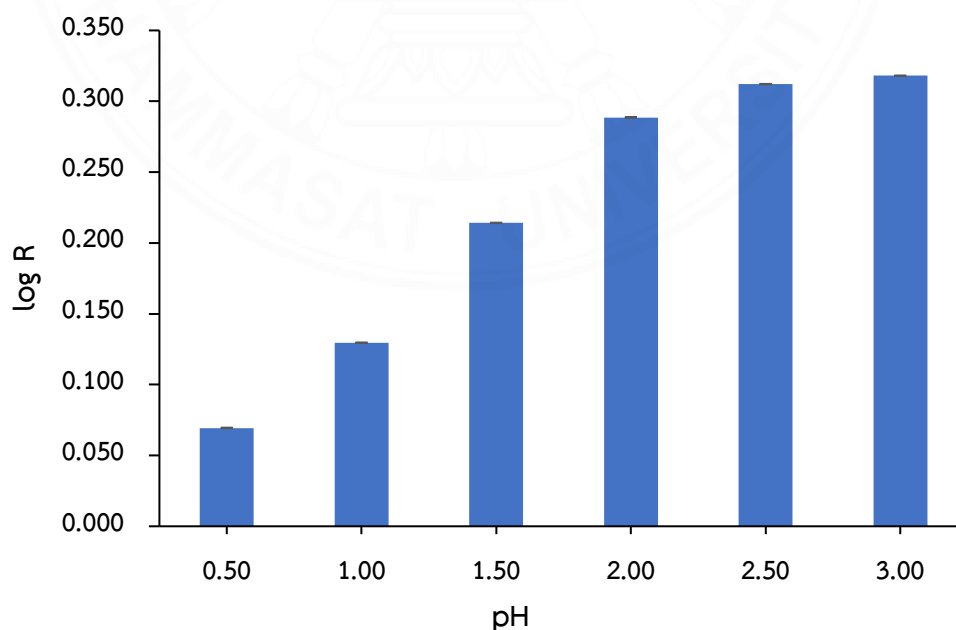


Figure 4.12. Effect of pH of acetate buffer.

4.2.4.3 Concentration of Fe(III)

The effect of Fe(III) concentration was studied in the range of $1.25 \times 10^{-3} - 2.5 \times 10^{-2} \text{ mol L}^{-1}$ (Figure 4.13). At $1.25 \times 10^{-3} \text{ mol L}^{-1}$, the lowest signal was presented, and at other concentrations, the signal was non-significantly different. Thus, $1.00 \times 10^{-2} \text{ mol L}^{-1}$ of Fe(III) was selected for further study.

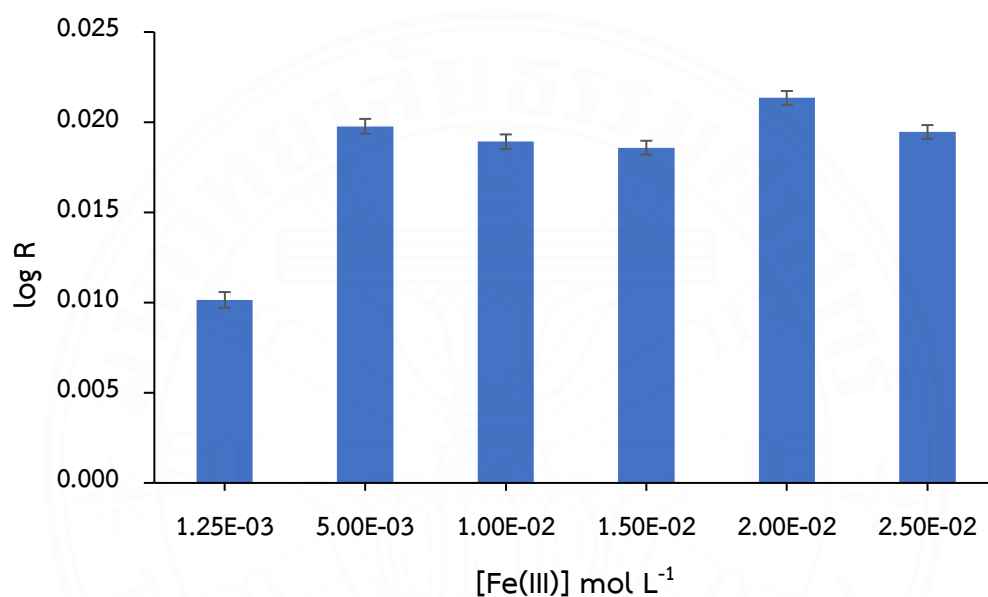


Figure 4.13. Effect of concentrations of Fe(III).

4.2.5 Some analytical features

Under the optimal conditions, some analytical features of this proposed laser-based spectrometer were studied, such as linearity, LOD, LOQ, precision, and accuracy, by comparing them to a commercial spectrophotometer (MAPADA).

4.2.5.1 Linearity

The standard graph was plotted between log R vs TCH concentration for the proposed laser-based spectrometer. In contrast, the commercial spectrophotometer presented a graph of the function of absorbance and TCH concentration (mol L^{-1}). The standard graphs of both methods were linear in the range

of 5.74×10^{-6} – 1.15×10^{-4} mol L⁻¹. The equation obtained from the proposed Laser-based spectrometer was $\log R = 2565[\text{TCH}] + 0.0005063$, with $0.9987 R^2$, demonstrating an excellent linear relationship between $\log R$ and TCH concentration. In contrast, those from the spectrophotometer were $\text{Absorbance} = 5057 [\text{TCH}] - 0.01575$ with R^2 0.9989. Both spectrometers presented excellent linearity ($R^2 > 0.99$) with a wide range of 5.74×10^{-6} to 1.15×10^{-4} mol L⁻¹ of TCH.

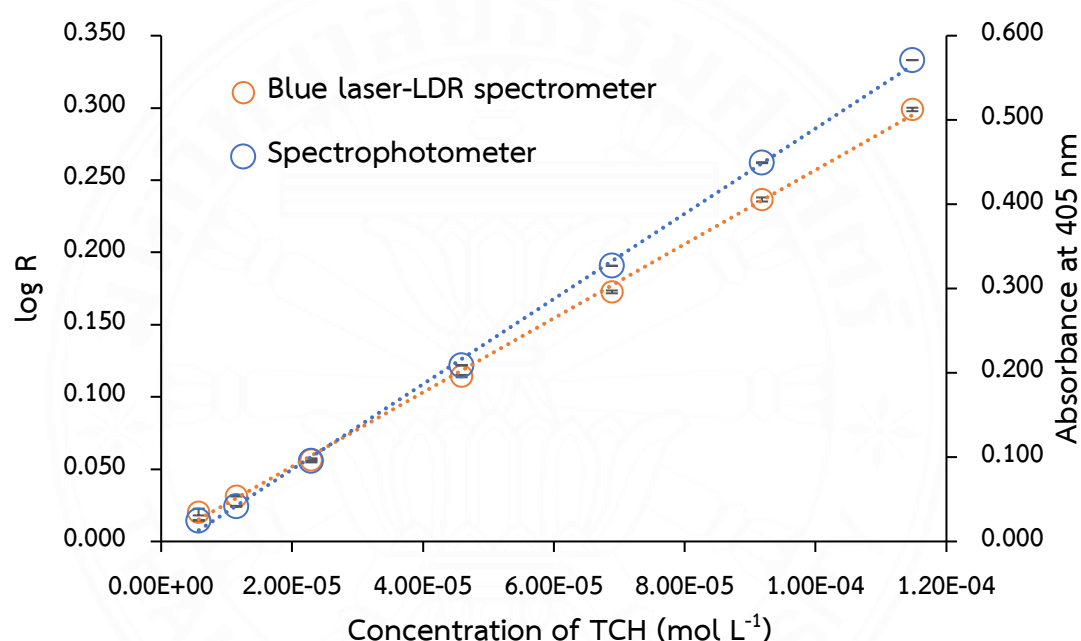


Figure 4.14. The linear graph of the laser-based spectrometer and spectrophotometer for determination of TCH.

4.2.5.2 Limit of detection (LOD) and limit of quantification (LOQ)

The limit of detection (LOD) and limit of quantification (LOQ) follow ICH Q2(R2) guidelines. The LOD and LOQ were calculated by equations $\text{LOD} = 3.3\sigma/S$ and $\text{LOQ} = 10\sigma/S$, respectively, where σ is the standard deviation of blank, and S is the slope of calibration. The LOD and LOQ of the purposed laser-based spectrometer were 1.44×10^{-6} and 4.35×10^{-6} mol L⁻¹, respectively, whereas those for the spectrophotometer were 3.15×10^{-7} and 9.55×10^{-7} mol L⁻¹.

4.2.5.3 Precision and Accuracy

The precision of the method was described in terms of repeatability and reproducibility. Ten times measurements and ten bottles of complex solution (2.30×10^{-5} mol L⁻¹ of TCH) were examined and presented in the percent relative standard deviation (%RSD). It was found that the %RSDs of repeatability and reproducibility of the signal measured by the purposed laser-based spectrometer were 1.30 and 3.26, respectively. In contrast, the %RSDs of those by the spectrophotometer were 0.21 and 2.03. Both methods provided excellent precision, in which % RSDs were less than 5.

The recovery was evaluated by spiking standards TCH in the sample solution at concentration levels of 1.04×10^{-5} – 4.16×10^{-5} mol L⁻¹. The percentage recoveries were found in the range of 85-97 for both methods, and the results are reported in **Table 4.1**. In the low concentration of TCH, the % recoveries are low (some are lower than 90). Therefore, we suggested preparing the sample solutions at a higher concentration of 3.12×10^{-5} mol L⁻¹.

Table 4.1.

The recovery studies.

Standard TCH added (mol L ⁻¹)	% Recoveries ± SD	
	Blue laser-LDR spectrometer	Commercial spectrophotometer
1.04×10^{-5}	87.31 ± 0.60	86.53 ± 0.66
2.08×10^{-5}	91.75 ± 0.28	85.10 ± 0.34
3.12×10^{-5}	93.60 ± 0.41	93.67 ± 0.12
4.16×10^{-5}	96.05 ± 0.39	96.90 ± 0.09

The concentration of TCH in the sample solution was 4.01×10^{-5} mol L⁻¹.

4.2.6 Application

The proposed laser-based spectrometer and spectrophotometer were used to analyze the amount of TCH in 6 brands of TCH capsules. There was no significant difference between those results between both methods at a 95% confidence level ($t_{\text{stat}} = -0.84$, $t_{\text{critical}} = 2.77$). Moreover, the amounts of TCH in each sample were found in the range of 91.8-112.2 and 94.3-113.1 % labeled amount for laser-based spectrometer and spectrophotometer, respectively. The assay of the drug content of all samples meets the compliance requirement of USP41¹¹ (Tetracycline Hydrochloride Capsules, 90.0-125.0 % labelled amount). Therefore, this lab-made spectrometer can be alternative equipment for the determination of TCH in pharmaceuticals and is suitable for field analysis and the example experiment in chemistry class, especially at home.

Table 4.2.

Assay of TCH in samples

Sample	Labelled amount of TCH (mg/cap)	Amount of TCH, Assay (mg/cap \pm SD)	
		Blue laser-LDR spectrometer	Commercial spectrophotometer
1	500	459.24 \pm 0.95	471.92 \pm 1.07
2	500	471.45 \pm 1.07	482.99 \pm 0.31
3	250	254.32 \pm 0.45	243.93 \pm 0.54
4	250	280.12 \pm 0.79	282.33 \pm 0.49
5	250	253.34 \pm 0.31	257.59 \pm 0.48
6	250	248.27 \pm 0.29	256.43 \pm 0.49

4.3 Red laser-LDR spectrometer for determination of MSG

4.3.1 Absorption spectrum of complex

The absorption spectrum of the Cu-MSG complex is shown in **Figure 4.15**. The maximum length of the complex solution is 680 nm. Thus, the red laser pointer was chosen as a light source because the wavelength of the red laser pointer is close to the maximum wavelength.

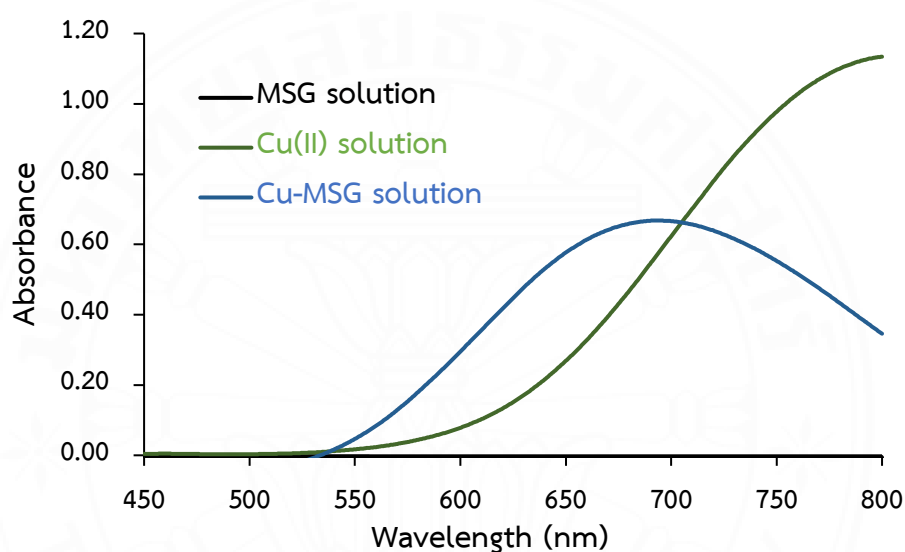


Figure 4.15. The absorption spectrum of Cu-MSG

4.3.2 Reaction time and stability

The reaction time and stability are shown in **Figure 4.16**. The complex reaction time between Cu(II) and MSG was rapid and presented a color change immediately. Then, the solution was measured at wavelength 650 nm, and it was found that the absorbance did not change until 120 minutes. Therefore, this reaction is stable for 2 hrs.

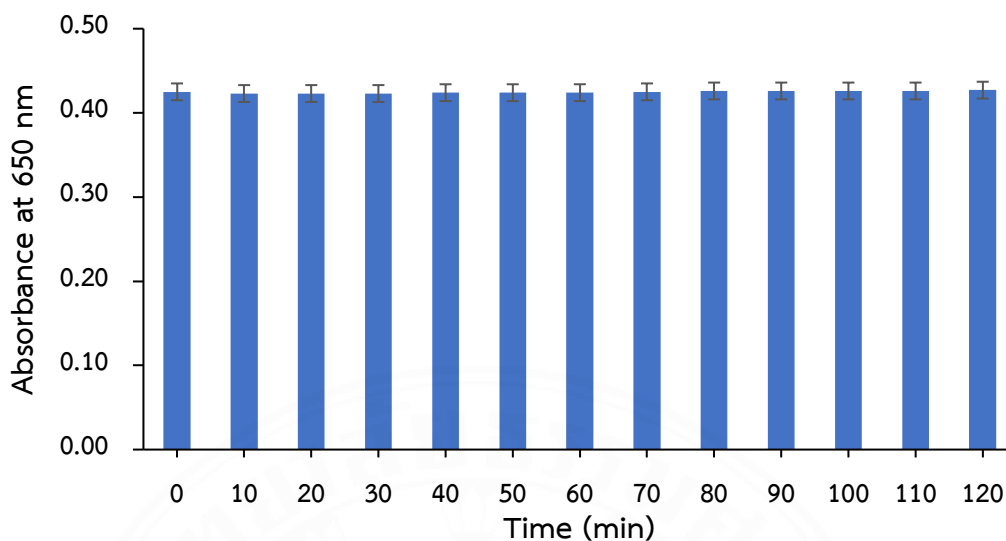


Figure 4.16. The reaction time and stability of complex between Cu(II) and MSG.

4.3.3 Stoichiometric ratio

The stoichiometric ratio between Cu(II) and MSG was studied using Job's method and the mole ratio method. The log R was measured by a laser-based spectrometer. The results are shown in **Figures 4.17 and 4.18** for Job's method and mole ratio method, respectively. The results of both methods showed that the stoichiometric ratio of Cu: MSG was 1:2. The result corresponds to the research of (Deschamps et al., 2003; Verdejo et al., 2005).

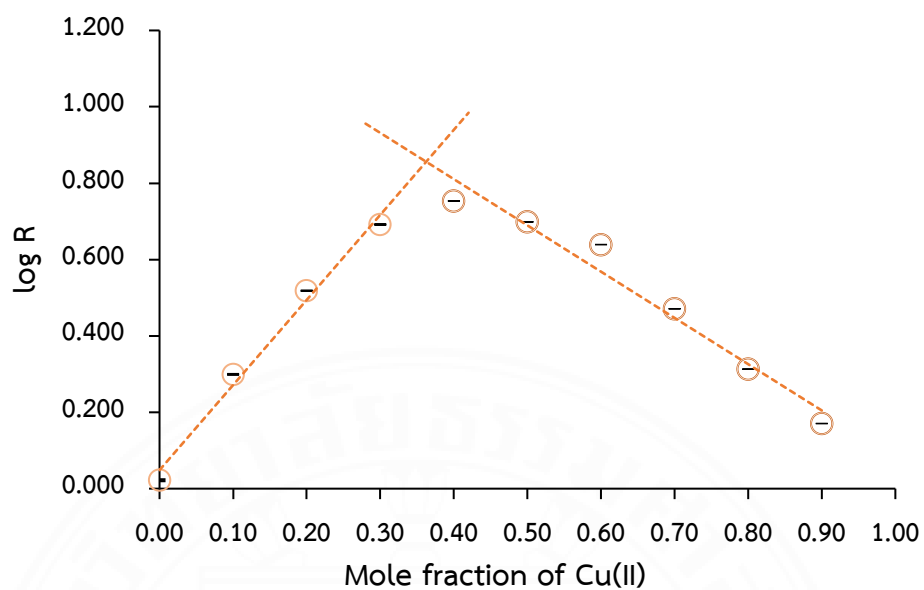


Figure 4.17. Job's method, a graph represents $\log R$ as a function of the mole fraction of Cu(II).

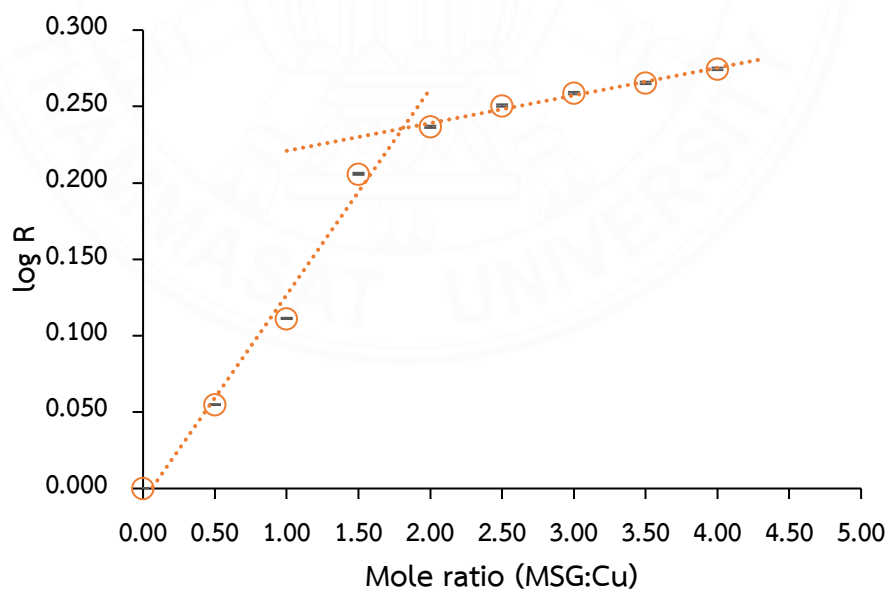


Figure 4.18. The mole ratio method, a graph represents $\log R$ as a function of the mole ratio (MSG: Cu).

4.3.4 Optimization

Univariate optimization was studied, and the initial conditions consisted of Cu(II) MSG at a concentration of $5.91 \times 10^{-2} \text{ mol L}^{-1}$.

4.3.4.1 Effect of Cu(II)

The effect of Cu(II) concentration was studied in the range of $1.25 \times 10^{-3} - 1.88 \times 10^{-2} \text{ mol L}^{-1}$ (Figure 4.19). At $1.25 \times 10^{-3} \text{ mol L}^{-1}$, the lowest signal was presented, and at other concentrations, the signal was increasing until $9.40 \times 10^{-3} \text{ mol L}^{-1}$. After that, the signal was non-significantly different. Thus, $1.25 \times 10^{-2} \text{ mol L}^{-1}$ of Cu(II) was selected for further study.

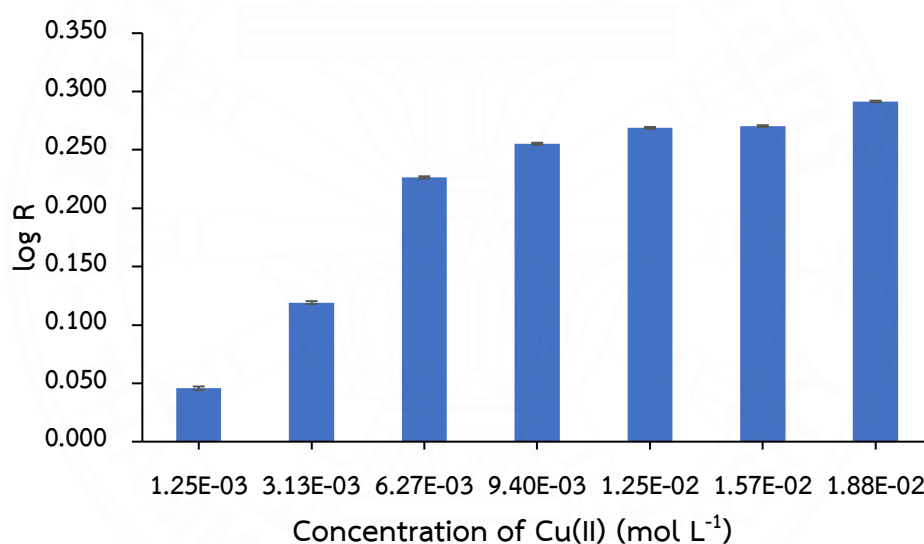


Figure 4.19. Effect of concentrations of Cu(II).

4.3.5 Some analytical features

Under the optimal conditions, some analytical features of this proposed laser-based spectrometer were studied, such as linearity, LOD, LOQ, precision, and accuracy, compared with a commercial spectrophotometer (MAPADA).

4.3.5.1 Linearity

The standard graph was plotted between log R vs MSG concentration (mol L^{-1}) for the proposed laser-based spectrometer. In contrast, the

commercial spectrophotometer presented a graph in function of absorbance and MSG concentration. The standard graphs of both methods were linear in the range of 5.91×10^{-3} - 4.73×10^{-2} mol L⁻¹. The equation obtained from the proposed Laser-based spectrometer was $\log R = 0.7945[\text{MSG}] + 0.0067$, with 0.9987 R², demonstrating an excellent linear relationship between log R and MSG concentration. In contrast, those from the commercial spectrophotometer were Absorbance = 0.9259 [MSG]-0.0229 with R² 0.9983. Both spectrometers presented excellent linearity (R² > 0.99) with a wide range of 5.91×10^{-3} - 4.73×10^{-2} mol L⁻¹ of MSG.

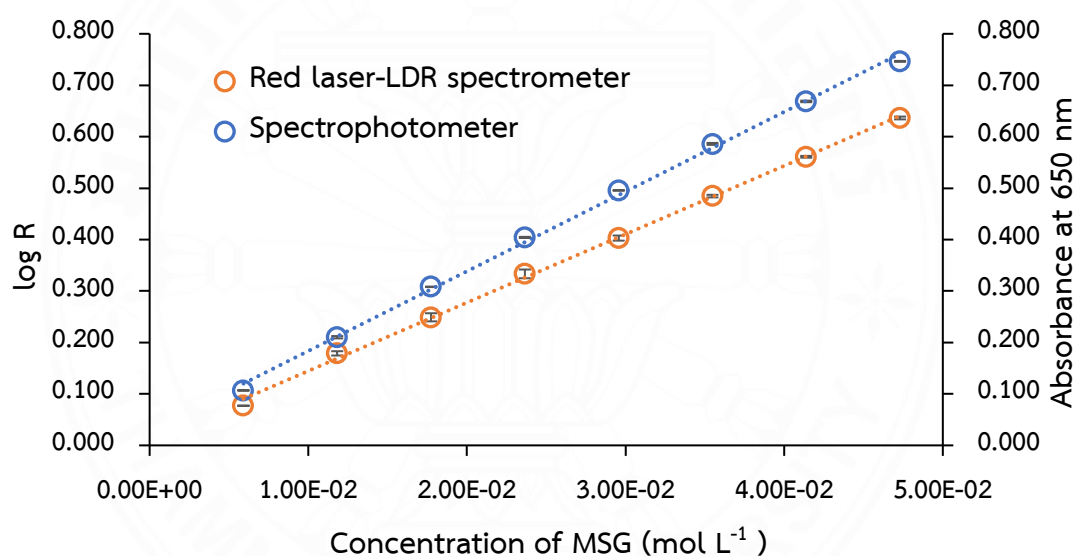


Figure 4.20. The linear graph of a laser-based spectrometer and spectrophotometer for determination of MSG.

4.3.5.2 Limit of detection (LOD) and limit of quantification (LOQ)

The limit of detection (LOD) and limit of quantification (LOQ) were followed by ICH Q2(R2) guideline¹⁰. The LOD and LOQ were calculated by equations $\text{LOD} = 3.3\sigma/S$ and $\text{LOQ} = 10\sigma/S$, respectively, where σ is the standard deviation of blank, and S is the slope of calibration. The LOD and LOQ of the proposed

laser-based spectrometer were 6.50×10^{-3} and 1.95×10^{-2} mol L⁻¹, respectively, whereas those for the spectrophotometer were 1.77×10^{-4} and 5.32×10^{-4} mol L⁻¹.

4.3.5.3 Precision and Accuracy

The precision of the method was described in terms of repeatability. Five times measurements of complex solution (2.96×10^{-2} mol L⁻¹ of MSG) were examined and presented in the percent relative standard deviation (%RSD). The %RSD of the repeatability of the proposed laser-based spectrometer was found to be 1.24. In comparison, the %RSDs of those by the spectrophotometer were 0.11. Both methods provided excellent precision, in which % RSDs were less than 5.

The recovery was evaluated by spiking standards MSG in the sample solution at concentration levels of 5.91×10^{-3} – 2.37×10^{-2} mol L⁻¹. The percentage recoveries were found in the range of 99-111 for both methods, and the results are reported in **Table 4.3**.

Table 4.3.

The recovery studies.

Standard MSG added (mol L ⁻¹)	% Recoveries \pm SD	
	Red laser-LDR spectrometer	Commercial spectrophotometer
5.91×10^{-3}	110.70 \pm 1.10	108.10 \pm 0.63
1.18×10^{-2}	110.30 \pm 0.50	107.70 \pm 0.63
1.77×10^{-2}	104.80 \pm 0.3	105.80 \pm 0.00
2.37×10^{-2}	99.40 \pm 0.5	103.50 \pm 0.16

The concentration of MSG in the sample solution was 1.20×10^{-2} mol L⁻¹.

4.3.6 Application

The proposed laser-based spectrometer and spectrophotometer were used to analyze the amount of MSG in three samples. There was no significant

difference between those results between both methods at a 95% confidence level ($t_{\text{stat}} = 1.23$, $t_{\text{critical}} = 12.71$). Moreover, the amounts of MSG in each sample were found in the range of 15.83 - 101.37 and 16.47 - 102.76 %w/w for laser-based spectrometer and spectrophotometer, respectively. Therefore, this lab-made spectrometer can be alternative equipment for the determination of MSG in flavor enhancers, suitable for field analysis and the example experiment in chemistry class, especially at home.

Table 4.4.

The amount of MSG in samples.

Sample	Amount of MSG (%w/w \pm SD)	
	Red laser-LDR spectrometer	Commercial spectrophotometer
1	15.83 \pm 0.00	16.47 \pm 0.14
2	16.95 \pm 0.23	17.20 \pm 0.13
3	100.37 \pm 1.67	102.76 \pm 0.31

4.4 Roadside test kit using the capillary-driven microfluidic paper-based device for the simultaneous colorimetric detection of THC and EtOH in synthetic saliva samples.

4.4.1 Flow behavior of synthetic salivas with varying viscosity

The human saliva has different viscosities. The SCMC solution was used to represent the viscosity in human saliva. The concentration of SCMC (0.1-1.17% SCMC) in this work is covered in the range of viscosity of natural saliva in humans [(Pungjunun et al., 2021)].

The effect of viscosity on the time of the solution flow to the detection zone is shown in **Figure 4.21**. The results showed that the saliva solution

with different viscosities can flow to the detection zone with the presence of a capillary-driven microfluidic channel on the paper-based device. At the lowest %SCMC in artificial saliva, the lowest time to reach the detection zone (3.00 s) was present. After that, the time to reach the detection zone was increased with an increase of the %SCMC in artificial saliva (0.10 – 1.17 %). The viscosity effect follows the Lucas-Wasburn-Radial equation (Berthier, Gosselin, & Berthier, 2015). The Lucas-Wasburn-Radial equation is shown in Equation 1.

$$z = 4 \sqrt{\frac{\gamma}{\mu}} \sqrt{\cos \Theta} \sqrt{\frac{D_H t}{FR_e}} \dots \dots \dots (1)$$

Where z is the distance of the interface from the inlet (m), γ is the surface tension between liquid and air ($\frac{N}{m}$), μ is the viscosity of the solution ($\frac{N \cdot s}{m^2}$), Θ is the contact angle, t is time (s), FR_e is the constant value depending on the shape of the channel (96), D_H is hydraulic diameter which is expressed in equation 2

$$D_H = 2h \dots \dots \dots (2)$$

Where h is the height (channel thickness, m).

According to equation 1, the viscosity of the solution is proportional to the time of the solution flow, which follows the result that the highest viscosity of %SCMC provides the highest time to reach the detection zone.

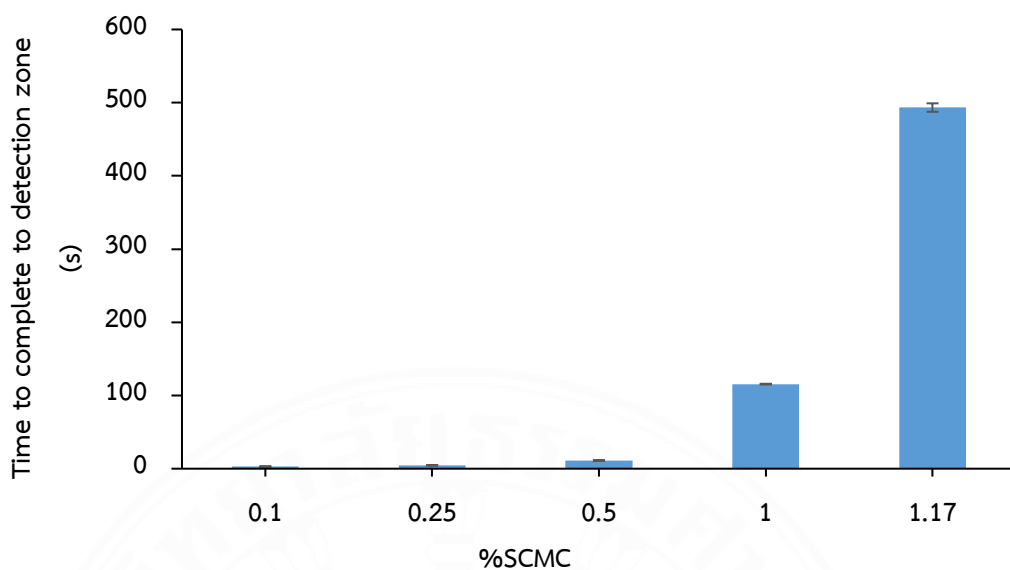


Figure 4.21. The effect of viscosity on time to reach the detection zone.

4.4.2 The effect of viscosity of synthetic salivas for colorimetric detection

EtOH was used as a model to study the effect of viscosity. The delta blue intensity ($B_{\text{EtOH}} - B_{\text{blank}}$) was used to determine EtOH since it provides the highest sensitivity compared to other color intensities. The effect of viscosity on the delta blue intensity of EtOH 1.00 %v/v in 0.100 - 1.17 %SCMC-based synthetic saliva is shown in **Figure 4.22**. The delta blue intensity of each concentration of SCMC-based synthetic saliva is in the range of 8.3 – 9.0, and the %RSD of each concentration is less than 5. Thus, the delta blue intensity was no significant difference in the range of SCMC 0.10 – 1.17%. Therefore, the viscosity is not affected by the colorimetric detection of EtOH.

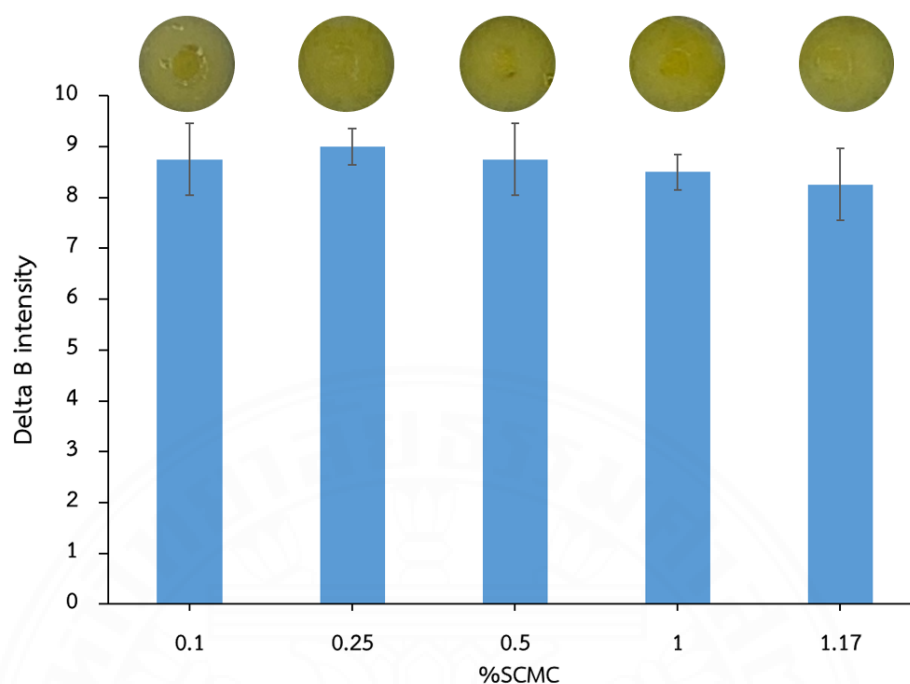


Figure 4.22. The effect of viscosity on the delta blue intensity of EtOH.

4.4.3 Optimization of the device design

The device design, including channel thickness and width, was considered to achieve the lowest time of the solution flow to the detection zone completely.

4.4.3.1 Channel thickness

The optimization of channel thickness is shown in **Figure 4.23**. The channel thickness was studied in the range of 0.1 – 0.5 mm by varying the thickness of the DSA and TPS layers. The time to reach the detection zone completely decreased with increasing channel thickness, which follows the Lucas-Wasburn-Radial equation (Berthier et al., 2015). The result at 0.5 mm of the channel thickness is provided completely at the lowest time of solution flow to the detection zone. So, channel height is indirectly proportional to the time of the solution flow. Thus, 0.5 mm of the channel thickness was selected for further study.

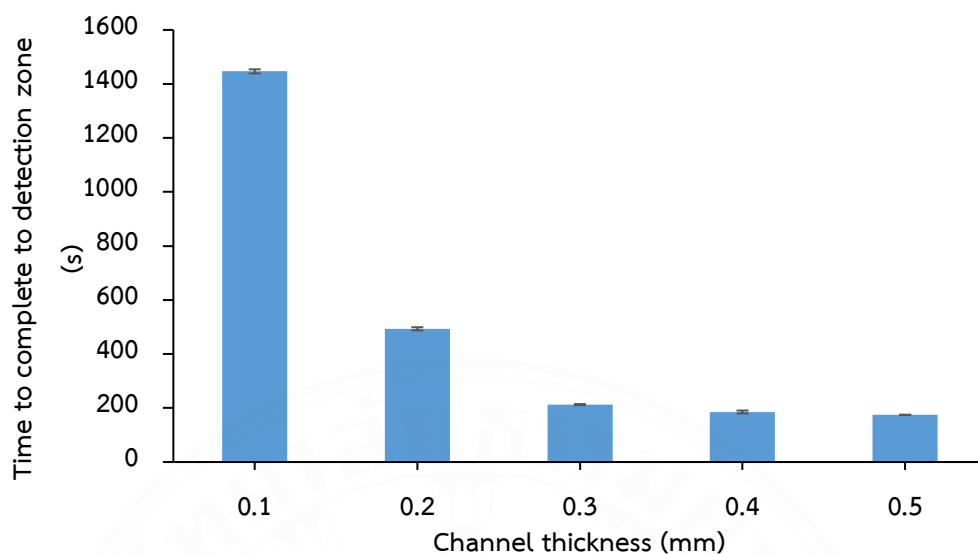


Figure 4.23. The optimization of channel thickness.

4.4.3.2 Channel width

The optimization of channel width is shown in **Figure 4.24**. The channel width was studied in the range of 1.5 – 3.5 mm. The time of solution flow to the detection zone completely was decreased with increasing the channel width. Increasing the channel width causes more solution flow to the detection zone, which makes the time of solution flow to the detection zone completely lower. Thus, the 3.5 mm of the channel width provides the lowest time of solution flow to the detection zone completely. Therefore, 3.5 mm of the channel thickness was selected for further study.

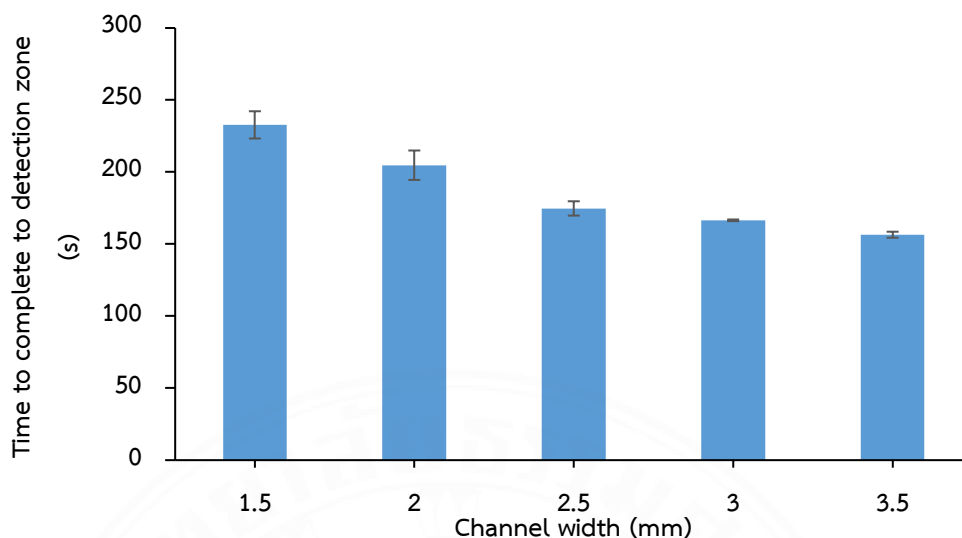


Figure 4.24. The optimization of channel width.

4.4.4 Optimization of the assay condition

To achieve the highest color intensity, the assay conditions were considered, including sample volume, the concentration of dichromate, reaction time of EtOH, reagent volume of fast blue B salt, and reaction time of THC.

4.4.4.1 Sample volume

The optimization of sample volume is shown in **Figure 4.25**. The sample volume was studied in the range of one hundred 100 – 200 μL . The delta blue intensity ($B_{\text{EtOH}} - B_{\text{blank}}$) was increased when the sample volume was increased from 100 to 125 μL . After that, the delta blue intensity showed no significant difference. Thus, the maximum capacity volume of the detection zone is 125 μL . The 125 μL sample volume was selected due to the lowest volume, which provides the highest delta blue intensity for further study.

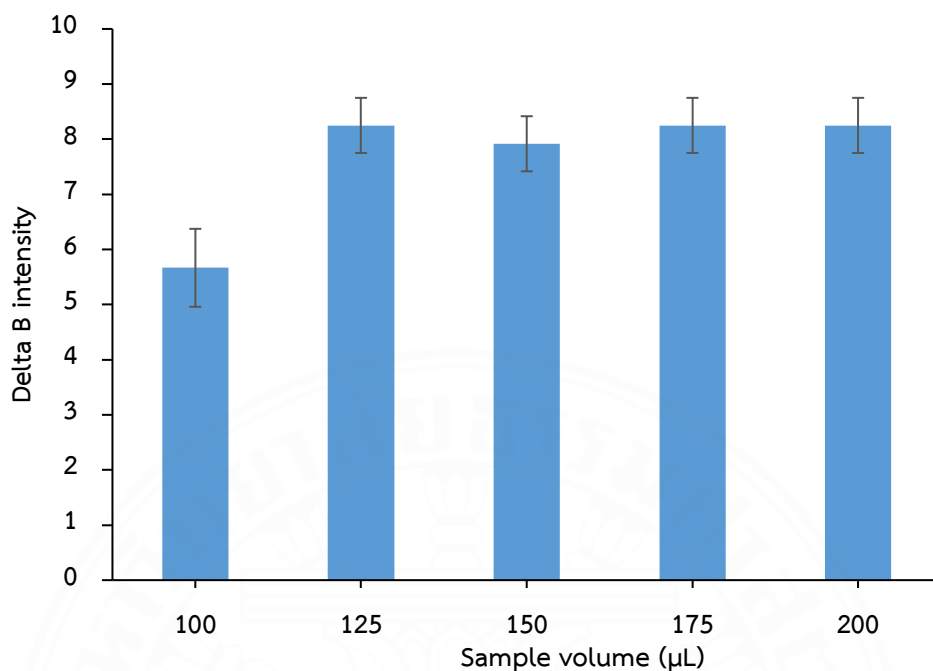


Figure 4.25. The optimization of sample volume.

4.4.4.2 Concentration of dichromate

The optimization concentration of dichromate is shown in Figure 4.26. The concentration of dichromate reagent was studied in the range of 0.1 – 1 mol L⁻¹. The delta blue intensity ($B_{\text{EtOH}} - B_{\text{blank}}$) was increased when the dichromate concentration reached 0.4 mol L⁻¹. After that, the delta blue intensity was decreased due to the high color background of the reagent. Thus, 0.4 mol L⁻¹ of dichromate was selected as an optimum value.

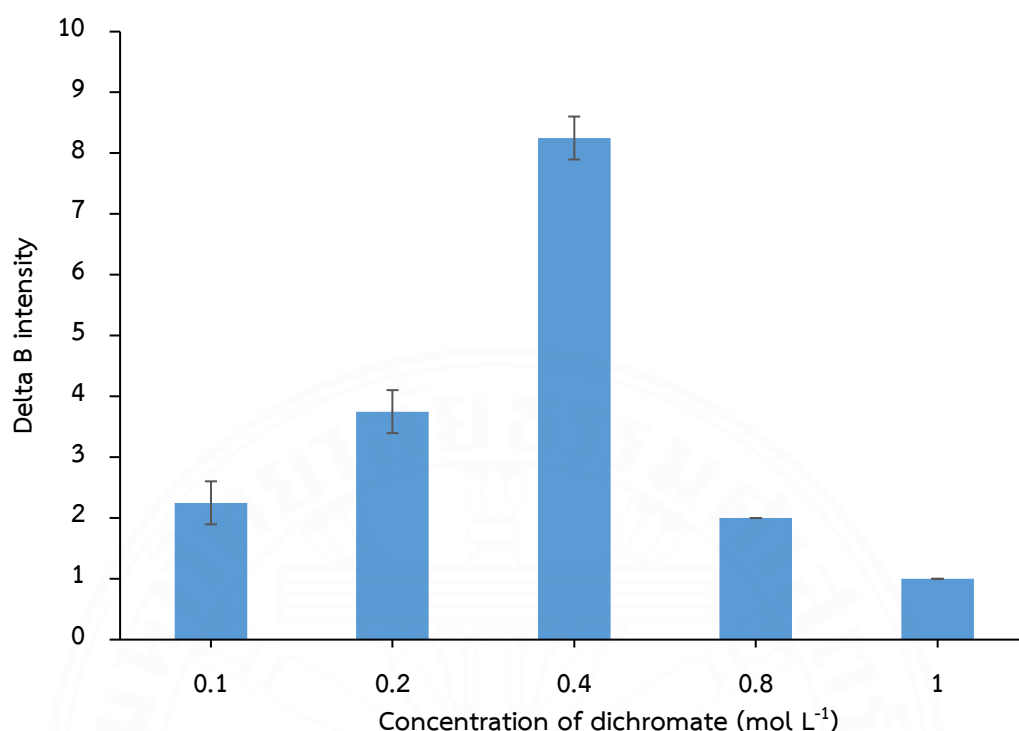


Figure 4.26. The optimization concentration of dichromate.

4.4.4.3 Reaction time of colorimetric detection of EtOH

The optimization of the reaction time of EtOH is shown in **Figure 4.27**. The reaction time of colorimetric detection of EtOH was studied in the range of 10 – 120 minutes. The delta blue intensity ($B_{\text{EtOH}} - B_{\text{blank}}$) was increased when the time was increased to 30 minutes because the concentration of Cr(III), which produces a green color, is increased due to ethanol not being fully oxidized to acetic acid. After 30 minutes, the delta blue intensity showed no significant difference because ethanol is fully oxidized to acetic acid. Thus, 30 minutes was selected as the optimal reaction time for ethanol.

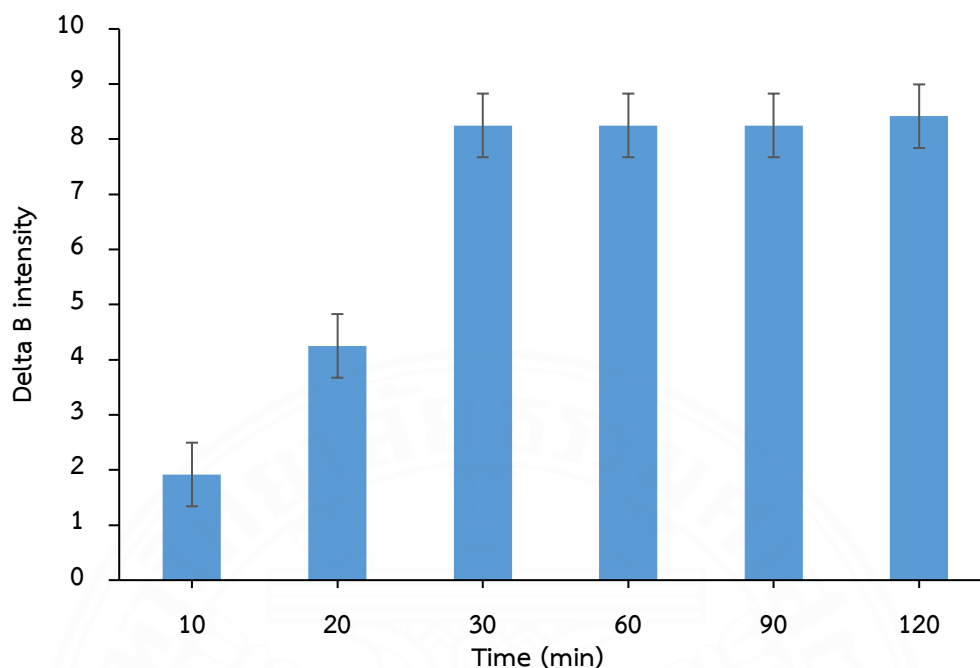


Figure 4.27. The optimization of reaction time of ethanol.

4.4.4.4 Reagent volume of fast blue B salt

According to 2.0 %w/v, the highest concentration of fast blue B salt can be prepared. The reagent volume of fast blue B salt was studied to achieve the highest color intensity. The delta green intensity ($G_{\text{blank}} - G_{\text{THC}}$) was used to determine THC provides the highest sensitivity compared to other color intensities. The optimization of the reagent volume of fast blue B salt is shown in **Figure 4.28**. The reagent volume of fast blue B salt was studied in the range of 1-5 μL . The delta green intensity was increased when the volume of fast blue B salt reagent increased until 3 μL due to the increased coupling product between THC and fast blue B salt. After 3 μL of the fast blue B salt reagent, the delta green intensity was no significant difference due to THC fully coupling with the fast blue B salt reagent. Therefore, 3 μL was selected as the optimum reagent volume of fast blue B salt.

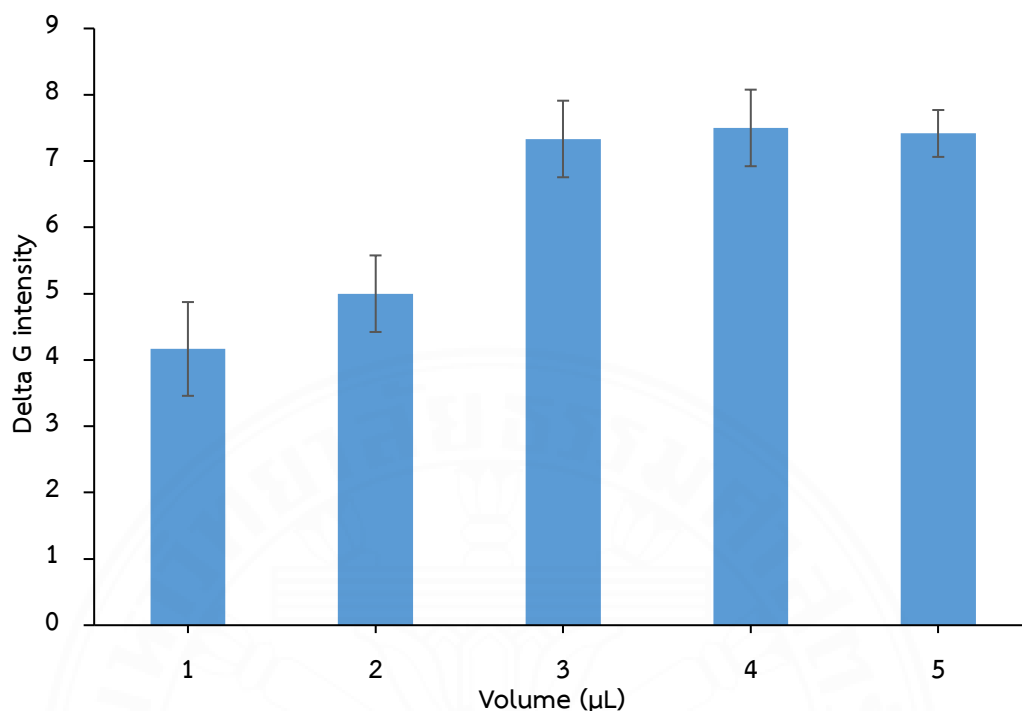


Figure 4.28. The optimization of reagent volume of fast blue B salt.

4.4.4.5 Reaction time of colorimetric detection of THC

The optimization of the reaction time of THC is shown in **Figure 4.29**. The reaction time of colorimetric detection of THC was studied in the range of 10 – 120 minutes. The delta green intensity ($G_{\text{blank}} - G_{\text{THC}}$) was increased when the time was increased to 30 minutes due to the increased coupling product between THC and fast blue B salt reagent. After 30 minutes, the delta green intensity showed no significant difference due to THC fully coupling with the fast blue B salt reagent. Thus, 30 minutes was selected as the optimal reaction time for THC.

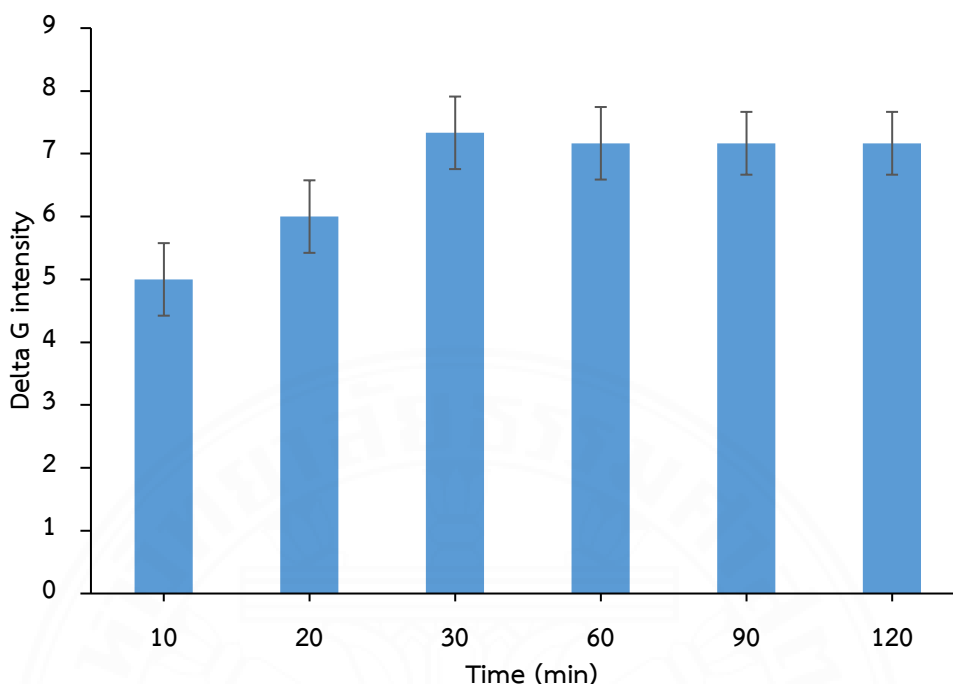


Figure 4.29. The optimization of reaction time of THC.

4.4.5 Some Analytical Features

Under the optimal conditions, some analytical features of the capillary-driven microfluidic paper-based device, such as linearity, LOD, and precision, were studied.

4.4.5.1 Linearity

The calibration curve of EtOH between delta blue intensity ($B_{\text{EtOH}} - B_{\text{blank}}$) and EtOH concentration was plotted. Also, the calibration curve of THC between delta green intensity ($G_{\text{blank}} - G_{\text{THC}}$) and THC concentration was plotted. The calibration curves of EtOH and THC are shown in **Figure 4.30 and 4.31**, respectively. Both calibration curves were linear in the range of 0.1 – 5.0 %v/v EtOH and 0.1 – 10 mg L⁻¹ THC, respectively. The equation obtained from the calibration curve of EtOH was $y = 5.5761x + 1.6938$, with R^2 of 0.9951. In contrast, those from the calibration curve of THC were $y = 4.557 \log(x) + 7.5707$ with R^2 of 0.9967, demonstrating an excellent linear relationship.

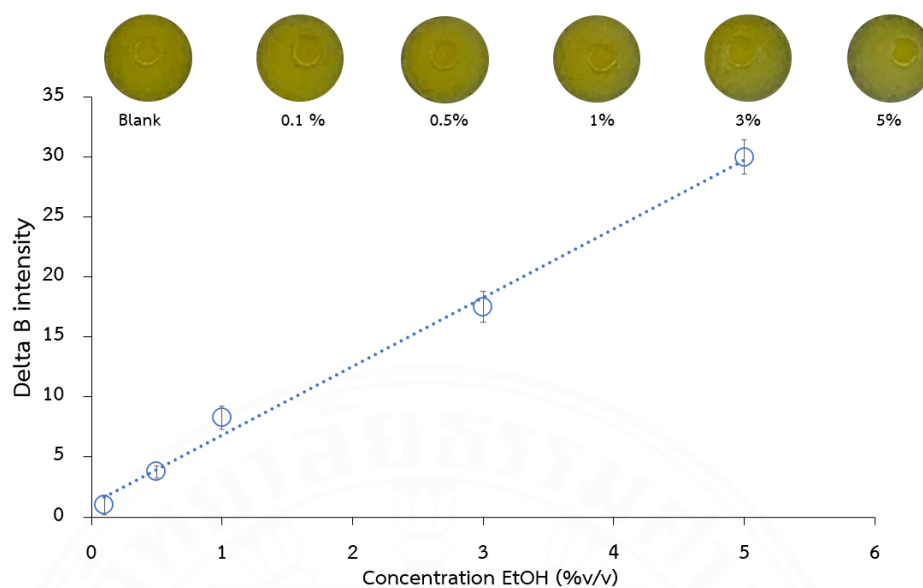


Figure 4.30. The calibration curve of EtOH.

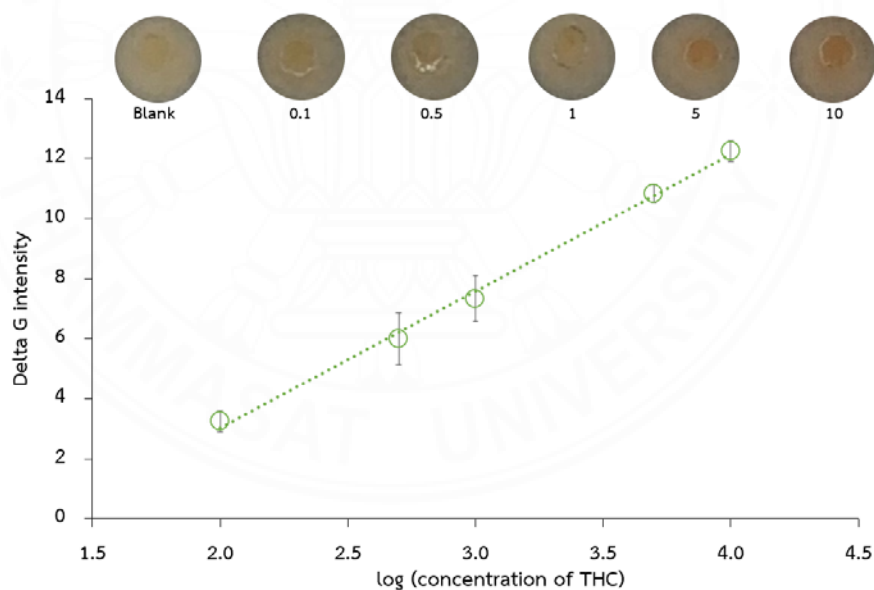


Figure 4.31. The calibration curve of THC.

4.4.5.2 Limit of detection (LOD)

The LOD was calculated by equations, $LOD = 3\sigma/S$, where σ is the standard deviation of blank, and S is the slope of calibration. The LOD of EtOH

and THC determination were 0.08 %v/v and 0.06 mg L⁻¹, respectively. The determination of EtOH and THC in saliva is shown in **Table 4.5**. The LOD of ethanol is sufficient to detect EtOH in saliva, which follows the legal blood alcohol concentration limit in some countries, such as Canada (0.64 %v/v) and Thailand (0.4 %v/v) (Kaewnu et al., 2021). However, the LOD of THC is not sufficient to detect THC in saliva, which follows the legal blood THC concentration limit in some countries, such as the state of Colorado, which is 5.00 × 10⁻³ mg L⁻¹ (Small, 2015). The proposed method provided better LOD of THC than other works in the list. Although the detection time for this work is inferior to some works, exploitations in terms of without sample preparation step, low LOD for THC, a more comprehensive linear range for THC, portable and sufficient to detect ethanol which follows legal limits are keys factors that make this work can be an alternative portable device for ethanol and THC detection in saliva.

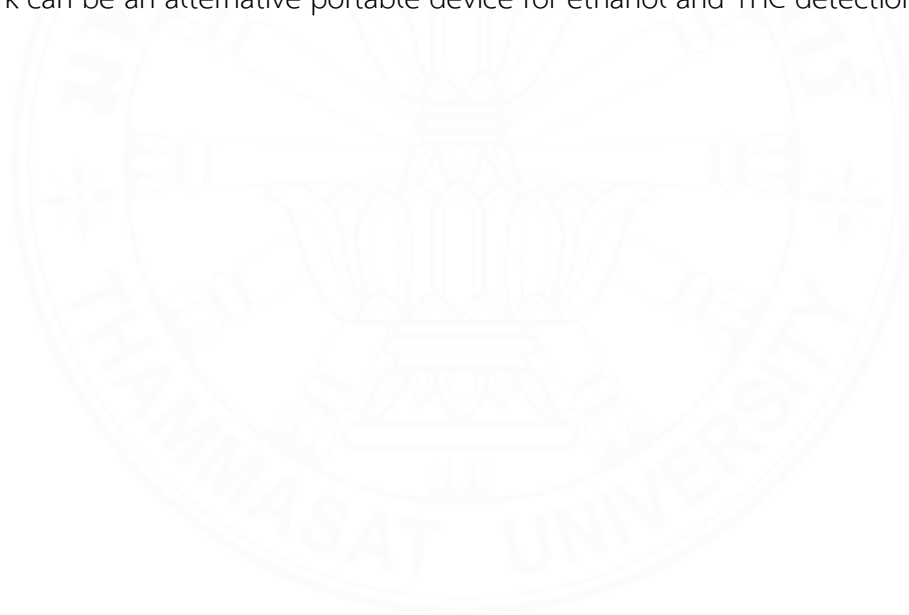


Table 4.5.

The determination of EtOH and THC in saliva.

Method	Sample preparation	Analyte		Linear range		LOD		Detection time (min)	Reference
		EtOH	THC	EtOH (%v/v)	THC (mg L ⁻¹)	EtOH (%v/v)	THC (mg L ⁻¹)		
Electrochemical sensor	✓	✗	THC	✗	3.14×10 ⁻² - 1.57	✗	31.0×10 ⁻²	5	(Majak et al., 2021)
Electrochemical sensor and colorimetric	✓	EtOH	THC	5.84×10 ⁻⁴ - 5.84×10 ⁻³	3.14 × 10 ⁻¹ - 1.89	✗	15.7×10 ⁻²	3	(Mishra et al., 2020)
Colorimetric sensor	✓	EtOH	✗	0.580-14.0	✗	3.00×10 ⁻²	✗	60	(Kaewnu et al., 2021)
Colorimetric sensor	✗	EtOH	THC	1.00×10 ⁻¹ - 5.00	1.00×10 ⁻¹ - 10.0	8.00×10 ⁻²	6.00×10 ⁻²	30	This work

4.4.5.3 Reproducibility

The reproducibility was expressed by %RSD with seven replicates of the measurement of 1.0 %v/v of EtOH and 1 mg L⁻¹ of THC. The %RSD of EtOH determination and THC determination is 4.81 and 6.69, respectively. Both reproducibilities follow the AOAC 2016 guideline, which shows good precision.

4.4.6 Stability

The Stability was expressed by %error compare with day 1 with three replicates of the measurement of 1.0 %v/v of EtOH and 1 mg L⁻¹ of THC for day 1-7. The stability study is shown in **Figure 4.32 and 4.33**. The %error of EtOH determination and THC determination for day 3, 5, 7 is in the range of 0-3% and 2-4%, respectively. Both shows good stability due to %error is less than 5%. Therefore, the fabricated device can be kept in desiccator at least 7 days before detection of EtOH and THC.

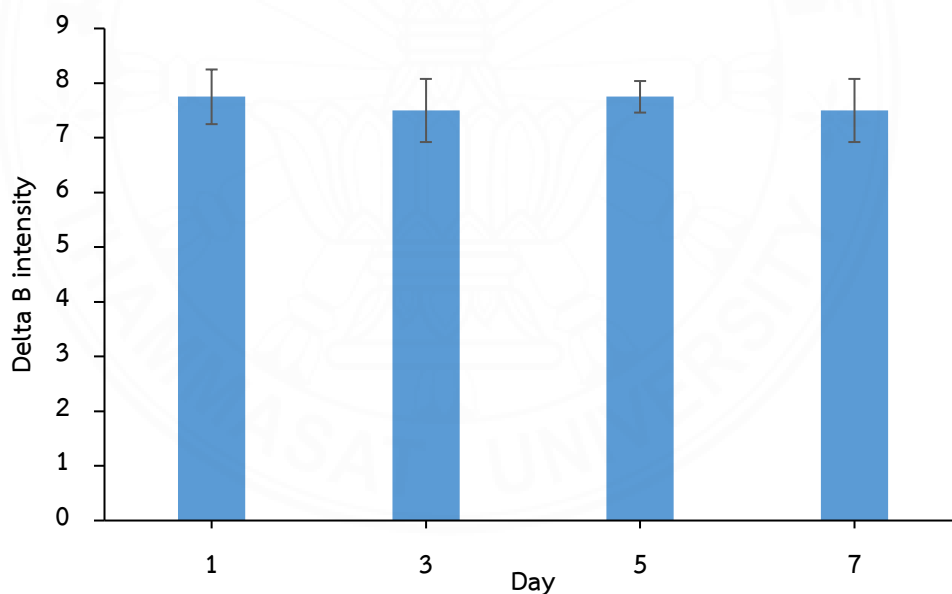


Figure 4.32. The stability study for EtOH detection.

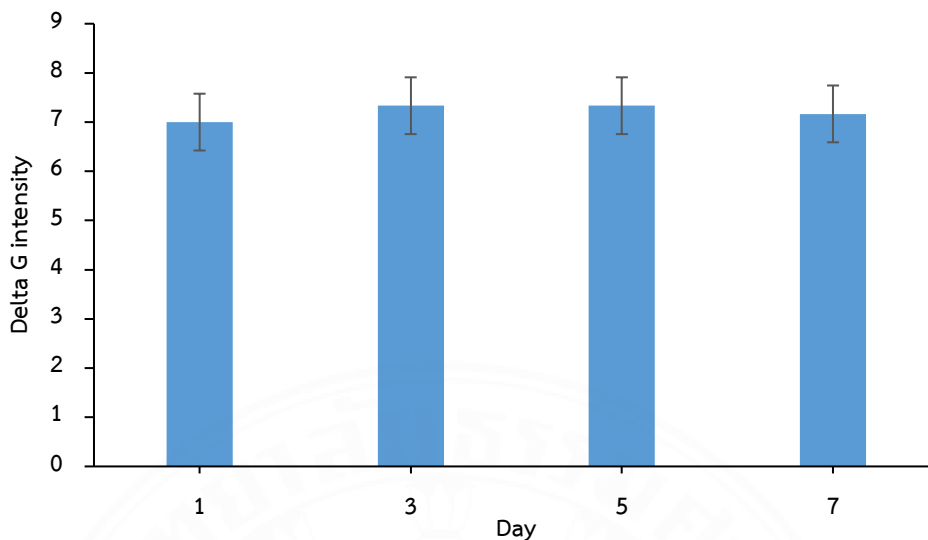


Figure 4.33. The stability study for THC detection.

4.4.7 Interference study

The common ions and compounds found in saliva were used to test. The concentration of each interference found in saliva is followed by (Ngamchuea, Chaisiwamongkhon, Batchelor-McAuley, & Compton, 2018) and (Dame et al., 2015) is shown in **Table 4.6**. The interference effect was expressed by equations, %error = ((delta color intensity of analyte with interference/delta color intensity of analyte) × 100) - 100.

Table 4.6.

The concentration of common ions and compounds in human saliva.

Ion/compound	Concentration (mmol L ⁻¹)
Na ⁺	80.0
HCO ³⁻	80.0
SCN ⁻	2.00
Ca ²⁺	1.00
K ⁺	20.0

Table 4.6.

The concentration of common ions and compounds in human saliva. (Cont.)

Ion/compound	Concentration (mmol L ⁻¹)
Cl ⁻	100
Mg ²⁺	0.200
PO ₄ ³⁻	4.00
Glucose	0.250
Sucrose	0.050
Ascorbic	0.010

4.4.7.1 Interference study for EtOH detection

The interference for EtOH detection is shown in **Figure 4.34**. The delta blue intensity ($B_{\text{EtOH}} - B_{\text{blank}}$) results between EtOH and EtOH with any interferences were compared. The delta blue intensity is not significantly different for only EtOH and EtOH with interferences. The %error is in the range of 1.01-3.03, which indicates that the typical concentration of the interference does not affect EtOH determination due to a %error of less than 5, which means there is no effect from the interference.

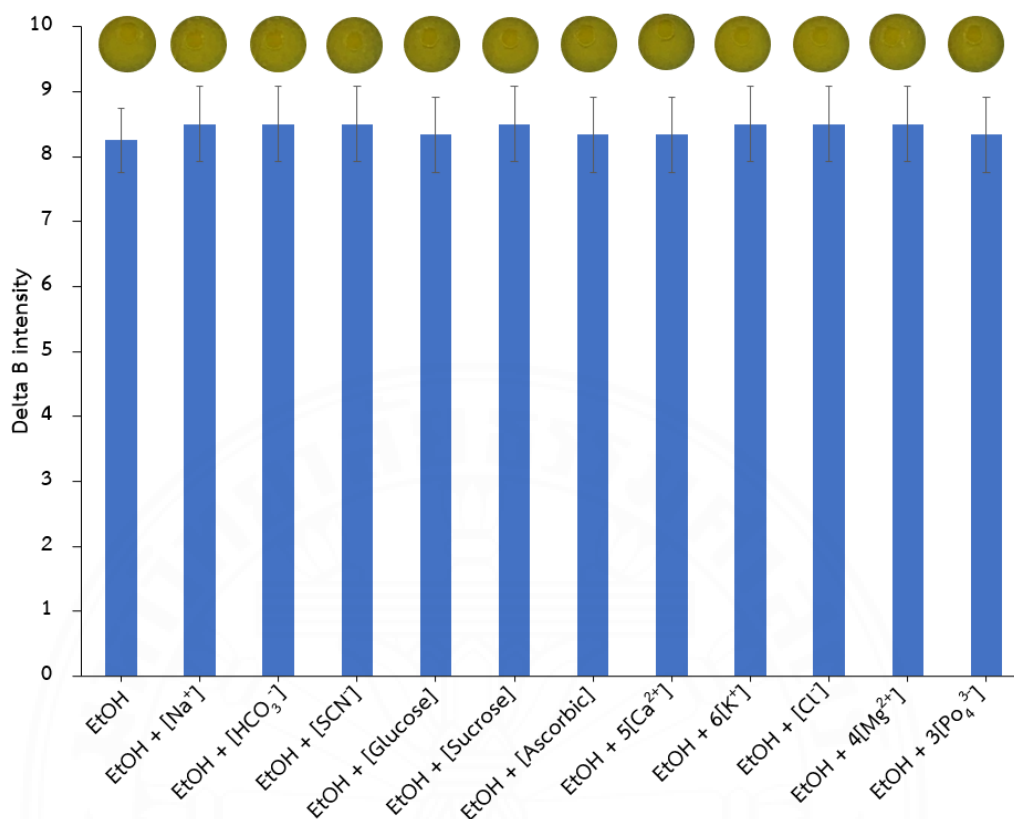


Figure 4.34. The interference study for EtOH detection.

4.4.7.2 Interference study for THC detection

The interference for THC detection is shown in **Figure 4.35**. The delta green intensity ($G_{\text{blank}} - G_{\text{THC}}$) results were compared between THC and THC with interference. The delta green intensity is not significantly different for only THC and THC with interference. The %error is in the range of 1.14-2.27, which indicates that the typical concentration of the interference does not affect THC determination because a %error of less than 5 means there are no effects from the interference.

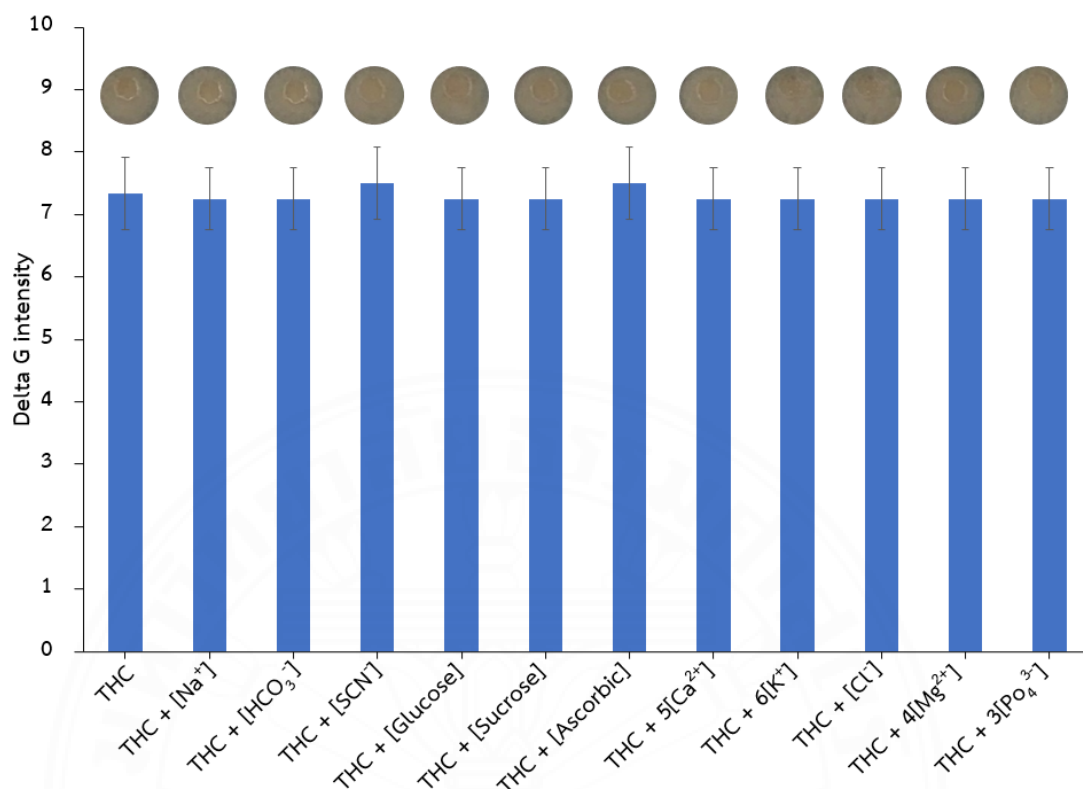


Figure 4.35. The interference study for THC detection.

4.4.8 Feasibility of developed device for simultaneous detection of EtOH and THC

The cross-talk detection between EtOH and THC is shown in **Figures 4.36 and 4.37**. In **Figure 4.36**, the delta blue intensity ($B_{\text{EtOH}} - B_{\text{blank}}$) between EtOH and a mixed solution of EtOH and THC showed no significant difference because the %error is less than 5. The delta blue intensity of THC is close to blank. Thus, EtOH in the presence of THC can be measured without concerning the interference effect of THC when using a dichromate reagent.

In **Figure 4.37**, the delta green intensity ($G_{\text{blank}} - G_{\text{THC}}$) between THC and a mixed solution of EtOH and THC showed no significant difference because the %error is less than 5. The delta green intensity of EtOH is close to blank. Thus, THC in the presence of EtOH can be measured without concerning the interference effect of EtOH when using a fast blue B salt reagent.

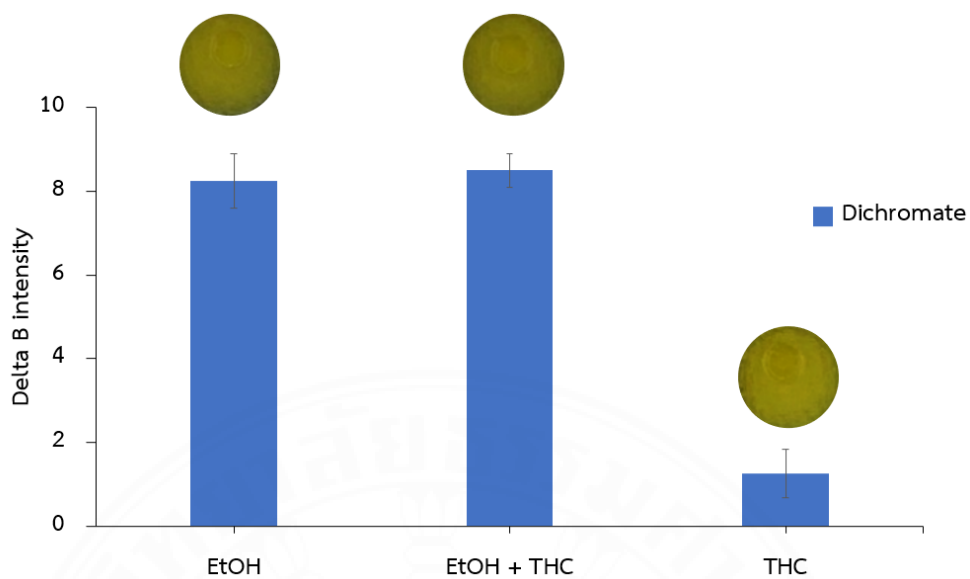


Figure 4.36. The detection of EtOH in the presence of THC.

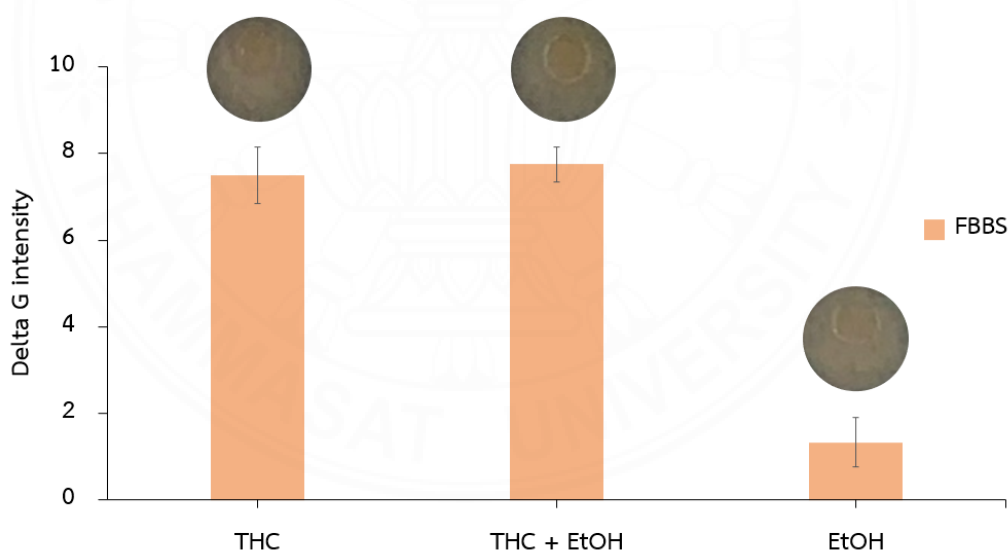


Figure 4.37. The detection of THC in the presence of EtOH.

4.4.9 Recovery

The feasibility of simultaneous detection of EtOH and THC is expressed in % Recovery. The feasibility of simultaneous detection of EtOH and THC results is shown in **Table 4.7**. 5 samples with different %SCMC were used to study the

% recovery. The % recovery for EtOH and THC are in the range of 98% – 102% and 95% – 105.2%, respectively, which follow the AOAC 2016 guideline. Thus, the capillary-driven microfluidic paper-based device can be used for simultaneous colorimetric detection of THC and EtOH in synthetic saliva samples with acceptable accuracy.



Table 4.7.

The feasibility of simultaneous detection of EtOH and THC.

No. sample	%SCMC	Analyte	Added	Found \pm SD	% Recovery \pm SD
1	1.17	EtOH (%v/v)	0.8	0.8 \pm 0.1	101 \pm 9
		THC (mg L ⁻¹)	0.8	0.8 \pm 0.1	95 \pm 7
		EtOH (%v/v)	2.0	2.0 \pm 0.1	98 \pm 4
		THC (mg L ⁻¹)	3.0	2.9 \pm 0.2	97 \pm 5
2	1.00	EtOH (%v/v)	0.8	0.8 \pm 0.1	98 \pm 9
		THC (mg L ⁻¹)	0.8	0.8 \pm 0.1	102 \pm 7
		EtOH (%v/v)	2.0	2.0 \pm 0.1	98 \pm 4
		THC (mg L ⁻¹)	3.0	3.0 \pm 0.2	100 \pm 5
3	0.50	EtOH (%v/v)	0.8	0.8 \pm 0.1	98 \pm 9
		THC (mg L ⁻¹)	0.8	0.8 \pm 0.1	102 \pm 7
		EtOH (%v/v)	2.0	2.0 \pm 0.1	101 \pm 5
		THC (mg L ⁻¹)	3.0	3.1 \pm 0.2	104 \pm 6
4	0.25	EtOH (%v/v)	0.8	0.8 \pm 0.1	98 \pm 9
		THC (mg L ⁻¹)	0.8	0.8 \pm 0.1	102 \pm 7

Table 4.7.

The feasibility of simultaneous detection of EtOH and THC. (Cont.)

No. sample	%SCMC	Analyte	Added	Found \pm SD	% Recovery \pm SD
		EtOH (%v/v)	2.0	2.0 \pm 0.1	98 \pm 7
		THC (mg L ⁻¹)	3.0	3.0 \pm 0.2	100 \pm 5
5	0.10	EtOH (%v/v)	0.8	0.8 \pm 0.1	101 \pm 9
		THC (mg L ⁻¹)	0.8	0.8 \pm 0.1	101 \pm 7
		EtOH (%v/v)	2.0	2.0 \pm 0.1	102 \pm 4
		THC (mg L ⁻¹)	3.0	3.2 \pm 0.2	105 \pm 5

CHAPTER 5

CONCLUSIONS AND RECOMMENDATIONS

This work is successful in inventing a spectrometer for colorimetric analysis of tetracycline hydrochloride (TCH), monosodium glutamate (MSG), delta-9-tetrahydrocannabinol (THC), and ethanol (EtOH) with two systems: laser pointer – light dependence resistor (LDR); and integrating of the capillary-driven microfluidic platform with the paper-based device.

5.1 Lab-made spectrometer

A simple spectrometer was designed and invented with simple components such as a laser pointer, light-dependent resistor (LDR), plastic holder, and multi-meter. Moreover, the car sun-protective films with various transmissions were used to test the relation of resistance and transmittance/absorbance. It was found that the relationships of absorbance and $\log R$ were linear with the coefficient of determination (R^2) > 0.990.

The systems were applied to determine tetracycline hydrochloride (TCH) and monosodium glutamate (MSG) using blue and red laser pointers, respectively. The determination of TCH and MSG is based on complex formation with Fe(III) and Cu(II), subsequently producing red and blue color solutions. The proposed systems presented the linearity in the concentration range of TCH and MSG were 1.15×10^{-4} – 5.74×10^{-6} mol L⁻¹ (R^2 0.9987) with LOD 1.44×10^{-6} mol L⁻¹; and 2.96×10^{-3} – 4.73×10^{-2} mol L⁻¹ (R^2 0.9987) with LOD 6.50×10^{-4} mol L⁻¹; respectively. The relative standard deviations (%RSDs) of repeatability were 1.30 for TCH and 1.24 for MSG. The proposed spectrometers successfully determined TCH in pharmaceuticals and MSG in flavor enhancers compared to a commercial spectrophotometer, with no significant difference at a 95% confidence level. This process of invention and testing is simple. Moreover, with the simple reaction, it should be an experiment or small project for

undergraduate students to understand the fundamentals of spectrometry and Beer's Law.

5.2 The capillary-driven microfluidic paper-based device

The capillary-driven microfluidic paper-based device successfully delivered the SCMC-based synthetic saliva from the sample insertion zone to the detection zone for all the concentrations of %SCMC-based synthetic saliva, including all the viscosity of human saliva range without sample dilution step. The proposed device is sufficient to determine ethanol in synthetic saliva, which follows the legal blood alcohol concentration limit in some countries, such as Canada (0.640 %v/v) and Thailand (0.400 %v/v). For THC detection, The proposed method provided a lower LOD of THC than other works in the list (Mishra et al., 2020) (Majak et al., 2021). Moreover, the device can measure THC and ethanol with the maximum concentration of some ions and compounds in real human saliva without interference. The device can simultaneously detect ethanol and THC without interference from each analyte and viscosity with acceptable accuracy. According to all of the studies, the developed device has the potential to be a prototype for a roadside testing platform.

REFERENCES

Books and Book Articles

- Driscoll, W. G. (1969). Chapter 4 - Spectrophotometers. In R. Kingslake (Ed.), *Applied Optics and Optical Engineering* (Vol. 5, pp. 85-104): Elsevier.
- Henry-Unaeze, H. N. (2022). Chapter 17 - Monosodium glutamate in foods and its biological importance. In A. Martinović, S. Oh, & H. Lelieveld (Eds.), *Ensuring Global Food Safety (Second Edition)* (pp. 341-357): Academic Press.
- Papich, M. G. (2021). Tetracycline, Tetracycline Hydrochloride. In M. G. Papich (Ed.), *Papich Handbook of Veterinary Drugs (Fifth Edition)* (pp. 883-885). St. Louis (MO): W.B. Saunders.
- Silva-Neto, H. A., Sousa, L. R., & Coltro, W. K. T. (2022). Chapter 4 - Colorimetric paper-based analytical devices. In W. R. de Araujo & T. R. L. C. Paixão (Eds.), *Paper-based Analytical Devices for Chemical Analysis and Diagnostics* (pp. 59-79): Elsevier.

Articles

- Acebal, C. C., Insausti, M., Pistonesi, M. F., Lista, A. G., & Band, B. S. F. (2010). A new automated approach to determine monosodium glutamate in dehydrated broths by using the flow-batch methodology. *Talanta*, *81*(1), 116-119.
doi:<https://doi.org/10.1016/j.talanta.2009.11.045>
- Acebal, C. C., Lista, A. G., & Fernández Band, B. S. (2008). Simultaneous determination of flavor enhancers in stock cube samples by using spectrophotometric data and multivariate calibration. *Food Chemistry*, *106*(2), 811-815.
doi:<https://doi.org/10.1016/j.foodchem.2007.06.009>
- Al Momani, F. A., & Örmeci, B. (2014). Measurement of polyacrylamide polymers in water and wastewater using an in-line UV-vis spectrophotometer. *Journal of Environmental Chemical Engineering*, *2*(2), 765-772.
doi:<https://doi.org/10.1016/j.jece.2014.02.015>

- Ali, H. M., Hammad, S. F., & El-Malla, S. F. (2021). Green spectrophotometric methods for determination of a monosodium glutamate in different matrices. *Microchemical Journal*, *169*, 106622.
doi:<https://doi.org/10.1016/j.microc.2021.106622>
- Alnokkari, A., Mounir, A., & Zaid, A. (2013). Colorimetric Determination of Monosodium Glutamate in Food Samples Using Colorimetric Determination of Monosodium Glutamate in Food Samples Using L-glutamate Oxidase-glutamate Oxidase. *Chinese Journal of Applied Environmental Biology*, *19*, 1069.
doi:10.3724/SP.J.1145.2013.01069
- Altunay, N., Elik, A., Tuzen, M., Lanjwani, M. F., & Mogaddam, M. R. A. (2023). Determination and extraction of acrylamide in processed food samples using alkanol-based supramolecular solvent-assisted dispersive liquid-liquid microextraction coupled with spectrophotometer: Optimization using factorial design. *Journal of Food Composition and Analysis*, *115*, 105023.
doi:<https://doi.org/10.1016/j.jfca.2022.105023>
- Andrews, J. L., de Los Rios, J. P., Rayaluru, M., Lee, S., Mai, L., Schusser, A., & Mak, C. H. (2020). Experimenting with At-Home General Chemistry Laboratories During the COVID-19 Pandemic. *Journal of Chemical Education*, *97*(7), 1887-1894.
doi:10.1021/acs.jchemed.0c00483
- Anirudhan, T. S., & Alexander, S. (2015). Selective determination of monosodium glutamate (Ajinomoto) in food samples using a potentiometric method with a modified multiwalled carbon nanotube based molecularly imprinted polymer. *RSC Advances*, *5*(117), 96840-96850. doi:10.1039/C5RA17885A
- Aronson, J. K. (2012). 25 - Penicillins, cephalosporins, other beta-lactam antibiotics, and tetracyclines. In J. K. Aronson (Ed.), *Side Effects of Drugs Annual* (Vol. 34, pp. 385-397): Elsevier.
- Aryal, P., Brack, E., Alexander, T., & Henry, C. S. (2023). Capillary Flow-Driven Microfluidics Combined with a Paper Device for Fast User-Friendly Detection of Heavy Metals in Water. *Analytical Chemistry*, *95*(13), 5820-5827.
doi:10.1021/acs.analchem.3c00378

- Aung, H.-P., & Pyell, U. (2016). In-capillary derivatization with o-phthalaldehyde in the presence of 3-mercaptopropionic acid for the simultaneous determination of monosodium glutamate, benzoic acid, and sorbic acid in food samples via capillary electrophoresis with ultraviolet detection. *Journal of Chromatography A*, 1449, 156-165.
doi:<https://doi.org/10.1016/j.chroma.2016.04.033>
- Bagheri, A. (2015). Thermodynamic Studies of Metal Complexes of Tetracycline and its Application in Drug Analysis. *Pharmaceutical Chemistry Journal*, 48(11), 765-769. doi:10.1007/s11094-015-1190-3
- Bao, J., & Nagayama, G. (2023). Optimization for ultrafast capillary-driven flow in open rectangular microchannels. *International Journal of Heat and Mass Transfer*, 201, 123629. doi:<https://doi.org/10.1016/j.ijheatmasstransfer.2022.123629>
- Benhabib, M., & Li, X. (2021). 14 - Paper-based microfluidic devices for low-cost assays. In X. Li & Y. Zhou (Eds.), *Microfluidic Devices for Biomedical Applications (Second Edition)* (pp. 551-585): Woodhead Publishing.
- Berthier, J., Gosselin, D., & Berthier, E. (2015). A generalization of the Lucas–Washburn–Rideal law to composite microchannels of arbitrary cross section. *Microfluidics and Nanofluidics*, 19(3), 497-507. doi:10.1007/s10404-014-1519-3
- Bourquin, D., & Brenneisen, R. (1987). Determination of the major Δ^9 -tetrahydrocannabinol metabolite in urine by high-performance liquid chromatography and photodiode array detection. *Analytica Chimica Acta*, 198, 183-189. doi:[https://doi.org/10.1016/S0003-2670\(00\)85018-7](https://doi.org/10.1016/S0003-2670(00)85018-7)
- Burckhardt-Herold, S., Klotz, J., Funk, F., Büchi, R., Petrig-Schaffland, J., & Geisser, P. (2007). Interactions between iron (III)-hydroxide polymaltose complex and commonly used drugs: Simulations and in vitro studies. *Arzneimittel-Forschung*, 57, 360-369. doi:10.1055/s-0031-1296684
- Cai, L., Wu, Y., Xu, C., & Chen, Z. (2013). A Simple Paper-Based Microfluidic Device for the Determination of the Total Amino Acid Content in a Tea Leaf Extract. *Journal of Chemical Education*, 90(2), 232-234. doi:10.1021/ed300385j

- Caroline Nava Pinheiro, A., Souza Ferreira, V., & Gabriel Lucca, B. (2022). Stamping method based on 3D printing and disposable napkin: Cheap production of paper analytical devices for alcohol determination in beverages aiming forensics and food control. *Microchemical Journal*, 180, 107604. doi:<https://doi.org/10.1016/j.microc.2022.107604>
- Casella, I. G., & Picerno, F. (2009). Determination of Tetracycline Residues by Liquid Chromatography Coupled with Electrochemical Detection and Solid Phase Extraction. *Journal of Agricultural and Food Chemistry*, 57(19), 8735-8741. doi:10.1021/jf902086y
- Cebi, N., Dogan, C. E., Olgun, E. O., & Sagdic, O. (2018). A survey of free glutamic acid in foods using a robust LC-MS/MS method. *Food Chemistry*, 248, 8-13. doi:<https://doi.org/10.1016/j.foodchem.2017.12.033>
- Chapman, J., Gangadoo, S., Truong, V. K., & Cozzolino, D. (2019). Spectroscopic approaches for rapid beer and wine analysis. *Current Opinion in Food Science*, 28, 67-73. doi:<https://doi.org/10.1016/j.cofs.2019.09.001>
- Chng, J. J. K., & Patuwo, M. Y. (2021). Building a Raspberry Pi Spectrophotometer for Undergraduate Chemistry Classes. *Journal of Chemical Education*, 98(2), 682-688. doi:10.1021/acs.jchemed.0c00987
- Dame, Z. T., Aziat, F., Mandal, R., Krishnamurthy, R., Bouatra, S., Borzouie, S., . . . Wishart, D. S. (2015). The human saliva metabolome. *Metabolomics*, 11(6), 1864-1883. doi:10.1007/s11306-015-0840-5
- Danchana, K., Iwasaki, H., Ochiai, K., Namba, H., & Kaneta, T. (2022). Determination of glutamate using paper-based microfluidic devices with colorimetric detection for food samples. *Microchemical Journal*, 179, 107513. doi:<https://doi.org/10.1016/j.microc.2022.107513>
- Deschamps, P., Naima, Z., Nicolis, I., Martens, T., Curis, E., Charlot, M. F., . . . Tomas, A. (2003). Copper(II)-L-glutamine complexation study in solid state and in aqueous solution. *Inorganica Chimica Acta - INORG CHIM ACTA*, 353, 22-34. doi:10.1016/S0020-1693(03)00218-4

- Devi, R., Gogoi, S., Barua, S., Sankar Dutta, H., Bordoloi, M., & Khan, R. (2019). Electrochemical detection of monosodium glutamate in foodstuffs based on Au@MoS₂/chitosan modified glassy carbon electrode. *Food Chemistry*, 276, 350-357. doi:<https://doi.org/10.1016/j.foodchem.2018.10.024>
- Elattar, R. H., Kamal, A. H., Mansour, F. R., & El-Malla, S. F. (2023). Spectrophotometric determination of monosodium glutamate in instant noodles' seasonings and Chinese salt by ligand exchange complexation. *Journal of Food Composition and Analysis*, 105404. doi:<https://doi.org/10.1016/j.jfca.2023.105404>
- Grasse, E. K., Torcasio, M. H., & Smith, A. W. (2016). Teaching UV-Vis Spectroscopy with a 3D-Printable Smartphone Spectrophotometer. *Journal of Chemical Education*, 93(1), 146-151. doi:10.1021/acs.jchemed.5b00654
- Haché, C., Shibusawa, S., Sasao, A., Suhama, T., & Sah, B. P. (2007). Field-derived spectral characteristics to classify conventional and conservation agricultural practices. *Computers and Electronics in Agriculture*, 57(1), 47-61. doi:<https://doi.org/10.1016/j.compag.2007.01.017>
- Hameedi, I. T. (2021). Determination of tetracycline hydrochloride in pure and pharmaceutical samples via oxidative coupling reaction. *Materials Today: Proceedings*, 42, 2953-2958. doi:<https://doi.org/10.1016/j.matpr.2020.12.802>
- Hind, H., & Ghadah, F. (2018). Sensitive Spectrophotometric Determination of Tetracycline Hydrochloride Indosage forms using Sodium Nitroprusside and Hydroxylamine Hydrochloride. *Al-Nahrain Journal of Science*, 17(3). Retrieved from <https://anjs.edu.iq/index.php/anjs/article/view/404>
- Huang, S., Qiu, R., Fang, Z., Min, K., van Beek, T. A., Ma, M., . . . Salentijn, G. I. J. (2022). Semiquantitative Screening of THC Analogues by Silica Gel TLC with an Ag(I) Retention Zone and Chromogenic Smartphone Detection. *Analytical Chemistry*, 94(40), 13710-13718. doi:10.1021/acs.analchem.2c01627
- Huy, B. T., Nghia, N. N., & Lee, Y.-I. (2020). Highly sensitive colorimetric paper-based analytical device for the determination of tetracycline using green fluorescent carbon nitride nanoparticles. *Microchemical Journal*, 158, 105151. doi:<https://doi.org/10.1016/j.microc.2020.105151>

- Ibarra, I. S., Rodriguez, J. A., Miranda, J. M., Vega, M., & Barrado, E. (2011). Magnetic solid phase extraction based on phenyl silica adsorbent for the determination of tetracyclines in milk samples by capillary electrophoresis. *Journal of Chromatography A*, 1218(16), 2196-2202. doi:<https://doi.org/10.1016/j.chroma.2011.02.046>
- Jang, I., Carrão, D. B., Menger, R. F., Moraes de Oliveira, A. R., & Henry, C. S. (2020). Pump-Free Microfluidic Rapid Mixer Combined with a Paper-Based Channel. *ACS Sensors*, 5(7), 2230-2238. doi:10.1021/acssensors.0c00937
- Jayawardane, B. M., McKelvie, I. D., & Kolev, S. D. (2015). Development of a Gas-Diffusion Microfluidic Paper-Based Analytical Device (μ PAD) for the Determination of Ammonia in Wastewater Samples. *Analytical Chemistry*, 87(9), 4621-4626. doi:10.1021/acs.analchem.5b00125
- Jayawardane, B. M., Wei, S., McKelvie, I. D., & Kolev, S. D. (2014). Microfluidic Paper-Based Analytical Device for the Determination of Nitrite and Nitrate. *Analytical Chemistry*, 86(15), 7274-7279. doi:10.1021/ac5013249
- Jiang, Q., Wu, J., Yao, K., Yin, Y., Gong, M. M., Yang, C., & Lin, F. (2019). Paper-Based Microfluidic Device (DON-Chip) for Rapid and Low-Cost Deoxynivalenol Quantification in Food, Feed, and Feed Ingredients. *ACS Sensors*, 4(11), 3072-3079. doi:10.1021/acssensors.9b01895
- Jumaev, R., Sadiq Hawezzy, H., & Abdullah, M. (2018). Spectrophotometric Determination of Tetracycline Hydrochloride Through Coupling with Sulphanilic Acid. *15*, 8. doi:10.26505/DJM/doi.org
- Kaewnu, K., Promsuwan, K., Phonchai, A., Thiangchanya, A., Somapa, D., Somapa, N., . . . Limbut, W. (2021). Cost-Effective Foam-Based Colorimetric Sensor for Roadside Testing of Alcohol in Undiluted Saliva. *Chemosensors*, 9(12). doi:10.3390/chemosensors9120334
- Kamal, A. H., El-Malla, S. F., Elattar, R. H., & Mansour, F. R. (2023). Determination of Monosodium Glutamate in Noodles Using a Simple Spectrofluorometric Method based on an Emission Turn-on Approach. *Journal of Fluorescence*. doi:10.1007/s10895-023-03143-0

- Kawamura, K., Nagayoshi, H., & Yao, T. (2010). In situ analysis of proteins at high temperatures mediated by capillary-flow hydrothermal UV-vis spectrophotometer with a water-soluble chromogenic reagent. *Analytica Chimica Acta*, 667(1), 88-95. doi:<https://doi.org/10.1016/j.aca.2010.04.013>
- Kolesnichenko, P. V., Eriksson, A., Lindh, L., Zigmantas, D., & Uhlig, J. (2023). Viking Spectrophotometer: A Home-Built, Simple, and Cost-Efficient Absorption and Fluorescence Spectrophotometer for Education in Chemistry. *Journal of Chemical Education*, 100(3), 1128-1137. doi:10.1021/acs.jchemed.2c00679
- Korać Jačić, J., Milenković, M. R., Bajuk-Bogdanović, D., Stanković, D., Dimitrijević, M., & Spasojević, I. (2022). The impact of ferric iron and pH on photo-degradation of tetracycline in water. *Journal of Photochemistry and Photobiology A: Chemistry*, 433, 114155. doi:<https://doi.org/10.1016/j.jphotochem.2022.114155>
- Kovarik, M. L., Clapis, J. R., & Romano-Pringle, K. A. (2020). Review of Student-Built Spectroscopy Instrumentation Projects. *Journal of Chemical Education*, 97(8), 2185-2195. doi:10.1021/acs.jchemed.0c00404
- Krishna, R., Patil, K., Dixit, A., Joseph, J., & Pandey, A. (2022). A novel paper-based microfluidic device and UV-visible spectroscopy coupled method for the field detection and analysis of seized marijuana samples. *Applied Research*, n/a(n/a), e202200068. doi:<https://doi.org/10.1002/appl.202200068>
- Kudo, H., Maejima, K., Hiruta, Y., & Citterio, D. (2020). Microfluidic Paper-Based Analytical Devices for Colorimetric Detection of Lactoferrin. *SLAS Technology*, 25(1), 47-57. doi:<https://doi.org/10.1177/2472630319884031>
- Kuntzleman, T. S., & Jacobson, E. C. (2016). Teaching Beer's Law and Absorption Spectrophotometry with a Smart Phone: A Substantially Simplified Protocol. *Journal of Chemical Education*, 93(7), 1249-1252. doi:10.1021/acs.jchemed.5b00844
- Kvittingen, E. V., Kvittingen, L., Sjursnes, B. J., & Verley, R. (2016). Simple and Inexpensive UV-Photometer Using LEDs as Both Light Source and Detector. *Journal of Chemical Education*, 93(10), 1814-1817. doi:10.1021/acs.jchemed.6b00156

- Lietard, A., Screen, M. A., Flindt, D. L., Jordan, C. J. C., Robson, J. M., & Verlet, J. R. R. (2021). A Combined Spectrophotometer and Fluorometer to Demonstrate the Principles of Absorption Spectroscopy. *Journal of Chemical Education*, 98(12), 3871-3877. doi:10.1021/acs.jchemed.1c00742
- Liu, C., Gomez, F. A., Miao, Y., Cui, P., & Lee, W. (2019). A colorimetric assay system for dopamine using microfluidic paper-based analytical devices. *Talanta*, 194, 171-176. doi:<https://doi.org/10.1016/j.talanta.2018.10.039>
- Liu, D., Huang, P., & Wu, F.-Y. (2022). Highly Specific and Rapid Colorimetric Detection of Tetracycline in Pills and Milk Based on Aptamer-Controlled Aggregation of Silver Nanoparticles. *Chemistry Africa*, 5(1), 107-114. doi:10.1007/s42250-021-00286-0
- Liu, G.-N., Xu, R.-D., Zhao, R.-Y., Sun, Y., Bo, Q.-B., Duan, Z.-Y., . . . Li, C. (2019). Hybrid Copper Iodide Cluster-Based Pellet Sensor for Highly Selective Optical Detection of o-Nitrophenol and Tetracycline Hydrochloride in Aqueous Solution. *ACS Sustainable Chemistry & Engineering*, 7(23), 18863-18873. doi:10.1021/acssuschemeng.9b03963
- Liu, M.-M., Li, S.-H., Huang, D.-D., Xu, Z.-W., Wu, Y.-W., Lei, Y., & Liu, A.-L. (2020). MoOx quantum dots with peroxidase-like activity on microfluidic paper-based analytical device for rapid colorimetric detection of H₂O₂ released from PC12 cells. *Sensors and Actuators B: Chemical*, 305, 127512. doi:<https://doi.org/10.1016/j.snb.2019.127512>
- Liu, Y., Brettell, T. A., Victoria, J., Wood, M. R., & Staretz, M. E. (2020). High performance thin-layer chromatography (HPTLC) analysis of cannabinoids in cannabis extracts. *Forensic Chemistry*, 19, 100249. doi:<https://doi.org/10.1016/j.forc.2020.100249>
- Lo, S.-C., Donahue, S. M., & Brown, C. W. (1993). Automated Drug Dissolution Monitor That Uses a UV-Visible Diode Array Spectrophotometer. *Journal of Pharmaceutical Sciences*, 82(4), 350-354. doi:<https://doi.org/10.1002/jps.2600820403>

- Majak, D., Fan, J., Kang, S., & Gupta, M. (2021). Delta-9-tetrahydrocannabinol (Δ^9 -THC) sensing using an aerosol jet printed organic electrochemical transistor (OECT). *Journal of Materials Chemistry B*, 9(8), 2107-2117. doi:10.1039/D0TB02951C
- Mano-Sousa, B. J., Maia, G. A. S., Lima, P. L., Campos, V. A., Negri, G., Chequer, F. M. D., & Duarte-Almeida, J. M. (2021). Color determination method and evaluation of methods for the detection of cannabinoids by thin-layer chromatography (TLC). *Journal of Forensic Sciences*, 66(3), 854-865. doi:<https://doi.org/10.1111/1556-4029.14659>
- Marlina, D., Amran, A., & Ulianas, A. (2018). Monosodium Glutamate Analysis in Meatballs Soup. *IOP Conference Series: Materials Science and Engineering*, 335, 012033. doi:10.1088/1757-899X/335/1/012033
- McCaig, T. N. (2002). Extending the use of visible/near-infrared reflectance spectrophotometers to measure colour of food and agricultural products. *Food Research International*, 35(8), 731-736. doi:[https://doi.org/10.1016/S0963-9969\(02\)00068-6](https://doi.org/10.1016/S0963-9969(02)00068-6)
- Mishra, R. K., Sempionatto, J. R., Li, Z., Brown, C., Galdino, N. M., Shah, R., . . . Wang, J. (2020). Simultaneous detection of salivary Δ^9 -tetrahydrocannabinol and alcohol using a Wearable Electrochemical Ring Sensor. *Talanta*, 211, 120757. doi:<https://doi.org/10.1016/j.talanta.2020.120757>
- Ngamchuea, K., Chaisiwamongkhol, K., Batchelor-McAuley, C., & Compton, R. G. (2018). Chemical analysis in saliva and the search for salivary biomarkers – a tutorial review. *Analyst*, 143(1), 81-99. doi:10.1039/C7AN01571B
- Nogueira, S. A., Lemes, A. D., Chagas, A. C., Vieira, M. L., Talhavini, M., Morais, P. A. O., & Coltro, W. K. T. (2019). Redox titration on foldable paper-based analytical devices for the visual determination of alcohol content in whiskey samples. *Talanta*, 194, 363-369. doi:<https://doi.org/10.1016/j.talanta.2018.10.036>
- O'Donoghue, J. (2019). Simplified Low-Cost Colorimetry for Education and Public Engagement. *Journal of Chemical Education*, 96(6), 1136-1142. doi:10.1021/acs.jchemed.9b00301

- Paiva, E. M., Ribessi, R. L., Pereira, C. F., & Rohwedder, J. J. R. (2020). Low-frequency Raman spectrophotometer with wide laser illumination on the sample: A tool for pharmaceutical analytical analysis. *Spectrochimica Acta Part A: Molecular and Biomolecular Spectroscopy*, 228, 117798. doi:<https://doi.org/10.1016/j.saa.2019.117798>
- Palaharn, S., Charoenraks, T., Wangfuengkanagul, N., Grudpan, K., & Chailapakul, O. (2003). Flow injection analysis of tetracycline in pharmaceutical formulation with pulsed amperometric detection. *Analytica Chimica Acta*, 499(1), 191-197. doi:[https://doi.org/10.1016/S0003-2670\(03\)00948-6](https://doi.org/10.1016/S0003-2670(03)00948-6)
- Placer, L., Lavilla, I., Pena-Pereira, F., & Bendicho, C. (2023). A 3D microfluidic paper-based analytical device with smartphone-assisted colorimetric detection for iodine speciation in seaweed samples. *Sensors and Actuators B: Chemical*, 377, 133109. doi:<https://doi.org/10.1016/j.snb.2022.133109>
- Pungjunun, K., Yakoh, A., Chaiyo, S., Praphairaksit, N., Siangproh, W., Kalcher, K., & Chailapakul, O. (2021). Laser engraved microcapillary pump paper-based microfluidic device for colorimetric and electrochemical detection of salivary thiocyanate. *Microchimica Acta*, 188(4), 140. doi:10.1007/s00604-021-04793-2
- Saridal, K., & Ulusoy, H. İ. (2019). A simple methodology based on cloud point extraction prior to HPLC-PDA analysis for tetracycline residues in food samples. *Microchemical Journal*, 150, 104170. doi:<https://doi.org/10.1016/j.microc.2019.104170>
- Senee Kruanetr, K. P. (2021). UV-Vis Spectrophotometric Method Using Natural Reagent from *Vigna unguiculata* subsp. *sesquipedalis* for Tetracycline Determination in Pharmaceutical Samples. *CURRENT APPLIED SCIENCE AND TECHNOLOGY*, 21, 51-64.
- Shen, L., Chen, J., Li, N., He, P., & Li, Z. (2014). Rapid colorimetric sensing of tetracycline antibiotics with in situ growth of gold nanoparticles. *Analytica Chimica Acta*, 839, 83-90. doi:<https://doi.org/10.1016/j.aca.2014.05.021>

- Shrestha, S., Chaudhary, N., Miya, T., Pokhrel, P., Chapagain, M., Krishna, P., & Rai. (2016). QUANTITATIVE ANALYSIS OF MONOSODIUM GLUTAMATE (MSG) IN INSTANT NOODLES BY HPLC-UV WITH PRE-COLUMN DERIVATIZATION.
- Sitanurak, J., Fukana, N., Wongpakdee, T., Thepchuay, Y., Ratanawimarnwong, N., Amornsakchai, T., & Nacapricha, D. (2019). T-shirt ink for one-step screen-printing of hydrophobic barriers for 2D- and 3D-microfluidic paper-based analytical devices. *Talanta*, *205*, 120113.
doi:<https://doi.org/10.1016/j.talanta.2019.120113>
- Small, E. (2015). Evolution and Classification of Cannabis sativa (Marijuana, Hemp) in Relation to Human Utilization. *The Botanical Review*, *81*(3), 189-294.
doi:10.1007/s12229-015-9157-3
- Solin, K., Vuoriluoto, M., Khakalo, A., & Tammelin, T. (2023). Cannabis detection with solid sensors and paper-based immunoassays by conjugating antibodies to nanocellulose. *Carbohydrate Polymers*, *304*, 120517.
doi:<https://doi.org/10.1016/j.carbpol.2022.120517>
- Songok, J., & Toivakka, M. (2016). Enhancing Capillary-Driven Flow for Paper-Based Microfluidic Channels. *ACS Applied Materials & Interfaces*, *8*(44), 30523-30530.
doi:10.1021/acsami.6b08117
- Taghdisi, S. M., Danesh, N. M., Ramezani, M., & Abnous, K. (2016). A novel M-shape electrochemical aptasensor for ultrasensitive detection of tetracyclines. *Biosensors and Bioelectronics*, *85*, 509-514.
doi:<https://doi.org/10.1016/j.bios.2016.05.048>
- Tang, X., Su, R., Luo, H., Zhao, Y., Feng, L., & Chen, J. (2022). Colorimetric detection of Aflatoxin B1 by using smartphone-assisted microfluidic paper-based analytical devices. *Food Control*, *132*, 108497.
doi:<https://doi.org/10.1016/j.foodcont.2021.108497>
- Thepchuay, Y., Sonsa-ard, T., Ratanawimarnwong, N., Auparakkitanon, S., Sitanurak, J., & Nacapricha, D. (2020). Paper-based colorimetric biosensor of blood alcohol

- with in-situ headspace separation of ethanol from whole blood. *Analytica Chimica Acta*, 1103, 115-121. doi:<https://doi.org/10.1016/j.aca.2019.12.043>
- Thongkam, T., & Hemavibool, K. (2020). An environmentally friendly microfluidic paper-based analytical device for simultaneous colorimetric detection of nitrite and nitrate in food products. *Microchemical Journal*, 159, 105412. doi:<https://doi.org/10.1016/j.microc.2020.105412>
- Thungon, P. D., Wang, H., Vagin, S. I., Dyck, C. V., Goswami, P., Rieger, B., & Meldrum, A. (2022). A Fluorescent Alcohol Biosensor Using a Simple microPAD Based Detection Scheme. *Frontiers in Sensors*, 3. Retrieved from <https://www.frontiersin.org/articles/10.3389/fsens.2022.840130>
- Tsai, W.-H., Huang, T.-C., Huang, J.-J., Hsue, Y.-H., & Chuang, H.-Y. (2009). Dispersive solid-phase microextraction method for sample extraction in the analysis of four tetracyclines in water and milk samples by high-performance liquid chromatography with diode-array detection. *Journal of Chromatography A*, 1216(12), 2263-2269. doi:<https://doi.org/10.1016/j.chroma.2009.01.034>
- Tsujikawa, K., Okada, Y., Segawa, H., Yamamuro, T., Kuwayama, K., Kanamori, T., & Iwata, Y. T. (2022). Thin-layer chromatography on silver nitrate-impregnated silica gel for analysis of homemade tetrahydrocannabinol mixtures. *Forensic Toxicology*, 40(1), 125-131. doi:10.1007/s11419-021-00592-9
- Verdejo, B., Aguilar, J., Doménech, A., Miranda, C., Navarro, P., Jiménez, H. R., . . . García-España, E. (2005). Binuclear Cu²⁺ complex mediated discrimination between l-glutamate and l-aspartate in water. *Chemical Communications*(24), 3086-3088. doi:10.1039/B503417E
- Walker, R., & Lupien, J. R. (2000). The Safety Evaluation of Monosodium Glutamate. *The Journal of Nutrition*, 130(4), 1049S-1052S. doi:10.1093/jn/130.4.1049S
- Wang, G.-S., & Hsieh, S.-T. (2001). Monitoring natural organic matter in water with scanning spectrophotometer. *Environment International*, 26(4), 205-212. doi:[https://doi.org/10.1016/S0160-4120\(00\)00107-0](https://doi.org/10.1016/S0160-4120(00)00107-0)
- Wen, Z., Song, S., Wang, C., Qu, F., Thomas, T., Hu, T., . . . Yang, M. (2019). Large-scale synthesis of dual-emitting-based visualization sensing paper for humidity and

ethanol detection. *Sensors and Actuators B: Chemical*, 282, 9-15.

doi:<https://doi.org/10.1016/j.snb.2018.11.041>

Xu, J.-J., An, M., Yang, R., Tan, Z., Hao, J., Cao, J., . . . Cao, W. (2016). Determination of Tetracycline Antibiotic Residues in Honey and Milk by Miniaturized Solid Phase Extraction Using Chitosan-Modified Graphitized Multiwalled Carbon Nanotubes. *Journal of Agricultural and Food Chemistry*, 64(12), 2647-2654. doi:10.1021/acs.jafc.6b00748

Yang, H. (2011). Spectroscopic Calibration for Soil N and C Measurement at a Farm Scale. *Procedia Environmental Sciences*, 10, 672-677.

doi:<https://doi.org/10.1016/j.proenv.2011.09.108>

Yang, M., Xu, Y., & Wang, J.-H. (2006). Lab-on-Valve System Integrating a Chemiluminescent Entity and In Situ Generation of Nascent Bromine as Oxidant for Chemiluminescent Determination of Tetracycline. *Analytical Chemistry*, 78(16), 5900-5905. doi:10.1021/ac060742w

Electronic Media

Amazon. (2023a). 3 Pack - DrugExam Made in USA Most Sensitive Marijuana THC 15 ng/mL Single Panel Drug Test Kit - Marijuana Drug Test with 15 ng/mL Cutoff Level for Detecting Any Form of THC. Retrieved from https://www.amazon.com/Pack-DrugExam-Sensitive-Marijuana-Detecting/dp/B08RN54V7P/ref=d_bmx_dp_b5muysxo_sccl_2_6/137-4024830-2276915?pd_rd_w=YFk0z&content-id=amzn1.sym.e3b35db1-c427-46b1-86ca-67bddaf5745a&pf_rd_p=e3b35db1-c427-46b1-86ca-67bddaf5745a&pf_rd_r=NMRO3HKZGEA8C0RV70RR&pd_rd_wg=DJA9l&pd_rd_r=e2346640-eb79-4e04-b2a9-d8f0cb609f7c&pd_rd_i=B08RN54V7P&psc=1

Amazon. (2023b). 3 Pack - DrugExam THC Advantage Made in USA Multi Level Marijuana Home Urine Test Kit. Highly Sensitive THC 5 Level Drug Test Kit. Detects at 15 ng/mL, 20 ng/mL, 50 ng/mL, 200 ng/mL and 300 ng/mL (3). Retrieved from <https://www.amazon.com/Pack-DrugExam-Advantage->

Marijuana-

[Sensitive/dp/B08VFC3DO4/ref=pd_day0fvt_vft_none_img_sccl_1/137-4024830-2276915?pd_rd_w=DqKeh&content-id=amzn1.sym.a400618b-650b-4c39-a4fe-66c3e0813a14&pf_rd_p=a400618b-650b-4c39-a4fe-66c3e0813a14&pf_rd_r=GBMYSCJYFA5S381WR4W3&pd_rd_wg=5LnXc&pd_rd_r=87331d08-1883-48fe-9ab1-8d0cbab753c2&pd_rd_i=B08VFC3DO4&psc=1](https://www.amazon.com/Sensitive/dp/B08VFC3DO4/ref=pd_day0fvt_vft_none_img_sccl_1/137-4024830-2276915?pd_rd_w=DqKeh&content-id=amzn1.sym.a400618b-650b-4c39-a4fe-66c3e0813a14&pf_rd_p=a400618b-650b-4c39-a4fe-66c3e0813a14&pf_rd_r=GBMYSCJYFA5S381WR4W3&pd_rd_wg=5LnXc&pd_rd_r=87331d08-1883-48fe-9ab1-8d0cbab753c2&pd_rd_i=B08VFC3DO4&psc=1)

Amazon. (2023c). Amazon.com: 15 Pack Easy@Home Marijuana (THC) Single Panel Drug Tests Kit - #EDTH-114 : Health & Household. Retrieved from https://www.amazon.com/Easy-Home-Marijuana-Single-Panel/dp/B00DVPS4IO?ref_=ast_sto_dp&th=1

Amazon. (2023d). Exploro Highly Sensitive at Home Marijuana Drug Test Kit, THC Drug Test Kit Marijuana/Weed, THC Drug Test Urine, Easy Home Drug Test Marijuana/THC Substance Abuse, 15 THC Test Strips/Sticks, 50 ng/ml. Retrieved from https://www.amazon.com/Exploro-Highly-Sensitive-Marijuana-Test/dp/B07BZ4KNKL/ref=d_bmx_dp_b5muysxo_sccl_2_1/137-4024830-2276915?pd_rd_w=EOTTS&content-id=amzn1.sym.e3b35db1-c427-46b1-86ca-67bddaf5745a&pf_rd_p=e3b35db1-c427-46b1-86ca-67bddaf5745a&pf_rd_r=TX4FA76G5XAEC1P5B1T&pd_rd_wg=pqkoy&pd_rd_r=01626c2e-183b-48fc-8317-efe8fa09a906&pd_rd_i=B07BZ4KNKL&th=1

Amazon. (2023e). UTest (2-Pack) 5-Levels of Detection THC Marijuana Home Urine Drug Test Kit - Highly Sensitive Testing Strips with 5 Panel Levels: 15 ng/mL, 50 ng/mL, 100, 200, & 300 ng/mL. Instant Results. Retrieved from https://www.amazon.com/UTest-Meter-Level-Marijuana-Strips/dp/B01N1Z975Y/ref=d_bmx_dp_b912yaon_sccl_2_4/137-4024830-2276915?pd_rd_w=zP6z7&content-id=amzn1.sym.e3b35db1-c427-46b1-86ca-67bddaf5745a&pf_rd_p=e3b35db1-c427-46b1-86ca-67bddaf5745a&pf_rd_r=F54TWTCKVAM8M34O1E4N&pd_rd_wg=KmqDL&pd_rd_r=464645e3-acf3-43f2-82b5-759bf4e49779&pd_rd_i=B01N1Z975Y&th=1

Amazon. (2023f). UTest Instant THC Home Drug Test | 15 ng/mL Single Panel Cannabis Detection Tests | Highly Sensitive Marijuana Urine Test Kit | Testing

- Strip (2 Pack). Retrieved from https://www.amazon.com/%C3%9CTest-Sensitive-Instant-Marijuana-Detection/dp/B00UCDYJU/ref=pd_vtp_h_vft_none_pd_vtp_h_vft_none_sccl_2/137-4024830-2276915?pd_rd_w=kTJeR&content-id=amzn1.sym.a5610dee-0db9-4ad9-a7a9-14285a430f83&pf_rd_p=a5610dee-0db9-4ad9-a7a9-14285a430f83&pf_rd_r=JDYC63973SJX2NTTOF0Y&pd_rd_wg=xjckb&pd_rd_r=461960cf-8301-41bf-9460-21a8d1b01629&pd_rd_i=B00UCDYJU&psc=1
- PharmaDrugTest. (2023). ETG Alcohol Test Strip. Retrieved from <https://www.pharmadrugtest.com/urine-drug-tests/90-etg-test-alcohol-urine.html>
- UK, H. H. (2023a). 10 x Alcohol Test Strips Urine Tester Kits ETG Testing Kit. Retrieved from https://homehealth-uk.com/all-products/10-x-etg-alcohol-ethanol-ethyl-glucuronide-urine-drug-test-strips/#tab_instructions
- UK, H. H. (2023b). 10 x Alcohol Testing Kits Saliva Strips Tester Kits (BAC) Tests. Retrieved from https://homehealth-uk.com/all-products/10-x-alcohol-saliva-test-strips/#tab_instructions
- UK, H. H. (2023c). Alcohol Breath Tester | One Step Breathalyzer | 2 Tests. Retrieved from https://homehealth-uk.com/all-products/one-step-test-and-drive-alcohol-breath-testers-nfc/#tab_healthinfo
- UK, H. H. (2023d). Breastmilk Alcohol Test Strips – 10 Test Pack. Retrieved from https://homehealth-uk.com/all-products/10-x-one-step-breast-milk-alcohol-check-screen-detection-home-test-kits/#tab_instructions
- UKDrugTesting. (2023a). ALLTEST 7 Panel Drug And Alcohol Saliva Drug Testing Kit DSD877 Workplace & Driver. Retrieved from <https://www.ukdrugtesting.co.uk/collections/workplace-drug-and-alcohol-testing-kits/products/alltest-7-drug-saliva-drug-testing-kit-dsd-877>
- UKDrugTesting. (2023b). ALLTEST 13 Panel Saliva Drug And Alcohol Testing Kits DSD-8135 Workplace And Civil Aviation. Retrieved from <https://www.ukdrugtesting.co.uk/collections/workplace-drug-and-alcohol-testing-kits/products/alltest-13-drug-saliva-drug-testing-kit-dsd-8135>

UKDrugTesting. (2023c). Alltest Saliva Alcohol Test Strips. Retrieved from

<https://www.ukdrugtesting.co.uk/collections/alcohol-test-strips/products/alcohol-test-strips>

UKDrugTesting. (2023d). ALLTEST Workplace Drug and Alcohol Test DSD-873ALC-MET 7 Panel Saliva Drug Testing Kits. Retrieved from

<https://www.ukdrugtesting.co.uk/collections/workplace-drug-and-alcohol-testing-kits/products/alltest-workplace-drug-and-alcohol-test-dsd-873alc-met-saliva-drug-testing-kits>



BIOGRAPHY

Name	Nattawat Bawornnithichaiyakul
Educational Attainment	Academic Year 2020: Bachelor of Science (Chemistry), Thammasat University, Thailand
Scholarship	Year 2020-2022: Talent student to study graduate program in the Faculty of Science and Technology, Thammasat University, Contract No.TB 4/2563
Publications	
	Nattawat, A. (2023). Lab-made spectrometer for determination of tetracycline in pharmaceuticals. <i>PACCON2023</i> , 36-40.